US Army Corps of Engineers

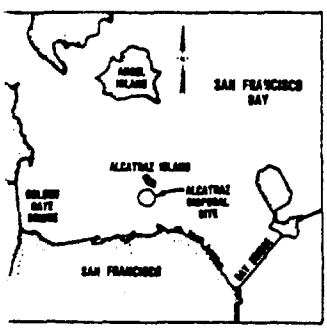

HYDRAULICS LABORATORY

MISCELLANEOUS PAPER HL-86-1

ALCATRAZ DISPOSAL SITE INVESTIGATION

Report 3

SAN FRANCISCO BAY-ALCATRAZ DISPOSAL SITE ERODIBILITY

by

Allen M. Teeter

Hydraulics Laboratory

DEPARTMENT OF THE ARMY
Waterways Experiment Station, Corps of Engineers
PO Box 631, Vicksburg, Mississippi 39180-0631

May 1987

Report 3 of a Series

Prepared for US Army Engineer District, San Francisco
San Francisco, California 94105-1905

Under IOMT Work Unit No. 31765

Unclassified
SECURITY CLASSIFICATION OF THIS PAGE

AD-A181837

REPORT DOCUMENTATION PAGE

Form Approved
OMB No 0704-0188
Exp Date Jun 30, 1986

1a REPORT SECURITY CLASSIFICATION Unclassified	1b RESTRICTIVE MARKINGS
2a SECURITY CLASSIFICATION AUTHORITY	3 DISTRIBUTION/AVAILABILITY OF REPORT Approved for public release; distribution unlimited.
2b DECLASSIFICATION/DOWNGRADING SCHEDULE	
4 PERFORMING ORGANIZATION REPORT NUMBER(S) Miscellaneous Paper HL-86-1	5 MONITORING ORGANIZATION REPORT NUMBER(S)
6a NAME OF PERFORMING ORGANIZATION USAEWES Hydraulics Laboratory 6b OFFICE SYMBOL (If applicable) WESHE-P	7a NAME OF MONITORING ORGANIZATION
6c ADDRESS (City, State, and ZIP Code) PO Box 631 Vicksburg, MS 39180-0631	7b ADDRESS (City, State, and ZIP Code)
8a NAME OF FUNDING/SPONSORING ORGANIZATION USAED, San Francisco 8b OFFICE SYMBOL (If applicable)	9 PROCUREMENT INSTRUMENT IDENTIFICATION NUMBER
8c ADDRESS (City, State, and ZIP Code) 211 Main Street San Francisco, CA 94105-1905	10 SOURCE OF FUNDING NUMBERS See reverse PROGRAM ELEMENT NO / PROJECT NO / TASK NO / WORK UNIT ACCESSION NO

11 TITLE (Include Security Classification)
Alcatraz Disposal Site Investigation; Report 3, San Francisco Bay-Alcatraz Disposal Site Erodibility

12 PERSONAL AUTHOR(S)
Teeter, Allen M.

13a TYPE OF REPORT	13b TIME COVERED	14 DATE OF REPORT (Year, Month, Day)	15 PAGE COUNT
Report 3 of a series	FROM _____ TO _____	May 1987	120

16 SUPPLEMENTARY NOTATION
Available from National Technical Information Service, 5285 Port Royal Road, Springfield, VA 22161.

17 COSATI CODES		
FIELD	GROUP	SUB-GROUP

18 SUBJECT TERMS (Continue on reverse if necessary and identify by block number)
Alcatraz Island (LC) Sedimentation and deposition (LC)
Erosion (LC)
San Francisco Bay (LC)

19 ABSTRACT (Continue on reverse if necessary and identify by block number)

Sediments from San Francisco Bay were subjected to laboratory erosion testing to provide information for the management of the Alcatraz disposal site, specifically to reduce the retention of disposed materials at the site. Erosion test results were used to estimate the erosion capacity of the site for a number of disposed material densities using data developed by this study. Erosion testing concentrated on fine-grained, cohesive sediment which makes up the bulk of the material disposed and retained at the Alcatraz site. Since the erodibility of such sediments is known to depend on interparticle cohesion, characterization testing was used to describe the cohesive nature of the sediments and their settling behavior.

Appendix A describes 18 erosion tests performed on remolded sediment sections in a 24.4-m recirculating saltwater flume at the US Army Engineer Waterways Experiment

(Continued)

20 DISTRIBUTION/AVAILABILITY OF ABSTRACT	21 ABSTRACT SECURITY CLASSIFICATION
☒ UNCLASSIFIED/UNLIMITED ☐ SAME AS RPT ☐ DTIC USERS	Unclassified
22a NAME OF RESPONSIBLE INDIVIDUAL	22b TELEPHONE (Include Area Code) / 22c OFFICE SYMBOL

DD FORM 1473, 84 MAR 83 APR edition may be used until exhausted
All other editions are obsolete

SECURITY CLASSIFICATION OF THIS PAGE
Unclassified

10. WORK UNIT ACCESSION NO. (Continued).

Additional funding provided by Improvement of Operations and Maintenance Techniques research program, Work Unit No. 31765, sponsored by Office, Chief of Engineers, US Army.

19. ABSTRACT (Continued).

Station. Two sediment materials were tested, each with three sand contents and three bulk densities. Flume flows were increased hourly during tests until appreciable erosion occurred. The critical shear stress for the onset of erosion τ_c was found to be highly dependent on the specific weight of the fine-grained sediments present. The addition of up to 40 percent sand had little effect on τ_c.

Additional erosion and characterization testing, discussed in Appendix B, was performed by the University of Florida at Gainesville using an annular flume. A sediment from Richmond Harbor on San Francisco Bay was used for these tests. One erosion test was performed on remolded sediment material, and four other tests were performed on deposited sediment beds. The settled beds were found to be more erodible than remolded beds.

PREFACE

The determination of the erodibility of materials disposed at the Alcatraz open-water disposal site, documented in this report, was performed for the US Army Engineer District, San Francisco, with additional support from the Improvement of Operations and Maintenance Techniques (IOMT) research program sponsored by the Office, Chief of Engineers, US Army, under IOMT Work Unit No. 31765, "Fine-Grained Shoaling in Navigation Channels."

This report is Report 3 of a series. The first report was published as "Alcatraz Disposal Site Investigation," Miscellaneous Paper HL-86-1. The second report was published under the same report number as "Alcatraz Disposal Site Investigation; Report 2, North Zone Disposal of Oakland Outer Harbor and Richmond Inner Harbor Sediments."

The study was conducted in the Hydraulics Laboratory (HL) of the US Army Engineer Waterways Experiment Station (WES) during the period January to April 1986 under the general supervision of Messrs. Frank A. Herrmann, Chief, HL; Richard A. Sager, Assistant Chief, HL; William H. McAnally, Jr., Chief, Estuaries Division; and George M. Fisackerly, Chief, Estuarine Processes Branch. Additional testing was performed by the University of Florida, Gainesville, under contract to WES.

The HL work was performed and this report prepared by Mr. Allen M. Teeter, Estuarine Processes Branch. Mr. James Hilbun was the technician for this study, with additional support from Messrs. Larry Caviness and Billy Moore, all of the Estuarine Processes Branch. This report was edited by Mrs. Marsha Gay, Information Technology Laboratory.

Cation exchange capacities and analyses necessary to compute sodium adsorption ratios were performed by the Analytical Support Group, Environmental Laboratory, WES, Ms. Ann B. Strong, Chief. The IOMT Technical Monitor was Mr. James Gottesman.

The University of Florida work was performed and Appendix B was written by Mmes. Catherine Villaret and Mary Paulic, Coastal and Oceanographic Engineering Department, University of Florida. Dr. Ashish J. Mehta was the principal investigator for the University of Florida work. Appendix B was also published as "Experiments on the Erosion of Deposited and Placed Cohesive Sediments in an Annular Flume and a Rocking Flume," UFL/COEL-86/007, sponsored by WES under Contract No. DACW39-84-C-0013.

COL Allen F. Grum, USA, was the previous Director of WES. COL Dwayne G. Lee, CE, is the present Commander and Director. Dr. Robert W. Whalin is Technical Director.

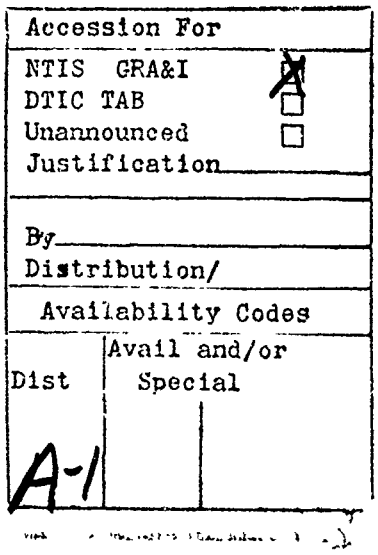

CONTENTS

	Page
PREFACE	1
PART I: INTRODUCTION	4
Background	4
Objectives	5
Approach	5
PART II: DISCUSSION OF EROSION TESTS	6
Test Materials	6
Description of Tests	6
Erosion Test Results	7
Variations in Results	9
PART III: APPLICATION OF RESULTS	12
Descent of Material to the Bed	12
Erosion Rate Estimates	13
Erosion Capacity of the Site	14
PART IV: CONCLUSIONS AND RECOMMENDATIONS	16
Conclusions	16
Recommendations	16
REFERENCES	17
TABLE 1	
APPENDIX A: SAN FRANCISCO BAY SEDIMENT EROSION TESTS IN THE WATERWAYS EXPERIMENT STATION FLUME	A1
TABLES A1-A3	
PLATES A1-A15	
APPENDIX B: SEDIMENT EROSION TESTS IN THE UNIVERSITY OF FLORIDA FLUMES	B1
APPENDIX C: NOTATION	C1

ALCATRAZ DISPOSAL SITE INVESTIGATION

SAN FRANCISCO BAY-ALCATRAZ DISPOSAL SITE ERODIBILITY

PART I: INTRODUCTION

Background

1. The Alcatraz dredged material disposal site in San Francisco Bay is classified as a dispersive site. It is intended that the strong ebb currents at the site prevent accumulation of disposed materials and transport them seaward in the direction of the Golden Gate Bridge. The disposal site has been in use for 90 years, and for the last 14 years has been the only authorized disposal site in the lower bay.

2. Recent loss of depth at the site has raised doubts as to the ability of the site to disperse new work and maintenance material disposed there. A mound of material developed which at one time reduced water depths to less than 9.1 m mllw.* Mound development at the Alcatraz disposal site has had the following effects:

a. Become a potential hazard to navigation in the existing shipping lane, which has a project depth of 12.2 m.

b. Threatened the capacity of the site to assimilate future dredged material.

c. Raised the possibility of new disposal sites, most probably increasing overall dredging costs.

To eliminate this disposal site mounding, the US Army Engineer District, San Francisco (SPN), has proposed specifications for the disposed material based on water content.

3 Sediments from San Francisco Bay were subjected to erosion tests at the Hydraulics Laboratory, US Army Engineer Waterways Experiment Station (WES), and at the Coastal and Oceanographic Engineering Department of the University of Florida at Gainesville (UF). The WES erosion studies are presented in Appendix A and the UF studies in Appendix B.

---

* All elevations (el) and stages cited herein are in metres referred to mean lower low water (mllw).

Objectives

4 The purpose of this study was to provide information for the management of the Alcatraz disposal site, specifically to reduce the retention of disposed materials at the site. The objective of the testing program was to provide this information by establishing the critical shear stress for erosion and erosion rates above threshold for a range of sediments typical of those disposed at the Alcatraz site. The objectives of this report were to summarize the erosion studies and to apply those laboratory results to the erodibility of the disposal site.

Approach

5. The two laboratory erosion studies form the basis for this report. The two studies are summarized and results compared in this report. Differences in the results of the two erosion studies are discussed. Results from the erosion studies are applied to the disposal site to assess the suspended settling of material to the bed, erosion rates for constant currents and varying bed density, and, finally, the erosion capacity of the site for varying bed density and actually occurring current speeds.

PART II: DISCUSSION OF EROSION TESTS

Test Materials

6. The WES erosion testing was conducted on two composite sediment materials. Core sections from the Alcatraz disposal site were supplied by SPN and combined into the first composite sample. Core sections from Redwood Harbor were combined into the second composite sample. The samples were sieved to remove coarse materials. Both composite samples tested had similar Atterberg limits and other characteristics.

7. UF tested a third composite sample made from five core sections from Larkspur-Richmond Longwharf provided by SPN.

Description of Tests

8. The WES tests were run in series with three levels of moisture or bulk wet density (BWD)* and three levels of added sand: 0, 15, and 40 percent. A total of 18 flume runs were made in this test matrix. A tilting flume was used for testing, and sediments were molded into small recessed chambers in the floor of the flume.

9. UF first tested the third composite material molded into their annular flume. Subsequent tests were performed in rocking and annular flumes on deposited material. In these subsequent tests, sediment was eroded and allowed to settle and consolidate before erosion testing was conducted. Five tests were performed. Descriptions of the testing facilities and procedures for the WES and UF tests are provided in Appendixes A and B.

10. Both the WES and UF erosion studies used the modified Partheniades erosion function as a basis for testing:

$$E = M\left(\frac{\tau_b}{\tau_c} - 1\right) \qquad \tau_c < \tau_b \tag{1}$$

---

* For convenience, symbols and abbreviations are listed in the Notation (Appendix C).

where

E = erosion rate

M = erosion rate constant

τ_b = bed shear stress, N/sq m

τ_c = critical shear stress for erosion, N/sq m

The objective of the testing was to determine M and τ_c.

Erosion Test Results

11. The WES tests showed that the addition of sand to the test sample had little or no effect on τ_c. A power law function was fit to the combined results, yielding an exponent of 3.29 and a constant of 17.62. The resulting equation is

$$\tau_c = 17.62\gamma_f^{3.29} \tag{2}$$

where γ_f is the specific weight of the fines in the material in grams per cubic centimetre. Average values of M were calculated for each material. There was a statistical difference between M values for the two sediments tested, but they were within a factor of 3 of each other. Sediment erodibility as a function of current speed U, as developed from the WES tests, is shown in Figure 1. The average M value of 0.048 g/sq cm/min determined from the WES tests was used to develop the curves in Figure 1.

12. The UF tests indicated a linear relation between ρ_b, UF's term for BWD, and τ_c:

$$\tau_c = 1.04(\text{BWD} - 1) \tag{3}$$

where BWD is expressed in grams per cubic centimetre. It should be noted that BWD in the WES tests and ρ_b in the UF tests are interchangeable. The UF tests had sufficient temporal resolution to determine M for individual tests. Results were combined into an expression

$$M = 0.00166 \exp(-2.33\tau_c) \tag{4}$$

where M is expressed in grams per square centimetre per minute. Curves developed from these expressions are given in Figure 2.

13. The values of τ_b required to develop the curves in Figures 1 and 2 were calculated using Manning's equation

$$\tau_b = \frac{\rho g n^2}{H^{1/3}} U^2 \tag{5}$$

where

ρ = flow density (1,025 kg/cu m)

g = gravity (9.81 m/sec^2)

n = friction coefficient (0.020)

H = flow depth (10 m)

U = depth-averaged current speed, m/sec

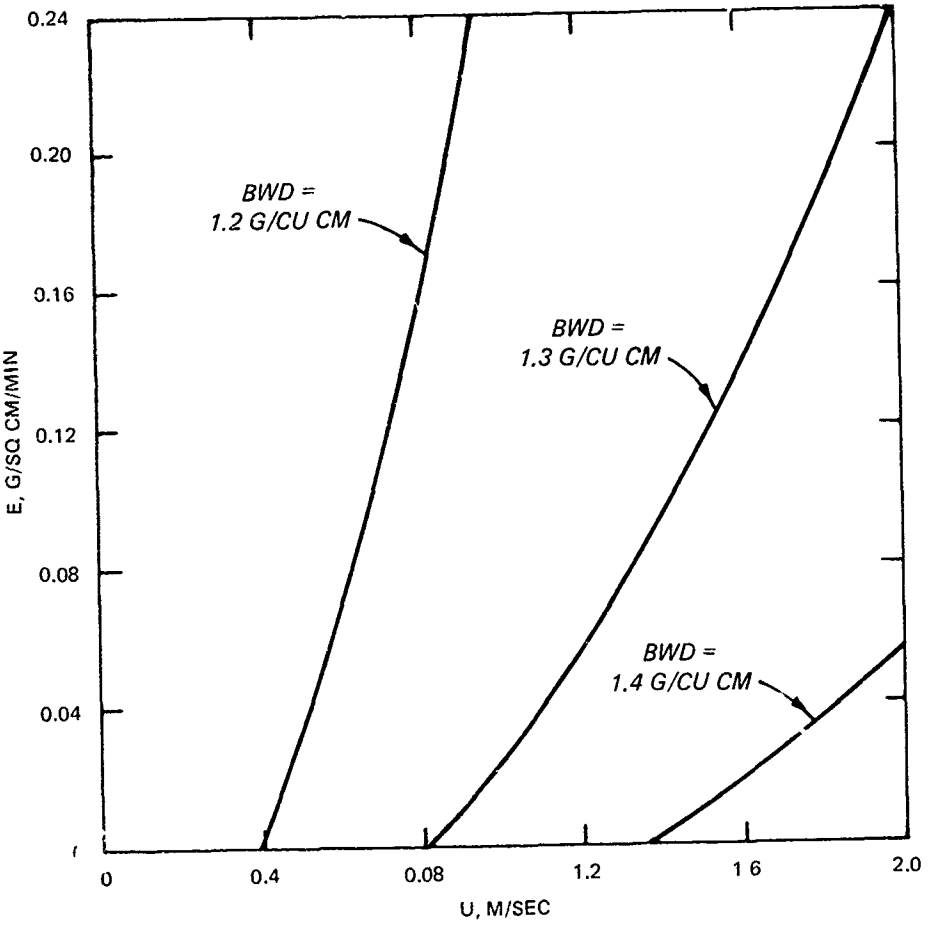

Figure 1. Erosion rates for constant currents based on WES flume tests

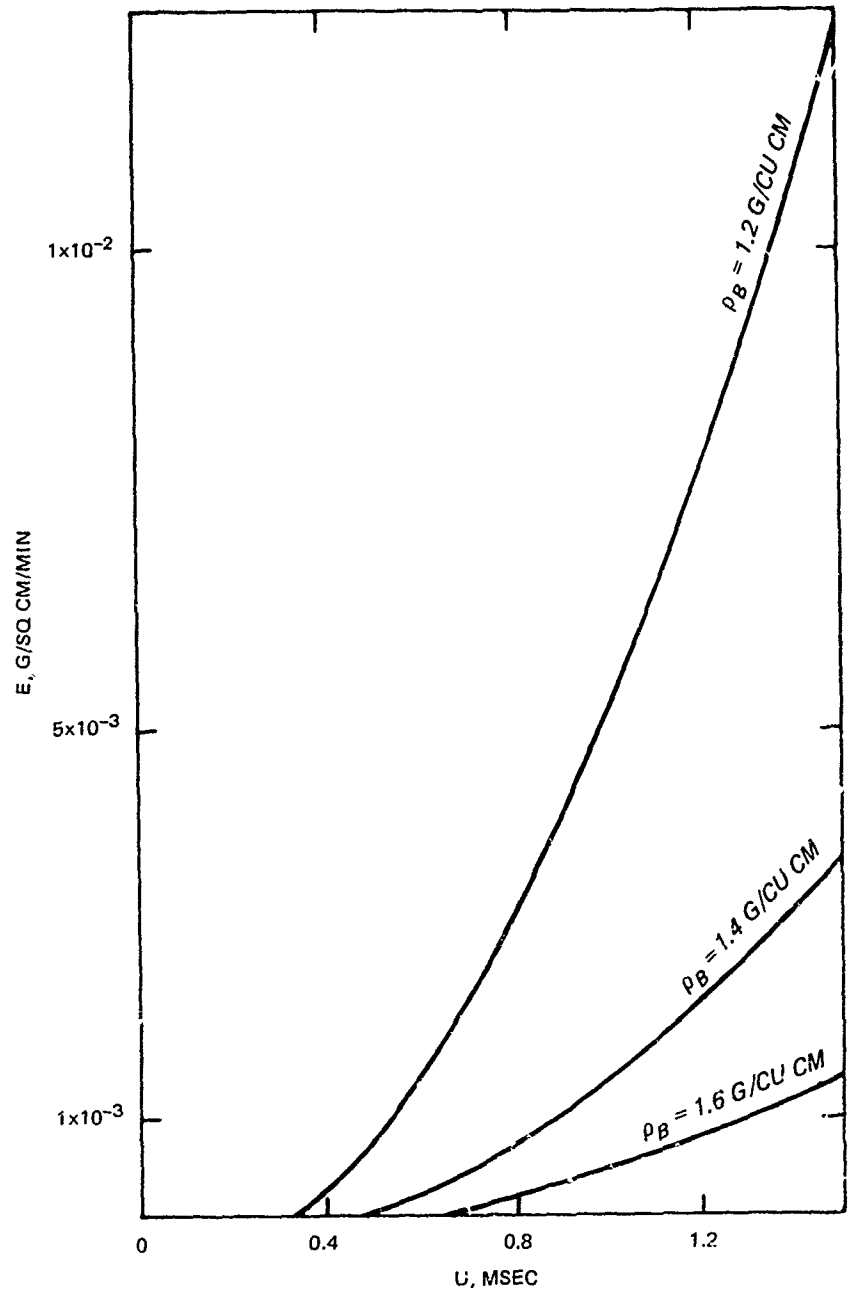

Figure 2. Erosion rates for constant currents based on UF flume tests

Variations in Results

14. Resistance to erosion is a combination of a sediment's τ_c and M . The WES tests showed a much stronger dependence of τ_c on BWD or ρ_b , or solids concentration. The τ_c values for a BWD of 1.2 g/cu cm were very

similar, 0.28 N/sq m for the WES tests and 0.20 N/sq m for the UF tests. However, at a BWD of 1.6 g/cu cm, WES tests indicated a τ_c of 14.1 N/sq m versus only 0.62 N/sq m for the UF tests. The WES tests therefore indicated a higher resistance to erosion in terms of the threshold for erosion than did the UF tests.

15. Results for M had an opposite trend. The value for M was found to be about 100 times greater in the WES tests than in the UF tests. The WES tests therefore indicated a lower resistance to erosion in terms of M than did the UF tests.

16. No standard testing procedure exists for the erodibility of unconsolidated marine sediments. Test procedures for these and other previous testing studies varied. Complete descriptions of test procedures used in the two erosion studies can be found in Appendixes A and B. Differences between the WES and UF results could be attributed to any of the following:

a. Different sediments were tested.

b. Different methods were used to prepare sediment beds for erosion.

c. The WES tests did not recirculate eroded sediment over the sediment beds, while UF tests did.

d. The WES sediment test beds had nearly uniform shear stresses across them, while UF test beds extended to sidewalls and had greater variation of shear stress across them.

e. The WES erosion rates were calculated by erosion depth measurements which detected only significant bed erosion, while UF erosion rates were calculated from suspension concentration changes which could detect much lower erosion rates.

Differences among sediments tested were probably not that important to their erosion characteristics, judging from other characterization test results and the repeatability found in the WES tests between sediments. The differences in bed preparation could have been important. The deposited beds used in the UF tests, although more natural, may have had sediment sorting from settling velocities, resulting in vertical variations in BWD. Also, sediment recirculation in the UF tests may have enhanced erosion above the critical shear stress level and may have changed the frictional characteristics of flows. Finally, lateral shear stress across channels in the UF tests would result in peak shear stresses being higher than average values, resulting in reported critical shear stress values lower than actually applied.

17. Typical laboratory relationships between E and τ_b show two

regimes or modes of erosion. At low shear stresses, erosion has been found by Hunt (1981) to proceed first as surface particle flaking which has a low threshold and a lower value of M. At higher values of τ_b, a break point is passed at which M increases sharply. Extrapolating the higher erosion mode yields a relatively high apparent critical erosion threshold. Figure 3 shows an example plot of the general form described. The UF and WES results might reflect measurements of the lower and higher modes, respectively, and may in fact be consistent from a phenomenological perspective.

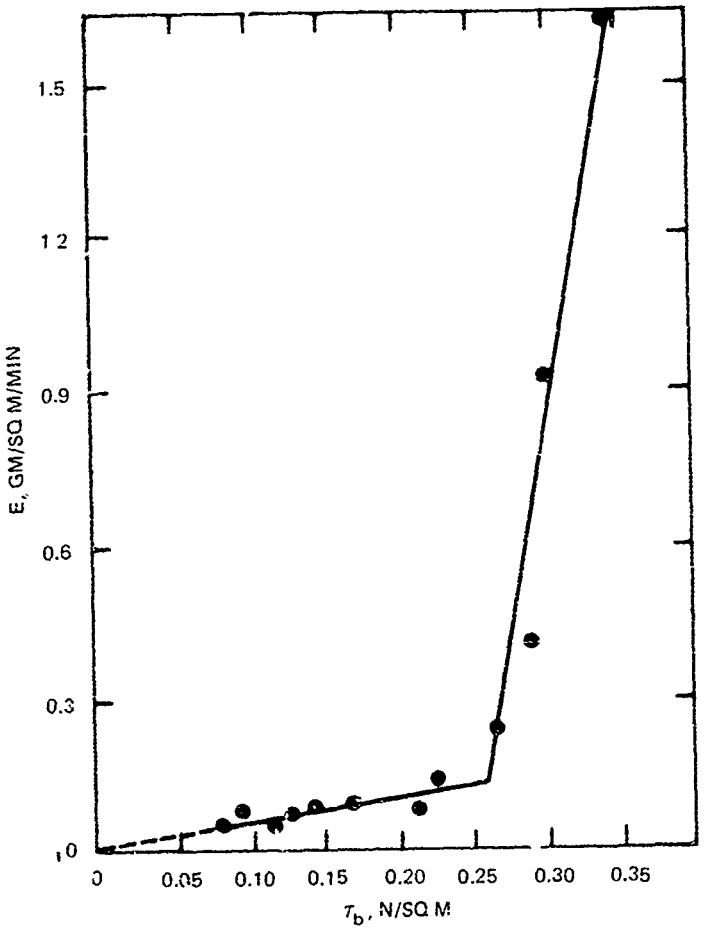

Figure 3. Typical nonlinear erosion behavior of cohesive sediment (data from Hunt 1981)

PART III: APPLICATION OF RESULTS

Descent of Material to the Bed

18. Sediment materials are initially diluted at the time of dredging, depending on the method. After disposal, materials descend based on their bulk density and initial momentum. Depending on specific sediment and disposal conditions, the dredged material can be considerably diluted before it impacts the bed and spreads horizontally to repose. The deeper the water at the disposal site and the greater the initial moisture of the disposed material, the greater the dilution attained during descent. Other factors can influence the dilution attained during the disposal operation, such as vessel speed and disposal rate. Trawle and Johnson (1986) present mathematical disposal modeling results for a companion WES study. If sufficient dilution is attained, fine sediment materials enter the ambient suspension, and their subsequent dynamic behavior is controlled by particle settling rates. A detailed analysis of the convective descent, dynamic collapse, and passive transport of dredged material disposed at the Alcatraz site is given by Trawle and Johnson (1986).

19. Krone (1962) found that the critical shear stress below which San Francisco Bay sediments deposited from suspension was 0.08 N/sq m, representing an average velocity of about 23 cm/sec. This velocity condition was observed to be exceeded about 85 percent of the time in the current data from the disposal site presented by Winzler and Kelly (1985).

20. Given an initial vertically uniform concentration C_o of sediment initially located at the center of the disposal site, an estimate of the concentration C of uniformly suspended material leaving the disposal site can be made using the expression:

$$\frac{C}{C_o} = \exp\left[-P\left(\frac{X}{U}\right)\left(\frac{W_s}{H}\right)\right] \tag{6}$$

where

P = probability of depositing once reaching the bed

X = radius of the site

W_s = settling velocity

Using a current speed U of 0.114 m/sec, which is half the critical value; a probability P of 0.5; a typical settling rate W_s of 0.5 mm/sec measured from WES characterization tests; and an average depth H of 20 m, Equation 6 estimates that about 99 percent of the suspended material would leave the disposal site.

21. Settling experiments on completely slurried sediments, performed as part of the WES characterization testing, indicated that the initial density of newly settled material was roughly 1.1 g/cu cm over a period of a couple of hours. Erosion tests indicate that material of this BWD is quickly eroded by currents typical of the disposal site.

22. Particle settling is therefore not an important factor when considering deposition of disposed material on the bed at the Alcatraz site. Turbidity clouds generated by the disposal of materials (generally which have been diluted to concentrations less than about 20 g/ℓ) either escape from the disposal site or reside at the bed only for a matter of minutes to hours until tidal currents increase.

23. Therefore, any measures increasing the fraction of disposed material which enters suspension, such as modified disposal practices, will decrease sediment retention in the site.

Erosion Rate Estimates

24. Once on the bed, material of sufficiently low density can flow or slump under the influence of gravity or stress imposed by the overlying flow. Material at higher density must be eroded to disperse from the disposal site.

25. Using the constants τ_c and M, determined from experiment, calculations can be made of E at the Alcatraz disposal site using Equation 1. The value of τ_b was estimated using Manning's equation (see Equation 5). Plots of the rates of erosion versus the depth-averaged flow velocity are given in Figures 1 (WES) and 2 (UF).

26. The calculated erosion rates and an estimated deposition rate can be compared for the site. Assuming 19,114 cu m/day are disposed at the site, and that material contains 0.6 g/cu cm or 43 percent by weight of solids (BWD ~1.39), the average deposition rate would be 0.24 g/sq cm/min, if all of the solids were deposited evenly over the disposal site. This type of disposal is often referred to as "thin layer" disposal. Erosion rates would have to

average about 0.24 g/sq cm/min, which represents the maximum erosion rate plotted in Figure 1, to balance the estimated deposition rate.

27. The surface of the disposal area has not been well characterized, but surface BWD's of roughly 1.48 g/cu cm in areas of fine sediment accumulation seem reasonable from a limited number of measurements, with higher values elsewhere. The average BWD of the Larkspur-Richmond Longwharf sediments is about 1.6 g/cu cm. Highly consolidated mud with a BWD of 1.6 g/cu cm would erode only about 2.5 cm after being subjected to a constant current speed of 1.5 m/sec for 24 hr based on the curves in Figure 2.

Erosion Capacity of the Site

28. Erosion rate expressions can be combined with current statistics to estimate the volumes of various sediments which would erode from the Alcatraz disposal site.

29. Current statistics, the average frequency of occurrence for certain speed ranges, were assembled from the data of Winzler and Kelly (1985) for the four middepth current meters deployed in the disposal site. A small portion of the data was depth averaged and compared with the middepth meter values, indicating that the latter values could be used to characterize the currents at the site. The current record covered 14-19 July 1985 at 15-min intervals.

30. The erosion capacity of the site was calculated and presented in Table 1, along with current statistics rounded to the nearest 0.1 percent. The erosion threshold and average erosion constant from the WES study and an average site depth of 20 m were used to compute erosion rates. The site diameter (610 m), the specific weight of the fines, and average current statistics were used to convert erosion rates into erosion volumes for the various current speed ranges and sediment BWD's. Sediment material was assumed to be 90 percent fines.

31. Table 1 shows that the extremely high current speeds are important to erosion of the denser material at the disposal site, even though they occur at very low frequencies. Erosion volumes decrease rapidly with increasing BWD, until little or no erosion occurs at a BWD of 1.5 g/cu cm.

32. The results presented in Table 1 are indirectly verified by the observed BWD's of the surface sediments, which are generally 1.5 g/cu cm and above. Sediment properties at the disposal site reflect the ability of the

sediments to resist erosion as much as the properties of the disposed material. Observations of surface sediment density are sparse, however. Also, the record length characterizing the current statistics is short. The record represented the time period from 14 to 19 July 1985. The highest current range frequency was based on a single observation.

33. Note that erosion capacities are directly proportional to the surface area used within the disposal site. Erosion capacity decreases in direct proportion to the underutilization of the site's area.

34. The BWD's indicated in Table 1 and Figures 1 and 2 are uniform average densities. An average BWD of 1.3 g/cu cm can consist of 40 percent (by volume) clumps of 1.6 g/cu cm and the remainder of 1.1 g/cu cm slurry, for instance. Such a material will erode differently from a completely slurried material which is uniformly 1.3 g/cu cm.

35. To estimate the site's erosion capacity for a graded distribution of sediment BWD's, apply class weight fractions to individual values from Table 1 and sum the results.

PART IV: CONCLUSIONS AND RECOMMENDATIONS

Conclusions

36. Individual fine-grained suspended sediment particles in suspension are not retained in the site, and any measures which increase the fraction of sediments immediately entering suspension subsequent to disposal will reduce sediment retention.

37. Clumps or highly consolidated sediments with BWD's greater than about 1.5 g/cu cm are very slow to erode at the disposal site. Most, if not all, of this material will be retained in the disposal site.

Recommendations

38. Disposal site management strategies should target a reduction in both the average and the maximum sediment densities or concentrations of disposed material to decrease retention of sediments in the disposal site. This might be accomplished by criteria placed on the disposed material, or by modification to disposal practices, or a combination of both. The combined effects from reducing maximum and average sediment densities could reduce or eliminate sediment retention at the Alcatraz disposal site by ensuring that

a. An appreciable amount of material will disperse immediately from the site in suspension.

b. Material which deposits at the site will be of low density.

c. Ambient currents can erode deposits faster than deposition can create them.

39. To increase the capacity of the Alcatraz disposal site, sediments disposed should be well slurried and of moderate solids content to ensure that the resulting bed deposits will be erodible by ambient currents. The entire disposal area should be continuously utilized to maximize the erodible area and to decrease burial of sediments.

40. Monitoring the distribution of disposed dredged material densities has never before been undertaken on a large scale, but it should be addressed. Long-term current records from the disposal site are needed to improve current statistics.

REFERENCES

Farmer, R. 1985. "Geotechnical Investigation, Alcatraz Disposal Site, San Francisco Bay, California," Draft Report, US Army Engineer District, San Francisco, San Francisco, Calif.

Hunt, S. D. 1981. "A Comparative Review of Laboratory Data on Frosion of Cohesive Sediment Beds," UFL/COEL/MP-81/7, Coastal and Oceancgraphic Engineering Department, University of Florida, Gainsville, Fla.

Krone, R. B. 1962. "Flume Studies of the Transport of Sediment in Estuarial Shoaling Processes," Hydraulic Engineering Laboratory and Sanitary Engineering Research Laboratory, University of California, Berkeley, Calif.

Owen, M. V. 1970. "A Detailed Study of the Settling Velocities of an Estuarine Mud," Report No. INT 78, Hydraulics Research Station, Wallingford, England.

Trawle, M. J., and Johnson, B. H. 1986 (Mar). "Alcatraz Disposal Site Investigation," Miscellaneous Paper HL-86-1, US Army Engineer Waterways Experiment Station, Vicksburg, Miss.

Vanoni, V. A. 1975. "Sedimentation Engineering," Report of Engineering Practice No. 54, American Society of Civil Engineers, New York, N. Y.

Winzler and Kelly. 1985 (Sep). "Oceanographic Investigation at the Alcatraz Disposal Site, San Francisco Bay, California," prepared by Winzler and Kelly, Consulting Engineers, San Francisco, Calif., for the US Army Engineer District, San Francisco, San Francisco, Calif.

Table 1

Alcatraz Disposal Site Erosion Capacity

Current Speed Range cm/sec	Frequency of Occurrence percent	Erosion Capacity, 1,000 cu yd* per month							
		BWD, g/cu cm							
		1.15	1.20	1.25	1.30	1.35	1.40	1.45	1.50
10-20	7.1	0	0	0	0	0	0	0	0
20-30	6.9	3,030	0	0	0	0	0	0	0
30-40	7.0	4,260	1,006	0	0	0	0	0	0
40-50	9.4	7,336	1,732	0	0	0	0	0	0
50-60	11.1	10,597	2,502	851	0	0	0	0	0
60-70	12.3	13,974	3,299	1,123	0	0	0	0	0
70-80	10.0	13,090	3,091	1,052	445	0	0	0	0
80-90	9.9	14,717	3,475	1,182	500	0	0	0	0
90-100	6.6	10,850	2,562	872	368	0	0	0	0
100-110	4.7	8,513	2,010	684	289	141	0	0	0
110-120	4.3	8,682	2,050	697	295	144	0	0	0
120-130	2.9	6,386	1,508	513	217	106	57	0	0
130-140	2.1	4,896	1,156	393	166	81	44	0	0
140-150	0.4	961	227	77	33	16	9	0	0
150-160	0.1	135	32	11	5	2	1	1	0
	Total	107,429	24,649	7,455	2,317	491	111	1	0

* 1,000 cu yd = 765 cu m.

APPENDIX A: SAN FRANCISCO BAY SEDIMENT EROSION TESTS IN THE WATERWAYS EXPERIMENT STATION FLUME

Introduction

1. Sediments from San Francisco Bay were subjected to erosion tests at the Hydraulics Laboratory, US Army Engineer Waterways Experiment Station (WES), to provide information on the erosion characteristics of disposed sediments. Direct testing was required to make good estimates of the erosion characteristics of fine-grained materials, as cohesion varies between sediments of different mineralogy, pore fluid composition, and other sediment conditions. The information is intended for evaluations of remedial measures by analytical evaluations and/or mathematical simulations of the sediment retention problem. The scope of the testing included the erosion behavior and characterization of the sediments.

Process Description

2. Because most of the material disposed at the Alcatraz disposal site is fine-grained, this study is primarily concerned with the erosion of fine-grained sediments. The hydraulic shear strength of these materials is related to their cohesive nature.

3. The process of fine-grained sediment erosion by tangential hydraulic stress in an open-channel, subcritical-flow environment has been studied by subjecting samples to erosive forces in the laboratory. Past studies have used two approaches to form test sediment beds:

a. Remold the sediment bed by pouring or trawling high-density material into a chamber, producing a relatively uniform condition.

b. Settle the sediment bed from a quiescent or slowly moving suspension, producing a vertically stratified bed in density and/or sediment properties.

Depending on bed conditions, laboratory fine-grained erosion experiments under constant flow conditions resulted in either a constant erosion rate if the bed was remolded (as in a), or an exponentially decreasing erosion rate with time if the bed was settled (as in b). The results are comparable, however, and the bed preparation is a matter of experimental convenience and of the specific application of results.

4. Previous erosion studies have found erosion rate to be proportional to the shear stress in excess of a critical value. The functional expression

known as the modified Partheniades function, given in Equation 1, paragraph 10, main text, was used as a basis for this testing. The objective of the testing was to determine the erosion rate constant* M and the critical shear stress for erosion τ_c for a range of sediment conditions.

5. A number of sediment bed conditions are known to have effects on resistance to erosion and erosion rate. A primary condition is the consolidation state of the bed as indicated by concentration parameters such as bed density, specific weight of solids, moisture content, and voids ratio. Table A1 gives the correspondence between several of these concentration parameters.

6. Two other conditions important to the erosion resistance of sediments are cohesiveness and grain size. Cohesiveness is known to increase the resistance to erosion and decrease erosion rates of sediments. Increased percentage of clay has been found to increase erosion resistance. The effect of the mixture of coarse- with fine-grained sediments has not been reported in the literature and is not known. Both of these conditions, along with bed density, were considered by this study.

Preliminary Tests and Characterizations

7. Before the test plan was developed and finalized, a number of preliminary tests and characterizations were performed. Comparisons were made between certain characterizations and values measured by the US Army Engineer District, San Francisco (SPN). Erosion test conditions were compared with field conditions using data also supplied by SPN. Limitations of experimental equipment in producing necessary flow conditions were evaluated.

8. The preliminary characterizations indicated the following results:

   a. The densities of the sediment core samples from the Alcatraz disposal site are relatively high, 1.5 to 1.75 g/cu cm, and are in agreement with SPN measurements.

   b. The liquid limits of sieved sediments were similar to one another, and only about half those of original, undisturbed values.

   c. Maximum flume currents of about 1.4 m/sec, or the associated shear stress of 2.1 N/sq m, were sufficient to erode sediments

---

* For convenience, symbols and abbreviations are listed in the Notation (Appendix C).

with moistures of greater than 120 percent (density less than 1.4 g/cu cm).

Results of liquid and plastic limits, density, and moisture content, and erodibility information from preliminary tests were used to set a framework for the main test series. Selected preliminary test data have been included in the main text.

Description of Tests

Test materials

9. WES performed erosion tests on two sediment materials. Core sections or samples designated by SPN as 93130 and 93263 from the Alcatraz disposal site were combined into one sample, designated CL. Farmer (1985)* provides the exact locations and geotechnical test results on these samples. Core sections from Redwood Harbor core sections 94974 and 97979 were combined into the other sample, designated CH-2. Samples were passed through a No. 200 sieve to remove coarse materials. Two other materials (designated CL-2 and CH) were constituted from core samples by WES, as described in the following tabulation, and used in characterization tests.

Core Sample	Test Sediment			
	CL	CL-2	CH	CH-2
1	93130	93146	93140	94974
2	93263		93162	97979

10. The sediment materials were combined with salt water from the flume to adjust density. The material was not dried at any stage of the testing. The fine-grained material appeared to contain large amounts of iron, which stained containers and even clung to magnetic stirring bars. Iron content has been found to increase the erosion resistance of fine-grained sediments in previous studies.

11. The salinity of salt water used in the flume was 32 ppt. The salt water was prepared by mixing about 250 kg of commercially available flaked sodium chloride with the water in the sump of the flume. The pH of the salt water used for the tests was 7.90, while the pH of the tap water used to make

* References cited in this Appendix are included in the References at the end of the main text.

the salt water was 7.77. The pH of the same salt water used in the consolidation tests and after settling was 7.54.

12. Sand from a Mississippi River bar south of Vicksburg, Mississippi, known as Reid Bedford, was added to the fine-grained test materials, as described in paragraph 14. The sand passed a No. 40 sieve and was retained on a No. 100 sieve.

Erosion test procedures

13. The following tests were performed:

a. Erosion threshold and rates on two sediments each for nine test conditions.

b. Settling rate on three sediments at various suspension concentrations and quiescent conditions.

c. Consolidation rate on two sediments at various high initial concentrations.

d. Atterberg (liquid and plastic) limits at various sediment conditions (sand content and sieve treatment).

e. Bulk wet density (BWD) of original and test materials.

f. Cation exchange capacity (CEC) on three test materials.

g. Sodium adsorption ratios (SAR) on three sediment pore fluids.

h. Loss on ignition on three sediments as a measure of organic content.

i. Size analysis on three undispersed sediments.

The following tabulation details how tests were applied to the four test sediments:

Test Performed	Test Sediment			
	CL	CL-2	CH	CH-2
Erosion	X			X
Settling	X	X	X	
Consolidation	X		X	
Atterberg	X		X	X
BWD	X	X	X	X
CEC	X		X	X
SAR	X		X	X
Percent loss on ignition	X		X	--
Particle size	X		X	X

14. Tests were carried out in accordance with the proposed scope of

work and the preliminary tests. Erosion tests were run on two sediments in series with three levels of moisture or BWD and three levels of added sand: 0, 15, and 40 percent. A total of 18 flume runs were made in this test matrix. A tilting flume was used for testing, and sediments were molded into small recessed chambers in the floor of the flume.

15. For each test, material was mixed to the desired consistency, tested for bulk density, and molded into the test chamber on the afternoon prior to the test day. The material in the chamber was covered with a thin layer of salt water and a dome lid to prevent drying. The tests started the following morning, allowing a setup or gelling period of about 16 hr for each test.

16. Before testing, the elevation of sediment surface was measured at 30 locations using a point gage. The accuracy of these measurements was ±0.0003 m.

17. Erosion tests were performed starting with a very gentle flow, then increasing flows in steps until the erosion thickness became appreciable or until the chamber edges became exposed. A maximum of eight steps of 1-hr duration were made until test termination. Tests lasted between 4 and 8 hr a day over a 6-week period. The flow, slope, and tailgate settings were adjusted to predetermined values within about one-half minute at the beginning of the step period.

18. After the termination of the tests, the sediment surfaces were regaged, and the remaining sediment removed.

Description of flume

19. The flume used for the erosion testing is called the temperature flume at WES because the temperature of the recirculating water and of the laboratory space the flume occupies can be controlled. Temperatures in the flume for this test were 20.6 to 21.7°C. The flume is a 24.4-m tilting channel constructed of aluminum, supported by a pivot at its center and mechanically coupled screw jacks along its length. The tilt can be adjusted within ±0.0003 m to produce uniform flow.

20. The flume is 0.92 m wide and has a maximum depth of about 0.3 m, controlled by an adjustable tailgate. Three pumps can be used to supply the head tank of the flume: a 0.14-cu m/sec centrifugal, a 0.057-cu m/sec centrifugal, or a 0.042-cu m/sec axial flow. For these tests the 0.042-cu m/sec axial flow pump was used because of the associated corrosion-resistant

plumbing available to handle salt water. The flume spills into a sump and the flow is recirculated. The volume of water in the system is about 11.33 cu m.

21. Flow in the flume was measured using a Data Industrial Series 900 flowmeter with a model 228 impeller sensor. The meter was calibrated with a V-notch weir, traceable to volumetric standards. The accuracy of the meter was 2 percent of the reading in the range used.

22. Water-surface slopes were measured with point gages located at 3, 12.2, and 21.4 m along the length of the flume. The point gages were read to ±0.0003 m, but the presence of ripples on the water surface limited accuracy to roughly ±0.0006 m. The shear stress on the flume bed was calculated from the bed and water-surface slopes, flow rates, and sidewall correction factors. Sidewall correction factors were computed using the method given by Vanoni (1975).

23. Two small chambers held sediments for erosion tests. The chambers were 0.20 m long in the direction of the flow by 0.15 m wide by 0.041 m deep, and were located 0.30 m from each wall and 22.9 m from the head of the flume. The chambers were specially constructed for these tests to accommodate the small samples available for erosion testing.

Characterization test procedures

24. Settling tests were performed by combining measured amounts of test sediments with 19.4 ℓ of natural seawater, vigorously mixing them for 5 min, introducing the suspension into a transparent 0.10-m-diam by 1.80-m-high settling column, and withdrawing samples over the following several hours. Samples were withdrawn from near the bottom of the column and analyzed for total nonfilterable solids using a standard method.

25. During most of the settling tests, it was possible to observe the thickness of the sediment deposit on the bottom of the column. As sediment settled to the bottom, the deposit thickness increased about linearly with time until the suspension concentration neared depletion. The peak deposit thickness then occurred, and subsequently thicknesses decreased. From the concentration and deposit thickness histories, average deposit densities were calculated.

26. Consolidation tests were performed by mixing test sediments with natural seawater and introducing the high-concentration (88 to 323 g/ℓ) suspensions into transparent cylinders. Cylinders were about 0.37 m high and had diameters of 0.060 m and 0.079 m, the latter used for higher test

concentrations. At these high concentrations, suspensions behaved as a mass and slowly collapsed. A sharp interface formed between the sediment and clear overlying layer. The initial rate of descent of the interface is equal to the hindered settling velocity W_h of the initial concentration C_o.

27. Atterberg limits were determined to characterize sediments. The test device was manufactured by Soiltest, Inc. (model CL-204). Standard methods were used, and modified only to accomplish specific testing variations such as sample sieving or sand addition.

28. BWD's were determined using 25-cu-cm widemouth pycnometers. The accuracy of these determinations was better than ±0.005 g/cu cm.

29. CEC and SAR are measures of the cohesiveness of the material and the ion balance of the pore fluid, respectively. A standard method was used to determine CEC which employed ammonium acetate extraction. Isopropyl alcohol was used to rinse dried sediments. SAR is derived from the amount of sodium (Na), calcium (Ca), and magnesium (Mg) in the pore water of the test material as shown in the following equation:

$$SAR = \frac{|Na|}{\left(\frac{1}{2}|Ca| + \frac{1}{2}|Mg|\right)^{1/2}}$$

30. Loss on ignition determination was used to characterize sediments for organic content. A standard method was used to measure the weight loss of dried samples after heating at 550°C for 1 hr. Several replicates of each sample were run.

31. Size analyses were performed to characterize test sediments. A 128-channel electronic particle counter (Particle Data model 80 X-Y) was used. A very small subsample of material was diluted in particle-free, 2 percent sodium chloride and analyzed immediately in an undispersed state. This method measures aggregate particle size distribution, representative of the dynamic behavior of sediments, rather than the dispersed, elemental particle size distribution used for geotechnical classification. The range of this analysis was from about 4 to 75 μm.

Data Analysis

Erosion tests

32. Raw data from the erosion tests consisted of the shear stress at the termination flow, the concentration of the test sediment, the volume eroded during the termination flow step, and the time over which the erosion took place. The τ_c for the sediments was between the shear stresses of the termination step and the previous step. Therefore to estimate the two unknown parameters τ_c and M, the following procedure was used:

a. The maximum excess shear stress was calculated as $\tau_i - \tau_{i-1}$ where τ_i is the bed shear stress at the termination step i and $i-1$ refers to the previous step.

b. An average M was calculated for both sediments by dividing the average erosion rate E by half the average maximum shear stress.

c. The average values of M for each sediment were then used in Equation 1, paragraph 10, main text, to estimate τ_c.

With this method, computed critical shear stresses were below the shear stress at the termination step. This difference depended on the ratio between the observed E for the test and the average M for all tests. If the value of E was high, the critical shear stress was well below the termination step, and if E was low, it was nearly the same as the termination step.

33. Another method of data analysis was employed which attempted to fit M and a constant and exponent of a τ_c function simultaneously by iterative nonlinear regression techniques. While the residuals were small, the resulting values of M were physically meaningless (negative), and results were not used.

Settling tests

34. Raw data from the settling tests consisted of total suspended solids at sampling times. A second-order polynomial regression equation was fit to the data by the least squares method. Coefficients from the regression equation were then used to calculate the settling velocity distributions by the pipette method.

35. Tests with values of C_o greater than about 1 g/ℓ exhibited interference among particles which made settling velocities almost uniform. For these tests, a method described by Owen (1970) of visually following the descent of the strong concentration gradient was also used to estimate median settling velocities.

36. The densities of deposited sediments were calculated from observed deposit thicknesses and mass of material settled from suspension. Average densities were determined at the peak thickness time and at an intermediate time.

Validity of tests

37. It is difficult to assess the validity of the erosion tests. No standard methods exist for erosion testing. No practical way exists to reproduce all aspects of prototype flow conditions in the laboratory. The flume must be considered as a physical model of the prototype and compromises must be made. Erosion rates were determined under known hydraulic shear stresses in the flume which reproduced the most important prototype hydraulic condition. However, the Reynolds numbers in the flume were much smaller than in the prototype.

38. Test sediments were representative of prototype sediment grain size and CEC, the main contributors to interparticle cohesion. Some other contributors to cohesiveness may have been altered in the flume. Organics within the test sediment matrix were disturbed and/or removed. Ion composition within the test sediment matrix and the flow had different SAR's from the prototype. The minimal amount of sediment transport in suspension could have affected results.

Results

39. A summary of the application of erosion and characterization tests to the four sediments is given in paragraph 13, this Appendix.

40. Erosion tests left sediments with a rough or jagged appearance, an unexpected result for sediments with such low BWD's and soupy consistencies. Erosion was often not uniform during flow steps, nor uniform across the surface of the sediment. Erosion rates were therefore spatial and temporal averages.

41. Table A2 gives test conditions for the main erosion test matrix. Figures A1 and A2 present values of τ_c plotted for each of the two test sediments and three concentrations of sand.

42. The average erosion rate constant M for the CL material was 0.0004 g/sq cm/sec, while the value of M for CH-2 was 0.0013 g/sq cm/sec. The average value of M for all tests was 0.0008 g/sq cm/sec.

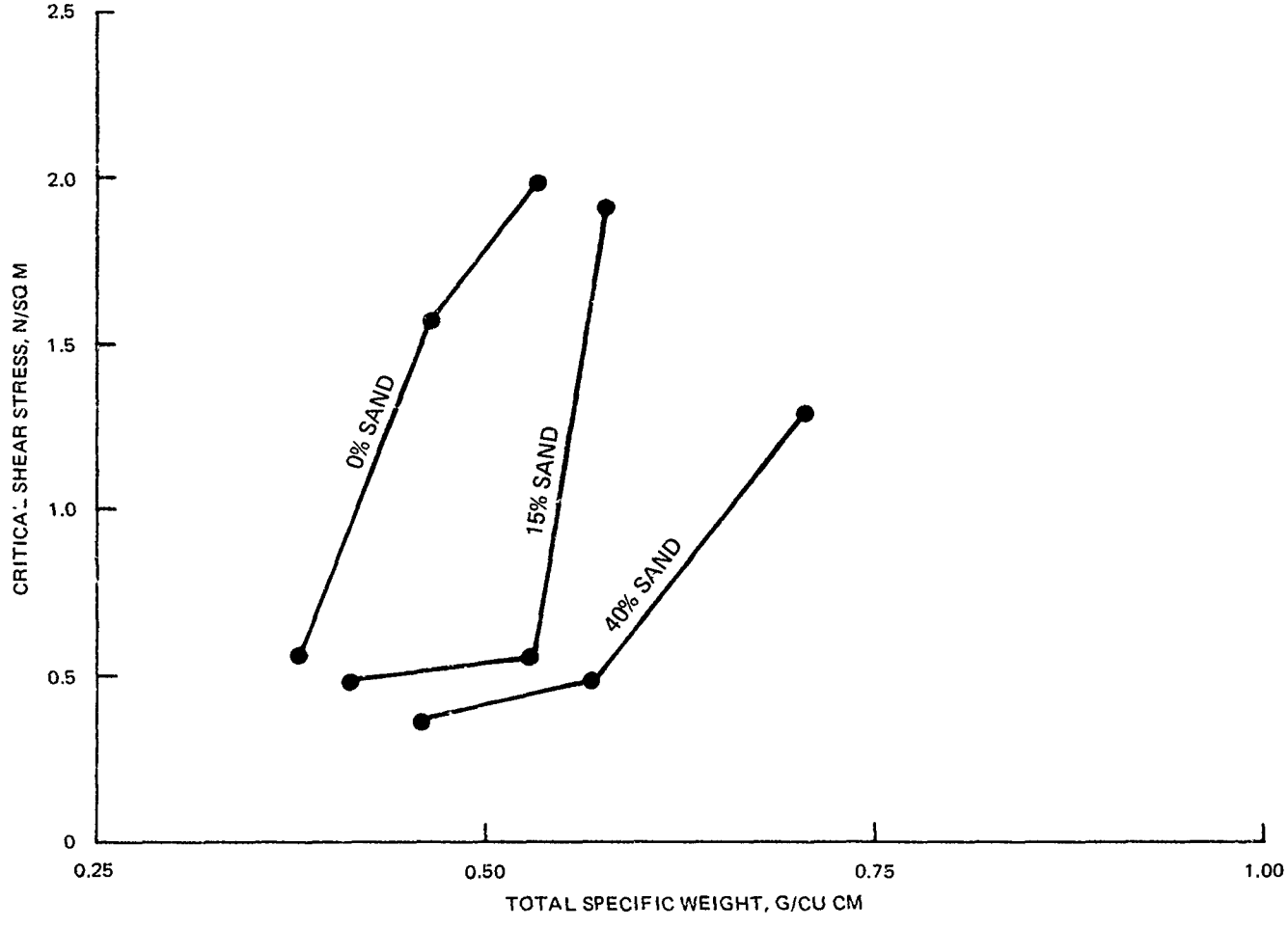

Figure A1. τ_c for sediment CL

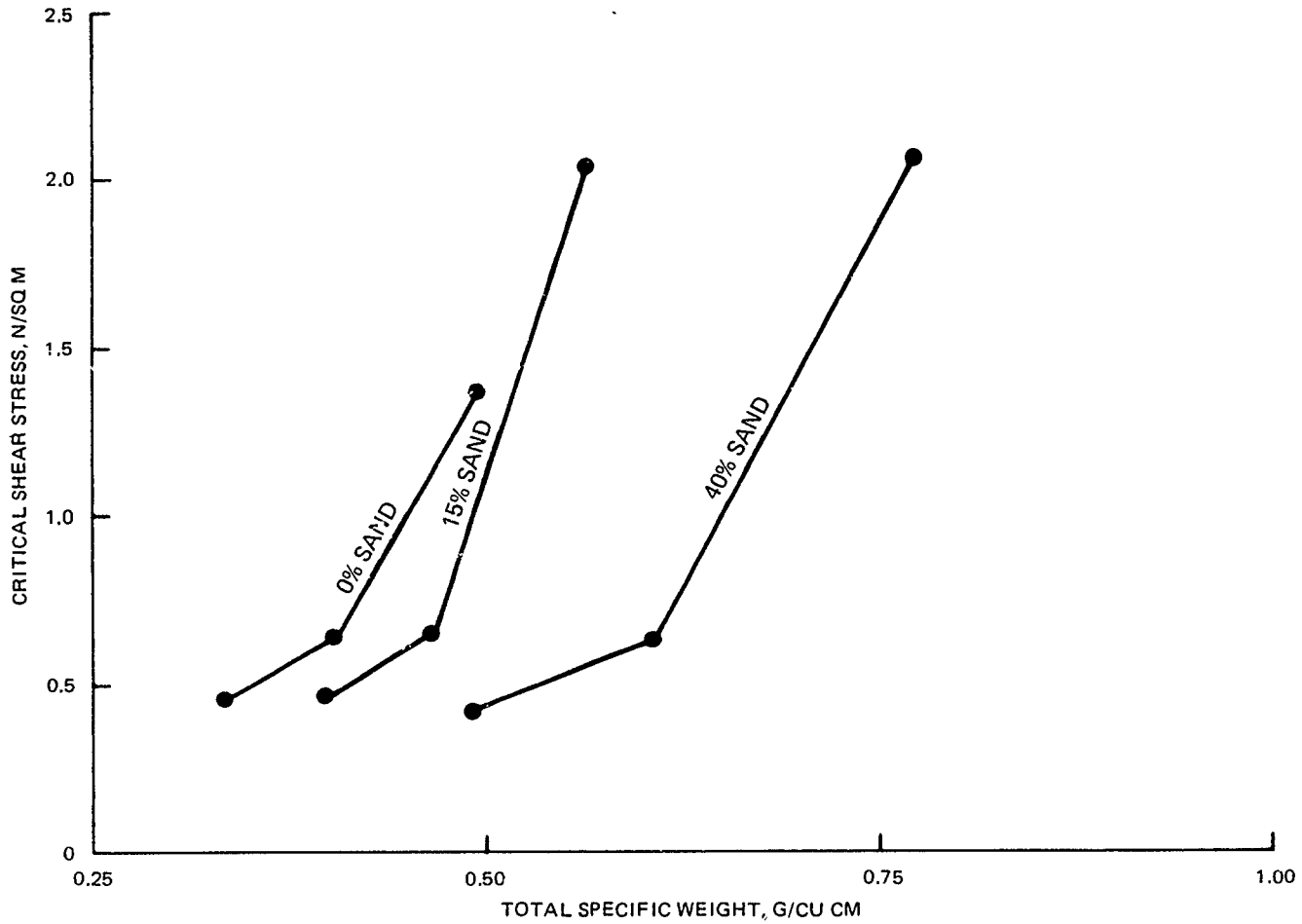

Figure A2. τ_c for sediment CH-2

43. Table A3 shows settling velocity distributions for three test sediments at various concentrations. The following tabulation presents the median settling velocity estimates made using Owen's method (Owen 1970) and the average densities of newly deposited sediments made during the settling tests:

Sediment	Initial Concentration of Suspension g/ℓ	Median Settling Velocity by Owen's Method mm/sec	Average Concentration of Deposit g/ℓ
CL	0.93	0.69	113
	3.33	0.55	78
	5.31	0.46	70
CL-2	0.94	-	117
	2.77	0.56	83
	4.91	0.43	84
CH	0.89	-	83
	3.27	0.50	79
	5.07	0.45	69

44. The following Atterberg test results compare WES and SPN values for the same core (but not the same sample):

	Core Sample	
	93156	93162
WES	77	90
SPN	84	93

Note: Core sample 93162 tested at 42 liquid limit after being passed through a No. 40 sieve.

The effects of the addition of sand to erosion test materials are shown in the following tabulation:

Percent Sand	Test	Sample CL	Sample CH-2
0	Liquid limit	44	41
	Plastic limit	34	31
40	Liquid limit	30	29
	Plastic limit	30	18

CEC and SAR values for test materials are as follows:

Sediment	CEC meq/100 g	SAR
CL	53.3	3.35
CH	71.9	0.61
CH-2	60.7	0.51

45. Plates A1-A3 show plots of the undispersed particle size, with mean, median, and modes of the distributions for three test sediments.

46. Plates A4-A15 show plots of consolidation test data, least-squares line fits to the beginning of interface descent curves, and values of W_h for the two test sediments over a range of C_o values.

Discussion of Results

47. Erosion tests showed a strong relationship between τ_c and density or specific weight of the sediment material. Sediment CL had higher values of τ_c and lower values of M than did CH-2 for the same bulk density, indicating a higher resistance to erosion (Figure A3).

48. The CL sediment had a lower CEC than the CH-2 and a much higher SAR value. Higher CEC's are normally associated with increased erosion resistance. Increases in SAR have been found in other studies to cause decreases in erosion resistance (Hunt 1981). It is not known what caused the SAR of the pore fluid of CH-2 sediment to be low, possibly some soluble material in that sediment. Both sediments were mixed with the same saltwater stock. The CL sediment was somewhat finer than the CH-2 sediment, and increased clay fractions are generally associated with increased resistance to erosion.

49. Apparently, among the factors of grain size, CEC, and SAR for these tests, the dominant factor in determining the erosion resistance of the material was the grain size.

50. The fine fraction of the solids concentration of the materials was correlated with τ_c. Figures A4 and A5 show plots of τ_c plotted against the specific weight of the fines γ_f in grams per cubic centimetre for the CL and CH-2 sediments, respectively. This again points to the importance of the fine fraction to the erosion resistance of the material.

51. A power law function was fit to the combined results, yielding an exponent of 3.29 and a constant of 17.62 (Figure A6):

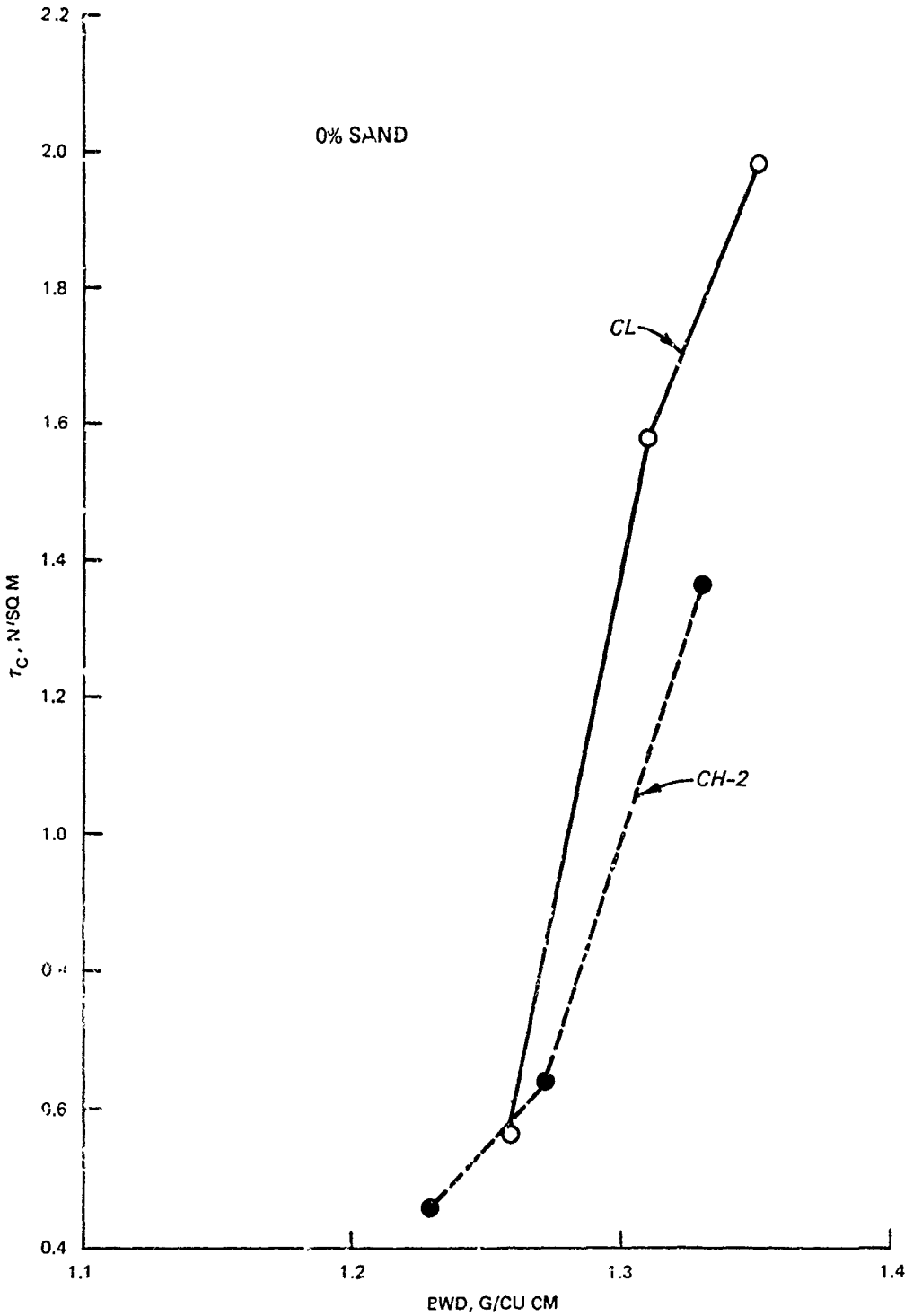

Figure A3. τ_c for 0 percent sand

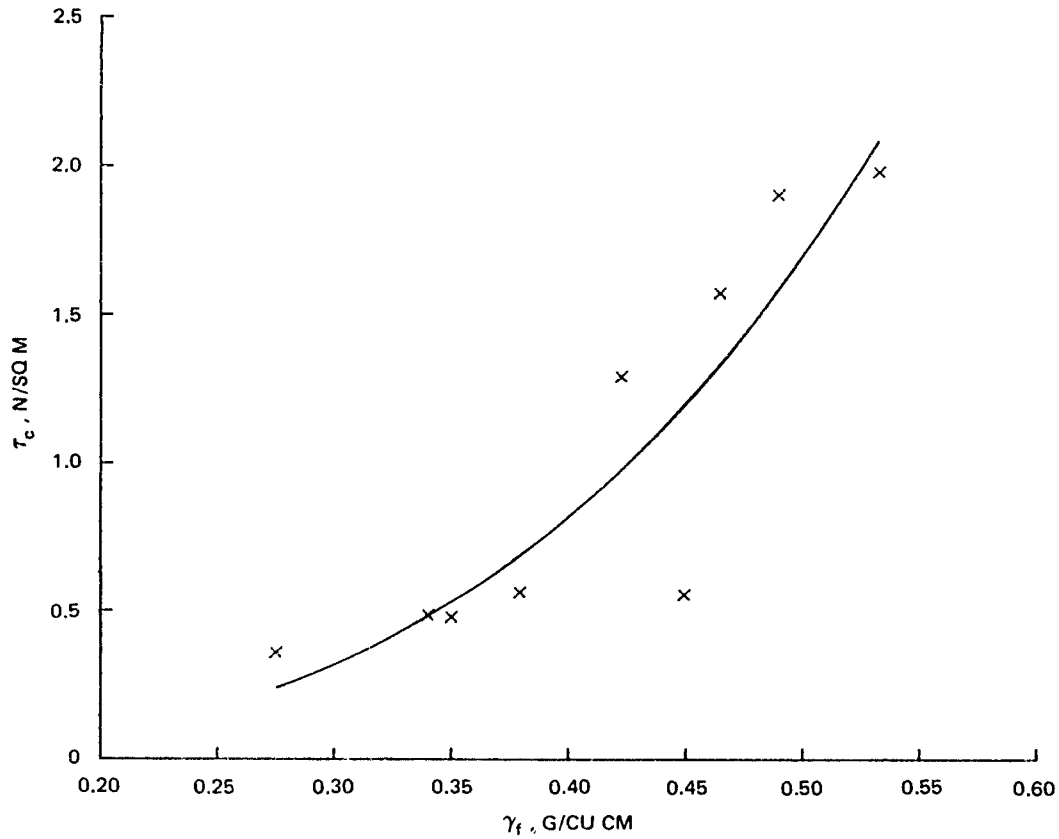

Figure A4. τ_c versus γ_f for sediment CL

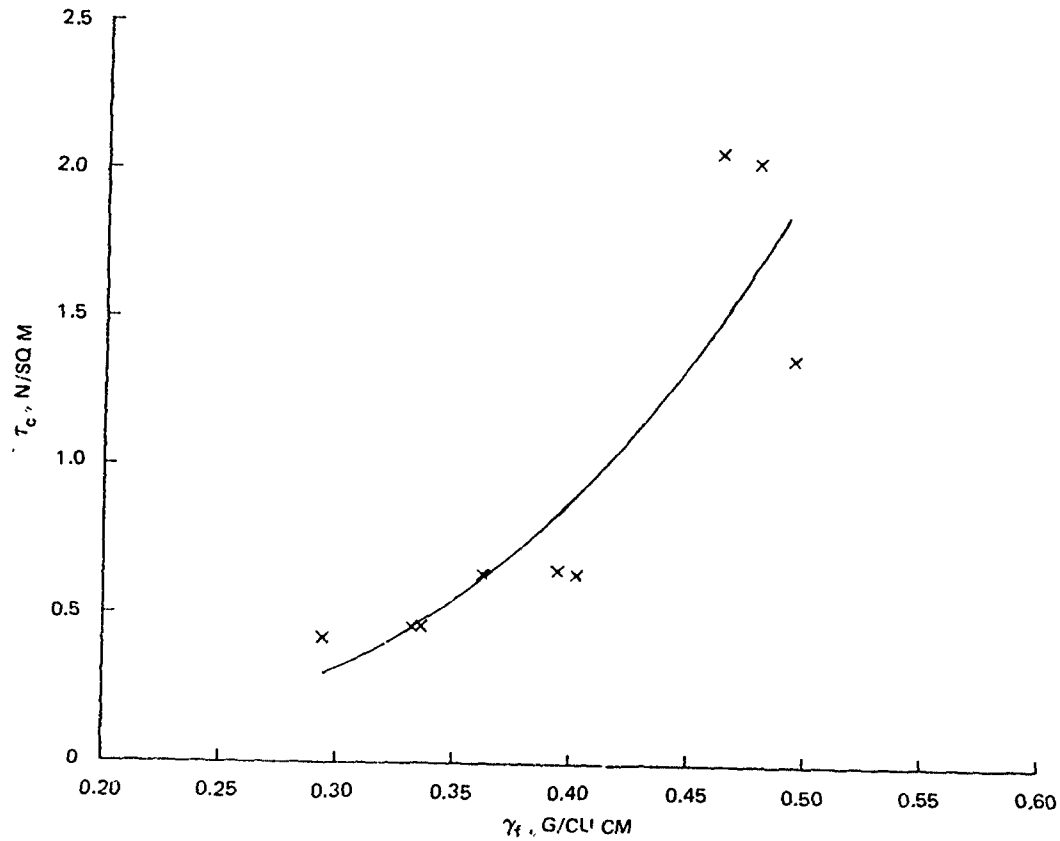

Figure A5. τ_c versus γ_f for sediment CH-2

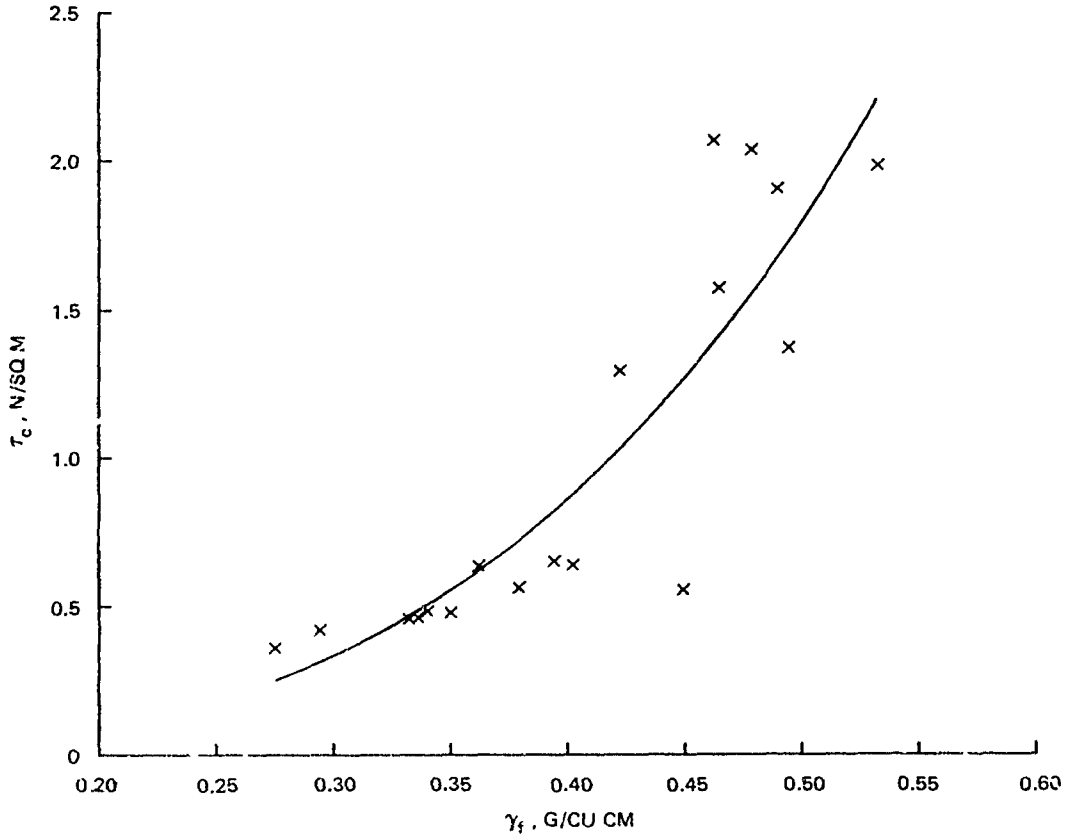

Figure A6. τ_c versus γ_f for both sediments

$$\tau_c = 17.67\gamma_f^{3.29}$$

52. Settling rates were higher than for most other fine-grained sediments from other areas tested previously by WES. Settling velocities were fairly uniform for the concentration range tested. Owen's method (Owen 1970) yielded results which were generally lower by about 15 percent than results from the pipette method.

53. Figures A7-A9 are plots of combined settling and consolidation test results. The onset of hindered settling occurred at 1- to 2-g/ℓ concentration for the CL-2 sediment. Although it could not be determined from the other tests, the onset appeared to be similar. The onset of layer formation (shown on log plots of Figures A7 and A9) was interpreted as occurring at about 20 g/ℓ for both sediments. Values of W_h were relatively high (about 0.01 mm/sec) for newly deposited sediments (70 to 120 g/ℓ), and decreased rapidly above about 150 g/ℓ.

Conclusions

54. Information on the erosion characteristics of San Francisco Bay muds was developed from flume tests. Characterization tests on the material were used to explain differences in experimental results, to relate results to previous studies, and to provide supplemental data for transport calculations.

55. Erosion test results can be combined with information of the flow regime at the disposal site and characteristics of the deposited materials to make estimates of erosion rates. Results can also be incorporated into numerical simulations, such as those using the US Army Engineers TABS numerical flow and sediment modeling system.

56. Characterization results for settling and consolidation can be used to improve disposal modeling and/or numerical sediment modeling of the disposal site.

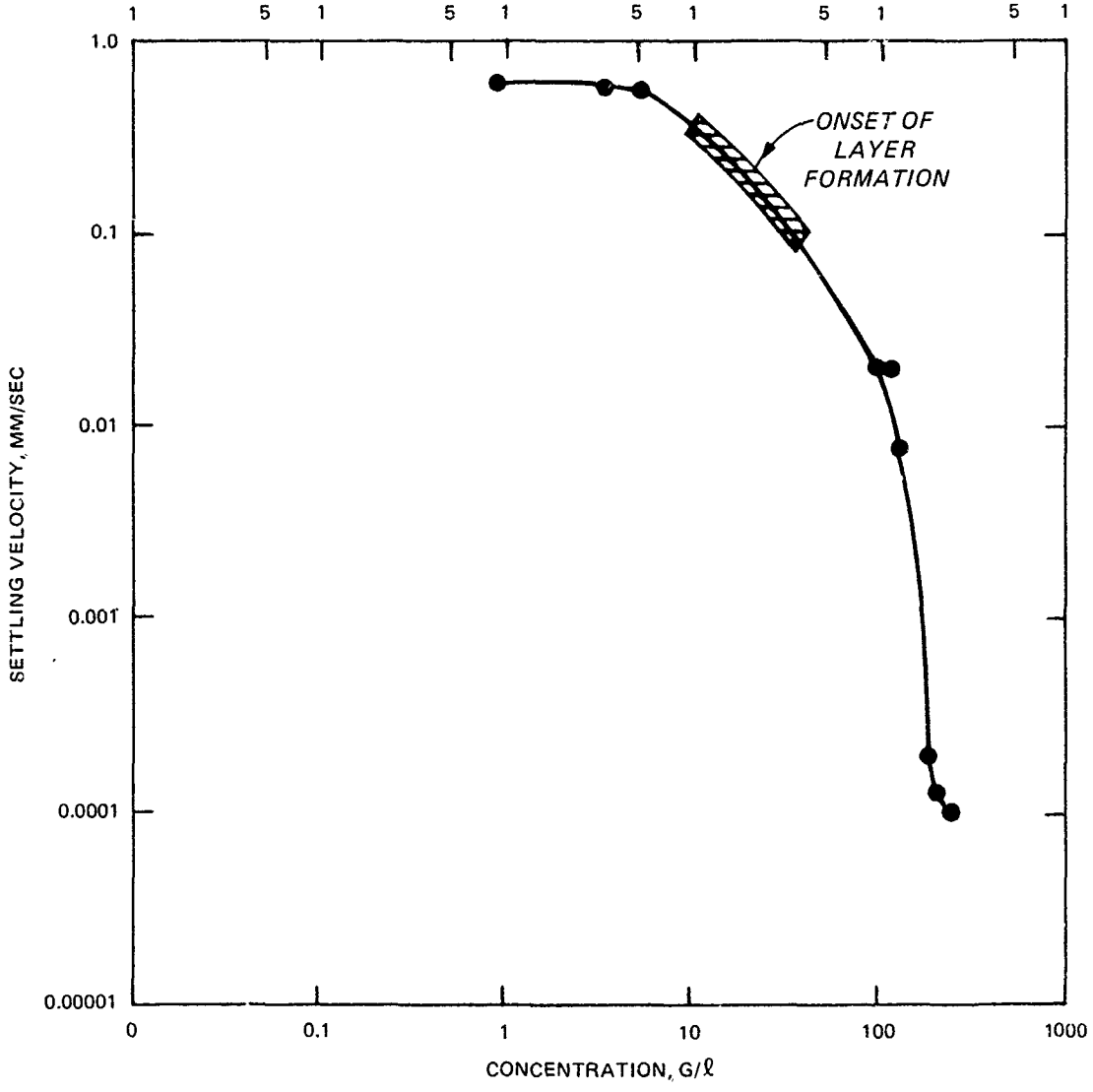

Figure A7. Settling rates for sediment CL

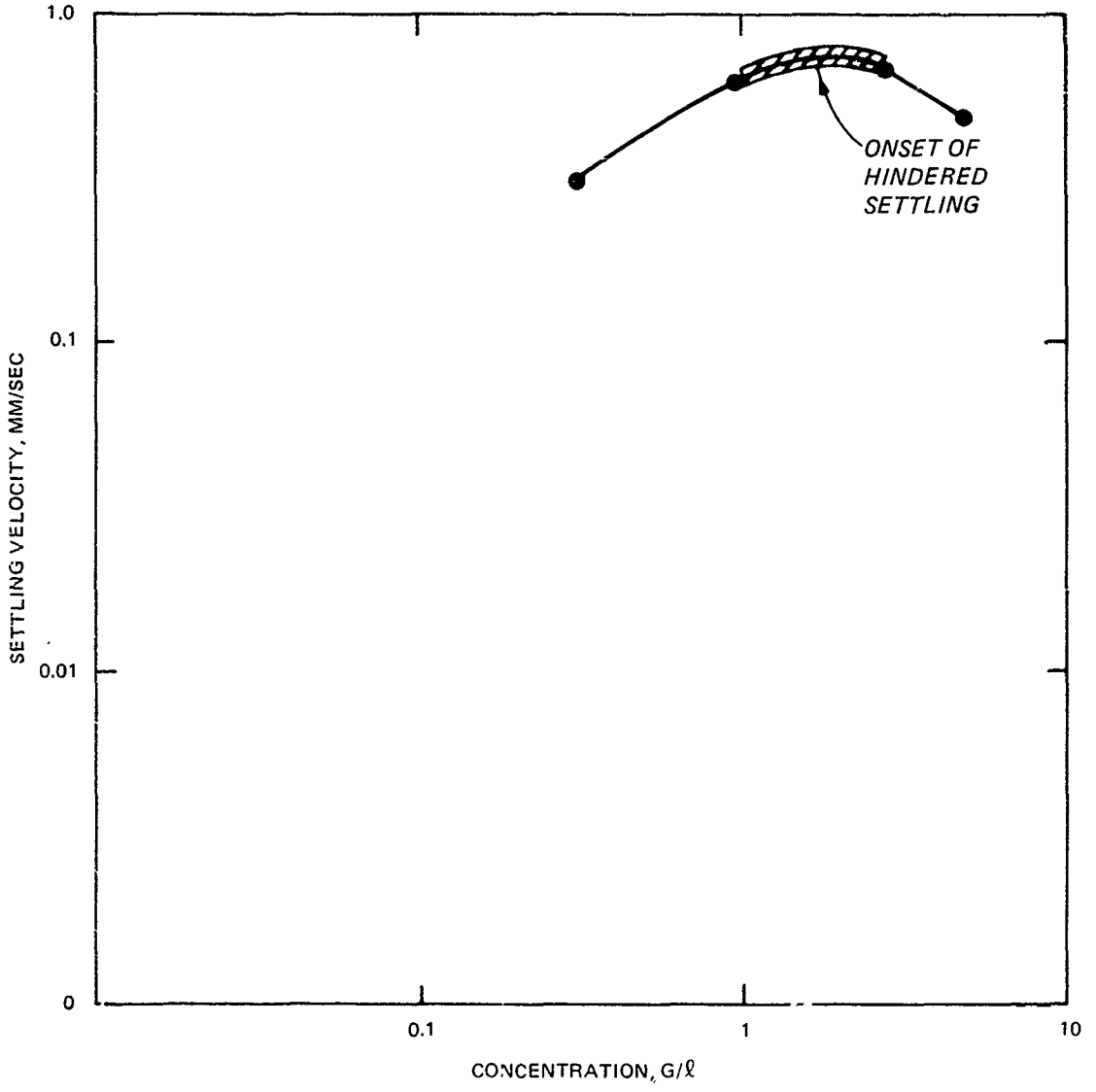

Figure A8. Settling rates for sediment CL-2

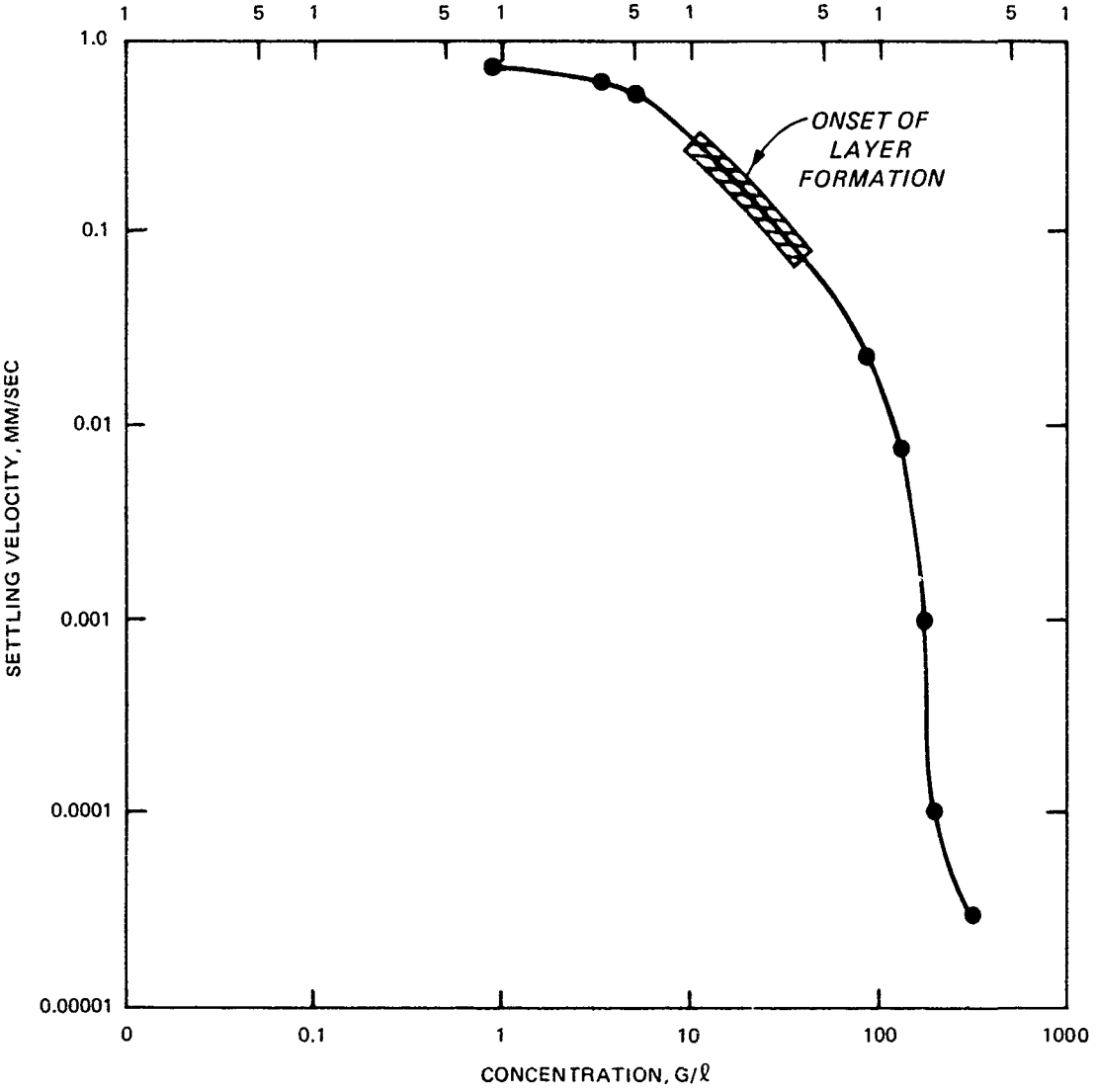

Figure A9. Settling rates for sediment CH

Table A1

Concentration Parameters

Specific Weight or Concentration g/ℓ	Moisture percent	Concentration by Volume	Concentration by Weight	BWD g/cu cm	Voids ratio
25	4,061	0.009	0.024	1.040	0.991
50	2,011	0.019	0.047	1.056	0.981
75	1,328	0.028	0.070	1.071	0.972
100	986	0.038	0.092	1.086	0.962
125	781	0.047	0.113	1.102	0.952
150	645	0.057	0.134	1.117	0.941
175	547	0.066	0.155	1.132	0.931
200	474	0.075	0.174	1.148	0.920
225	417	0.085	0.193	1.163	0.909
250	371	0.094	0.212	1.178	0.898
275	334	0.104	0.230	1.194	0.887
300	303	0.113	0.248	1.209	0.875
325	277	0.123	0.265	1.224	0.864
350	254	0.132	0.282	1.240	0.852
375	235	0.142	0.299	1.255	0.839
400	218	0.151	0.315	1.270	0.827
425	202	0.160	0.331	1.286	0.814
450	189	0.170	0.346	1.301	0.800
475	177	0.179	0.361	1.316	0.787
500	166	0.189	0.375	1.332	0.773
525	157	0.198	0.390	1.347	0.759
550	148	0.208	0.404	1.362	0.744
575	140	0.217	0.417	1.378	0.730
600	132	0.226	0.431	1.393	0.714
625	125	0.236	0.444	1.408	0.699
650	119	0.245	0.457	1.424	0.683
675	113	0.255	0.469	1.439	0.667
700	108	0.264	0.481	1.454	0.650
725	103	0.274	0.493	1.470	0.633
750	98	0.283	0.505	1.485	0.615
775	94	0.292	0.517	1.500	0.597
800	89	0.302	0.528	1.516	0.578

(Continued)

Note: Values are given for a liquid density of 1.025 and a solids density of 2.650 g/cu cm.

Table A1 (Concluded)

Specific Weight or Concentration g/ℓ	Moisture percent	Concentration by Volume	Concentration by Weight	BWD g/cu cm	Voids ratio
825	86	0.311	0.539	1.531	0.559
850	82	0.321	0.550	1.546	0.539
875	78	0.330	0.560	1.562	0.519
900	75	0.340	0.571	1.577	0.498
925	72	0.349	0.581	1.592	0.477
950	69	0.358	0.591	1.608	0.455
975	66	0.368	0.601	1.623	0.432
1,000	64	0.377	0.610	1.638	0.409
1,025	61	0.387	0.620	1.654	0.385
1,050	59	0.396	0.629	1.669	0.360
1,075	57	0.406	0.638	1.684	0.334
1,100	55	0.415	0.647	1.700	0.308
1,125	52	0.425	0.656	1.715	0.280
1,150	50	0.434	0.665	1.730	0.252
1,175	49	0.443	0.673	1.746	0.223
1,200	47	0.453	0.681	1.761	0.193

Table A2

Erosion Results for Test Matrix

Sediment/ Percent Sand	Specific Weight Total g/cu cm	Specific Weight Fines g/cu cm	Terminal Bed Shear Stress N/sq m	Maximum Excess Shear Stress* N/sq m	Erosion Time sec	Erosion Rate Total g/sq cm/sec	τ_c** N/sq m
CL/0	0.533	0.533	2.13	0.32	3,600	2.94E-5	1.98
	0.465	0.465	1.62	1.38	3,600	1.16E-5	1.57
	0.380	0.380	0.68	0.33	1,200	3.11E-5	0.56
CL/15	0.577	0.490	2.13	0.32	1,800	4.69E-5	1.90
	0.530	0.450	0.68	0.33	3,600	8.8E-5	0.56
	0.413	0.351	0.68	0.33	1,200	1.65E-4	0.48
CL/40	0.705	0.423	1.62	1.38	1,800	1.00E-4	1.29
	0.569	0.341	0.68	0.33	900	1.58E-4	0.49
	0.460	0.276	0.68	0.33	600	3.51E-4	0.36
CH-2/0	0.495	0.495	1.62	1.38	300	2.37E-4	1.37
	0.403	0.403	0.68	0.33	1,200	8.09E-5	0.64
	0.333	0.333	0.68	0.33	300	6.23E-4	0.46
CH-2/15	0.564	0.479	2.13	0.32	2,400	6.09E-5	2.03
	0.465	0.395	0.68	0.33	3,600	5.24E-5	0.65
	0.397	0.337	0.68	0.33	300	6.09E-4	0.46
CH-2/40	0.771	0.463	2.13	0.32	2,700	4.00E-5	2.06
	0.605	0.363	0.68	0.33	2,820	8.51E-5	0.64
	0.491	0.295	0.68	0.33	300	7.99E-4	0.42

* $\tau_i - \tau_{i-1}$ (See paragraph 32 of this Appendix.)

** Based on average erosion rate constant for each sediment, M = 3.96E-4 g/sq cm/min for CL and 1.30E-3 g/sq cm/min for CH-2.

Table A3

Set\ . ng Velocity Distributions

Salinity ppt	Initial Concentration mg/ℓ	Average Settling Velocity mm/sec	Geometric Mean Settling Velocity mm/sec	Standard Deviation	Skewness	Kortosis	Cumulative: Percent Greater than Settling Velocity	Cumulative: Settling Velocity mm/sec	Differential: Settling Velocity Range mm/sec	Differential: Concentration mg/ℓ
					Alcatraz CL					
32.0	927	0.825	0.610	1.5	0.00	0.32	10	1.013E+00	1.9683-0.6561	410.4
							20	8.925E-01	0.6561-0.2187	516.6
							30	7.862E-01	0.2187-0.0729	0.0
							40	6.926E-01	0.0729-0.0243	0.0
							50	6.102E-01	0.0243-0.0081	0.0
							60	5.375E-01	0.0081-0.0027	0.0
							70	4.735E-01	0.0027-0.0009	0.0
							80	4.171E-01	0.0009-0.0003	0.0
							90	3.675E-01	Total	927.0
32.0	3,330	0.437	0.604	1.4	0.17	0.41	10	9.642E-01	1.9683-0.6561	1,218.0
							20	8.144E-01	0.6561-0.2187	2,112.1
							30	7.102E-01	0.2187-0.0729	0.0
							40	6.311E-01	0.0729-0.0243	0.0
							50	5.679E-01	0.0243-0.0081	0.0
							60	5.158E-01	0.0081-0.0027	0.0
							70	4.719E-01	0.0027-0.0009	0.0
							80	4.342E-01	0.0009-0.0003	0.0
							90	4.014E-01	Total	3,330.1
32.0	5,310	0.680	0.581	1.3	0.16	0.39	10	7.894E-01	1.9683-0.6561	1,448.4
							20	7.098E-01	0.6561-0.2187	3,783.0
							30	6.493E-01	0.2187-0.0729	0.0
							40	6.005E-01	0.0729-0.0243	0.0
							50	5.597E-01	0.0243-0.0081	0.0
							60	5.246E-01	0.0081-0.0027	0.0
							70	4.940E-01	0.0027-0.0009	0.0
							80	4.669E-01	0.0009-0.0003	0.0
							90	4.427E-01	Total	5,231.4

(Continued)

Table A3 (Continued)

Salinity ppt	Initial Concentration mg/ℓ	Average Settling Velocity mm/sec	Geometric Mean Settling Velocity mm/sec	Standard Deviation	Skewness	Kortosis	Cumulative: Percent Greater than Settling Velocity	Cumulative: Settling Velocity mm/sec	Differential: Settling Velocity Range mm/sec	Differential: Concentration mg/ℓ
					Alcatraz CL-2					
31.3	303	0.304	0.352	2.4	0.13	0.37	10	1.060E+00	1.9683-0.6561	71.8
							20	7.403E-01	0.6561-0.2187	125.7
							30	5.405E-01	0.2187-0.0729	105.4
							40	4.071E-01	0.0729-0.0243	0.0
							50	3.139E-01	0.0243-0.0081	0.0
							60	2.465E-01	0.0081-0.0027	0.0
							70	1.965E-01	0.0027-0.0009	0.0
							80	1.586E-01	0.0009-0.0003	0.0
							90	1.294E-01	Total	302.9
31.2	940	0.840	0.560	1.6	0.21	0.54	10	9.200E-01	1.9683-0.6561	416.4
							20	8.406-01	0.6561-0.2187	487.8
							30	7.634E-01	0.2187-0.0729	0.0
							40	6.880E-01	0.0729-0.0243	0.0
							50	6.141E-01	0.0243-0.0081	0.0
							60	5.410E-01	0.0081-0.0027	0.0
							70	4.676E-01	0.0027-0.0009	0.0
							80	3.917E-01	0.0009-0.0003	0.0
							90	3.059E-01	Total	904.2
33.1	2,770	0.892	0.732	1.7	0.15	0.39	10	1.434E+00	1.9683-0.6561	1,439.1
							20	1.137E+00	0.6561-0.2187	1,330.9
							30	9.355E-01	0.2187-0.0729	0.0
							40	7.882E-01	0.0729-0.0243	0.0
							50	6.752E-01	0.0243-0.0081	0.0
							60	5.857E-01	0.0081-0.0027	0.0
							70	5.132E-01	0.0027-0.0009	0.0
							80	4.532E-01	0.0009-0.0003	0.0
							90	4.030E-01	Total	2,770.0

(Continued)

Table A3 (Continued)

Salinity ppt	Initial Concentration mg/ℓ	Average Settling Velocity mm/sec	Geometric Mean Settling Velocity mm/sec	Standard Deviation	Skewness	Kortosis	Cumulative: Percent Greater than Settling Velocity	Cumulative: Settling Velocity mm/sec	Differential: Settling Velocity Range mm/sec	Differential: Concentration mg/ℓ
					Alcatraz CL-2 (Continued)					
33.1	4,910	0.587	0.506	1.3	0.16	0.40	10	7.428E-01	1.9683-0.6561	823.2
							20	6.481E-01	0.6561-0.2187	3,977.1
							30	5.795E-01	0.2187-0.0729	0.0
							40	5.259E-01	0.0729-0.0243	0.0
							50	4.821E-01	0.0243-0.0081	0.0
							60	4.452E-01	0.0081-0.0027	0.0
							70	4.136E-01	0.0027-0.0009	0.0
							80	3.860E-01	0.0009-0.0003	0.0
							90	3.617E-01	Total	4,800.3
					Alcatraz CH					
25.1	887	0.437	0.716	1.8	0.06	0.33	10	1.496E+00	1.9683-0.6561	470.0
							20	1.219E+00	0.6561-0.2187	417.0
							30	1.002E+00	0.2187-0.0729	0.0
							40	8.301E-01	0.0729-0.0243	0.0
							50	6.919E-01	0.0243-0.0081	0.0
							60	5.802E-01	0.0081-0.0027	0.0
							70	4.891E-01	0.0027-0.0009	0.0
							80	4.144E-01	0.0009-0.0003	0.0
							90	3.526E-01	Total	887.0
30.7	3,270	0.782	0.591	1.4	0.02	0.32	10	8.551E-01	1.9683-0.6561	1,289.3
							20	7.823E-01	0.6561-0.2187	1,980.7
							30	7.149E-01	0.2187-0.0729	0.0
							40	6.527E-01	0.0729-0.0243	0.0
							50	5.952E-01	0.0243-0.0081	0.0
							60	5.422E-01	0.0081-0.0027	0.0
							70	4.933E-01	0.0027-0.0009	0.0
							80	4.488E-01	0.0009-0.0003	0.0
							90	4.069E-01	Total	3,270.0

(Continued)

Table A3 (Concluded)

Salinity ppt	Initial Concentration mg/ℓ	Average Settling Velocity mm/sec	Geometric Mean Settling Velocity mm/sec	Standard Deviation	Skewness	Kortosis	Cumulative: Percent Greater than Settling Velocity	Cumulative: Settling Velocity mm/sec	Differential: Settling Velocity Range mm/sec	Differential: Concentration mg/ℓ
				Alcatraz CH (Continued)						
30.7	5,070	0.621	0.535	1.3	0.14	0.38	10	7.397E-01	1.9683-0.6561	1,066.1
							20	6.629E-01	0.6561-0.2187	4,003.9
							30	6.036E-01	0.2187-0.0729	0.0
							40	5.554E-01	0.0729-0.0243	0.0
							50	5.150E-01	0.0243-0.0081	0.0
							60	4.803E-01	0.0081-0.0027	0.0
							70	4.501E-01	0.0027-0.0009	0.0
							80	4.234E-01	0.0009-0.0003	0.0
							90	3.995E-01	Total	5,070.0

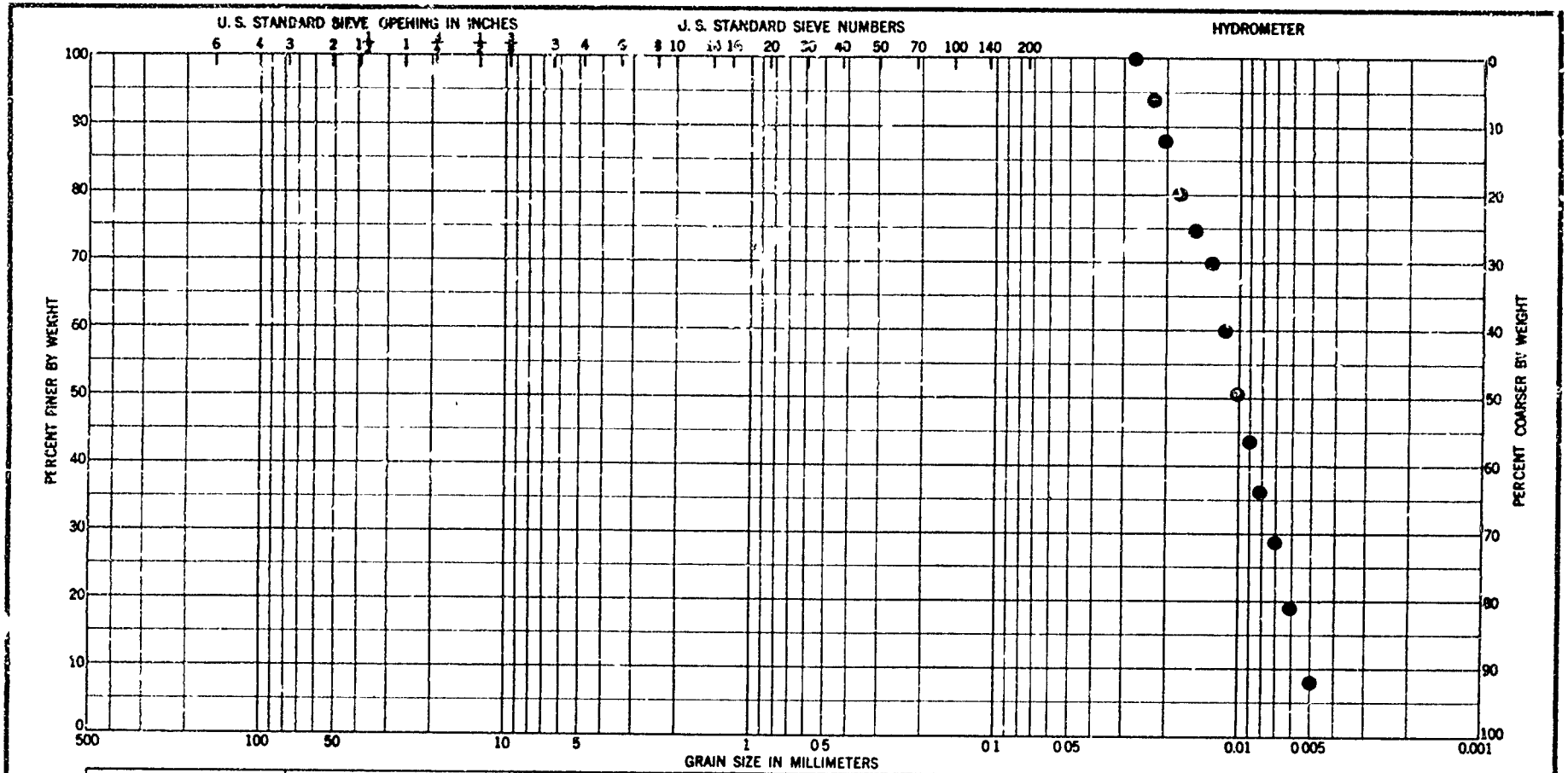

Sample No.	Elev or Depth	Classification	Nat w %	LL	PL	PI
CL		Mean 10.53 μm				
		Median 10.06 μm				
		Mode 25.5 μm				

GRADATION CURVES

Project: UNDISPERSED PARTICLE SIZE

Area: CL SEDIMENT SAMPLE

Boring No

Date

PLATE A1

ENG FORM 1 MAY 63 2087

PLATE A2

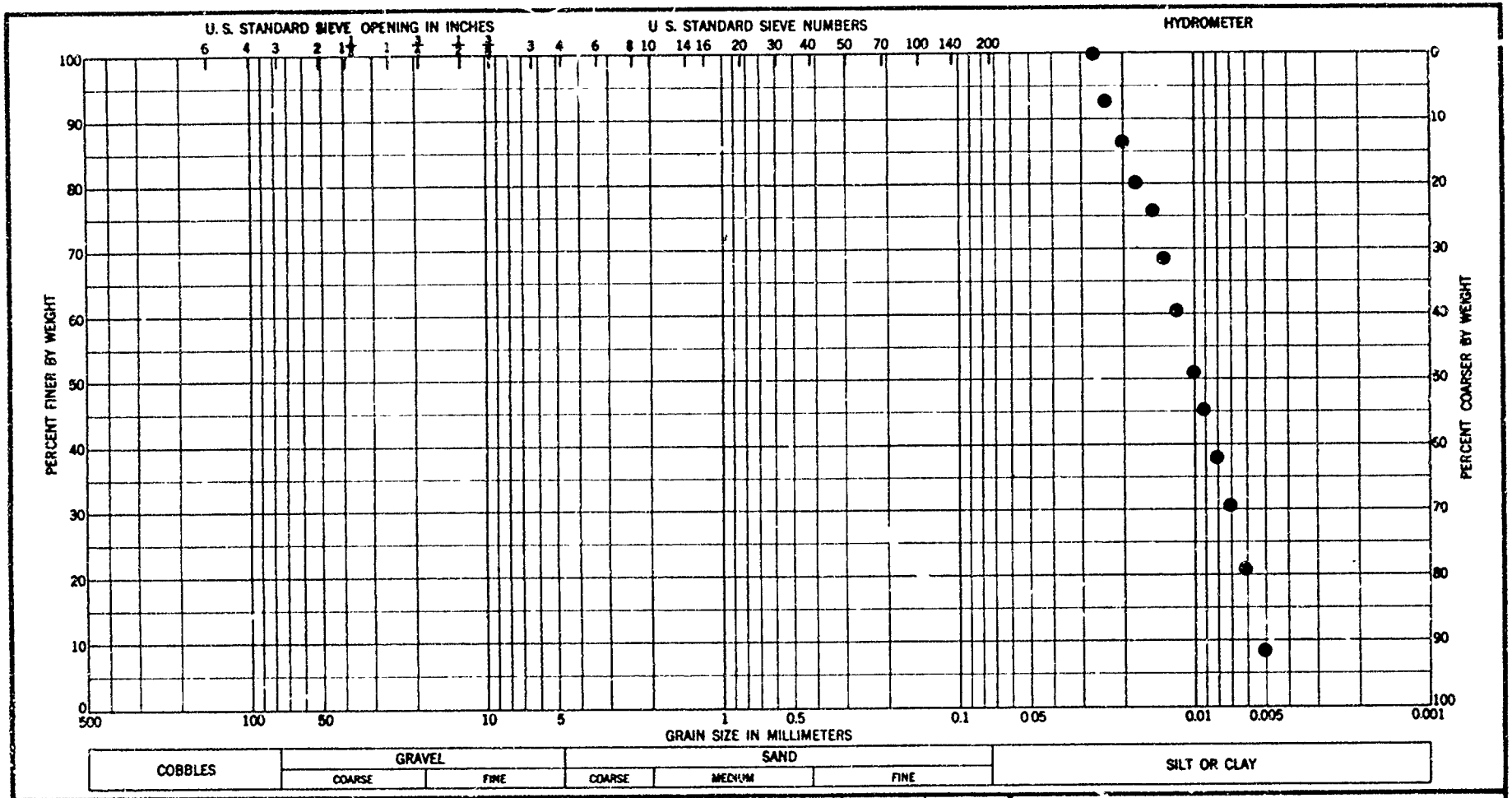

Sample No	Elev or Depth	Classification	Nat w %	LL	PL	PI
CH		Mean 10.22 μm				
		Median 9.77 μm				
		Mode 21.89 μm				

GRADATION CURVES

Project: UNDISPERSED PARTICLE SIZE

Area: CH SEDIMENT SAMPLE

Boring No

Date

ENG FORM 1 MAY 63 2087

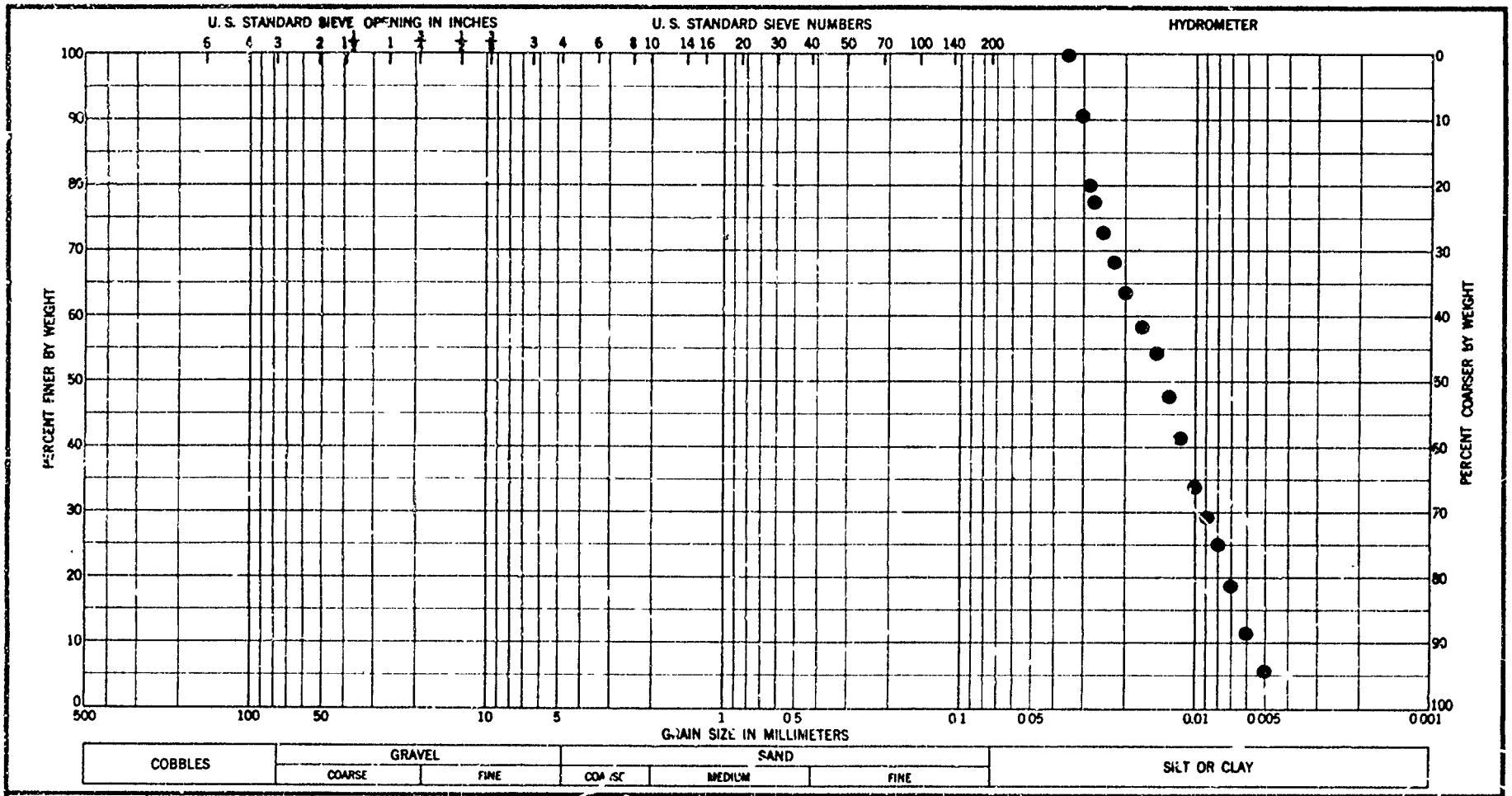

Sample No	Elev or Depth	Classification	Nat w %	LL	PL	PI
CH-2		Mean 14.26 μm				
		Median 14.91 μm				
		Mode 28.16 μm				

GRADATION CURVES

Project: UNDISPERSED PARTICLE SIZE

Area: CH-2 SEDIMENT SAMPLE

Boring No

Date

PLATE A3

ENG FORM 1 MAY 63 2087

PLATE A4

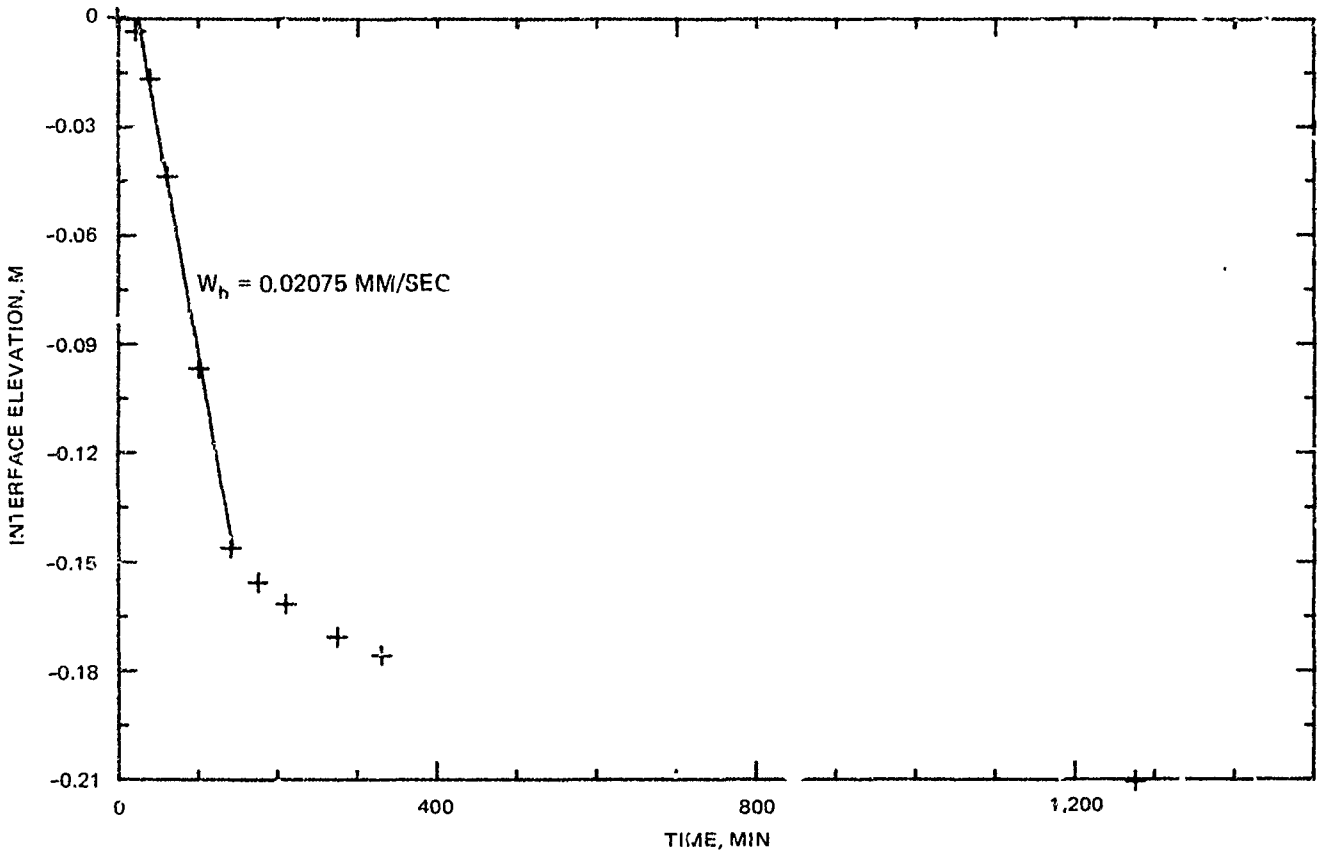

CONSOLIDATION TEST
CL SEDIMENT SAMPLE
C_o = 98 g/ℓ

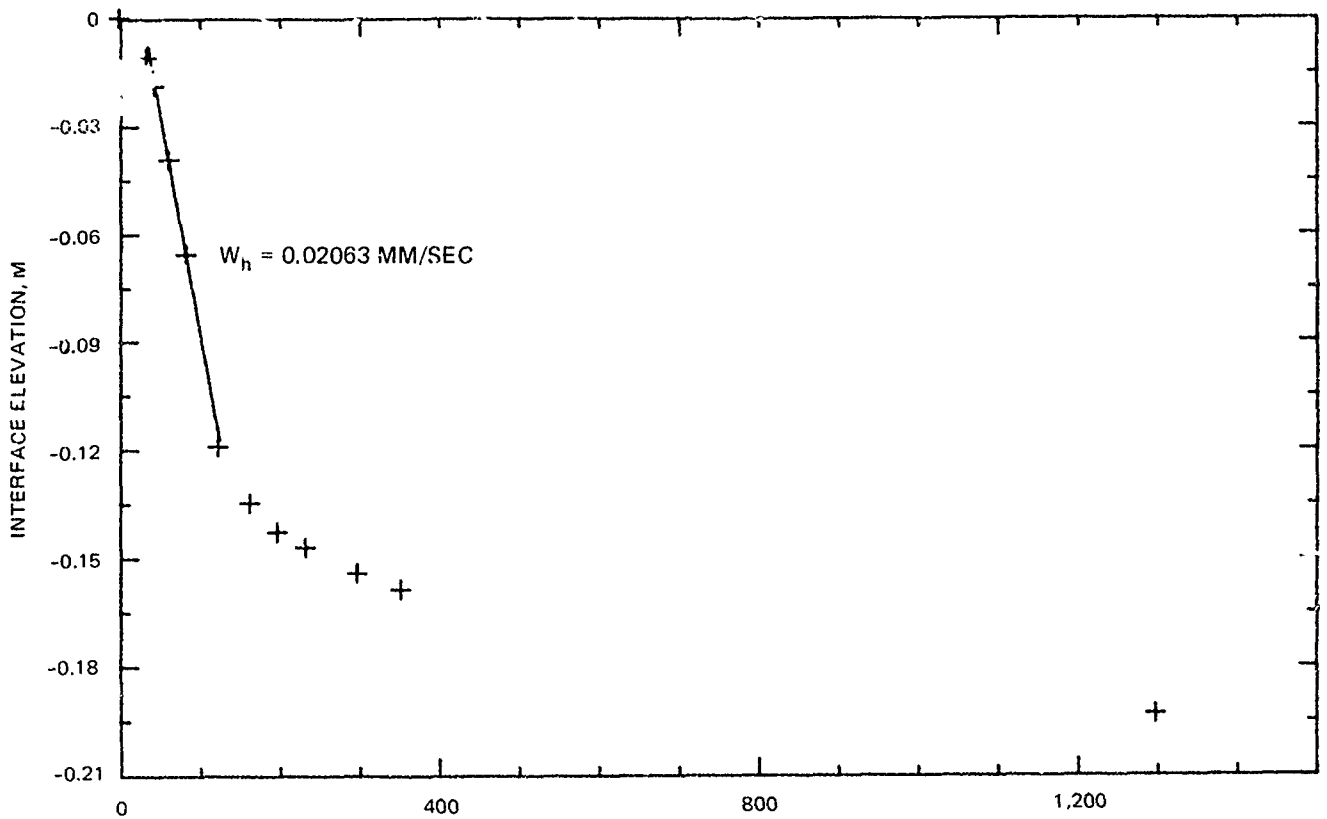

CONSOLIDATION TEST
CL SEDIMENT SAMPLE
C_o = 119 g/ℓ

PLATE A5

PLATE A6

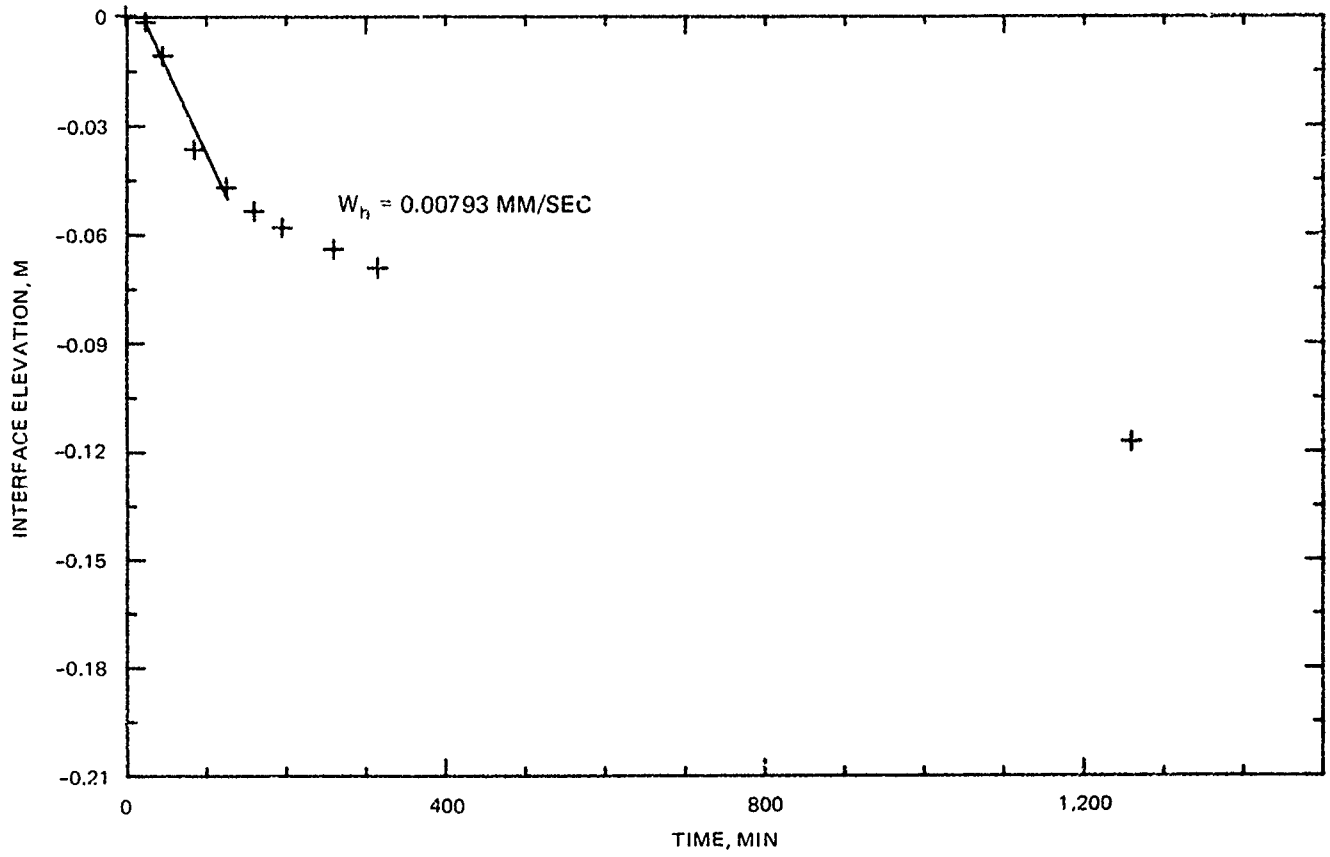

CONSOLIDATION TEST
CL SEDIMENT SAMPLE
C_o = 130 g/ℓ

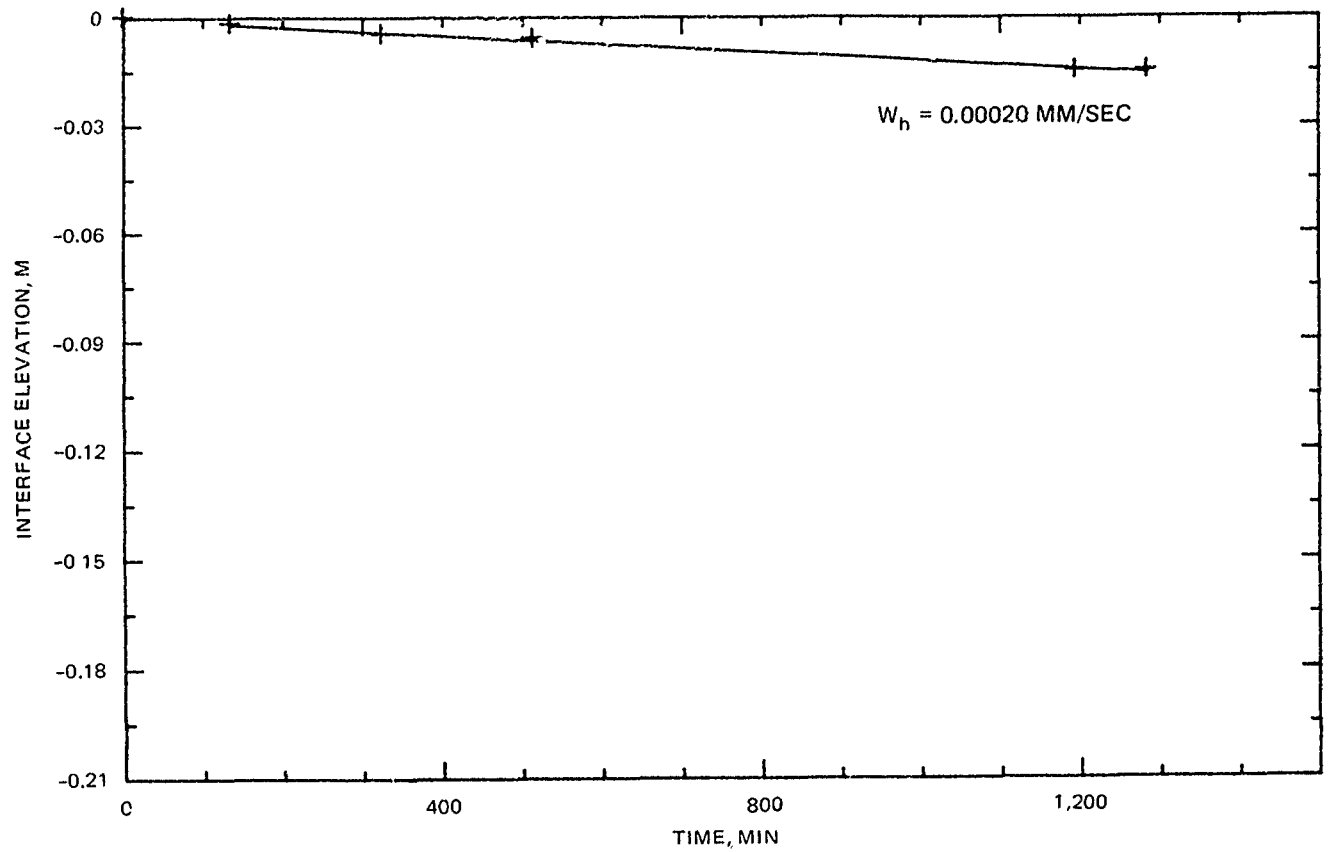

CONSOLIDATION TEST
CL SEDIMENT SAMPLE
C_o = 187 g/ℓ

PLATE A7

PLATE A8

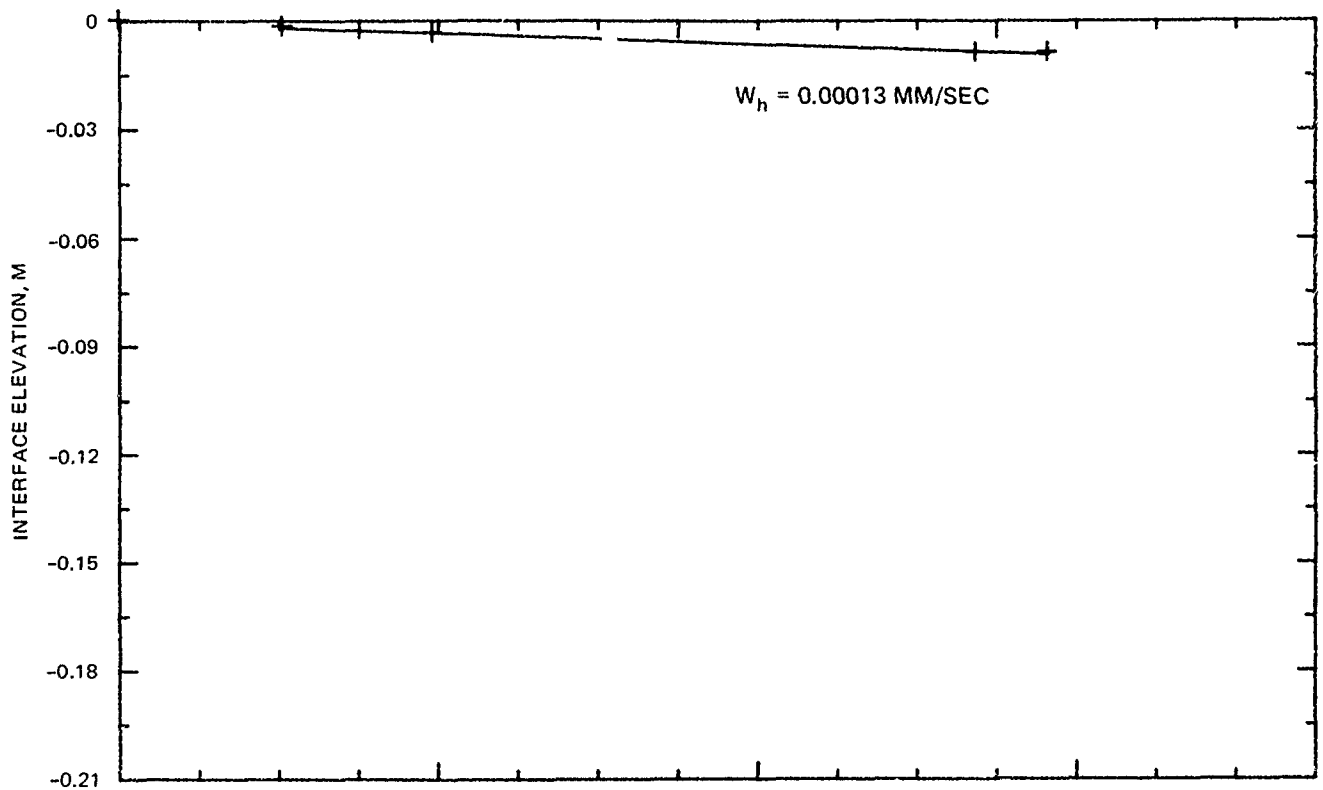

CONSOLIDATION TEST
CL SEDIMENT SAMPLE
C_o = 210 g/ℓ

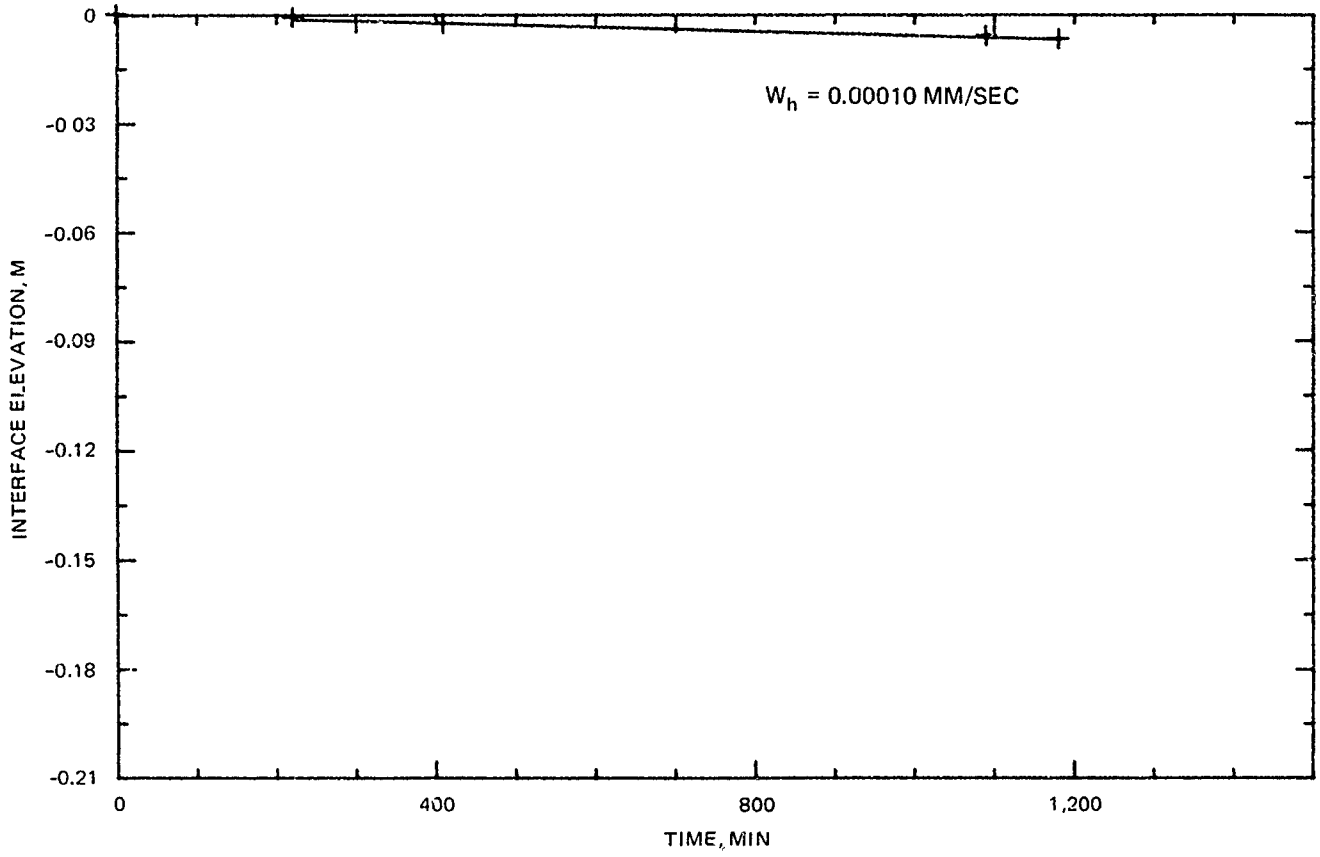

CONSOLIDATION TEST
CL SEDIMENT SAMPLE
C_o = 262 g/ℓ

PLATE A9

PLATE A10

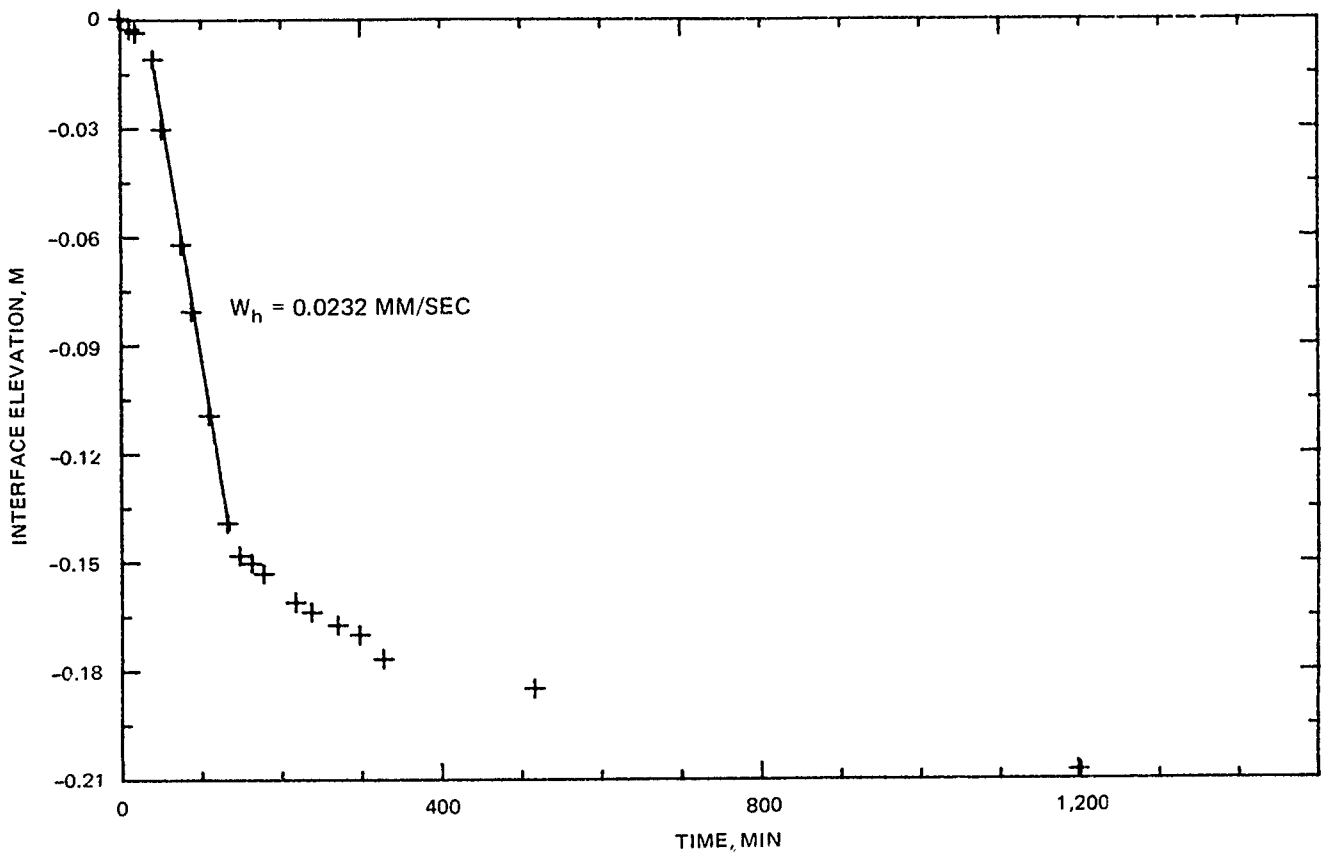

CONSOLIDATION TEST
CH SEDIMENT SAMPLE
C_o = 87.5 g/ℓ

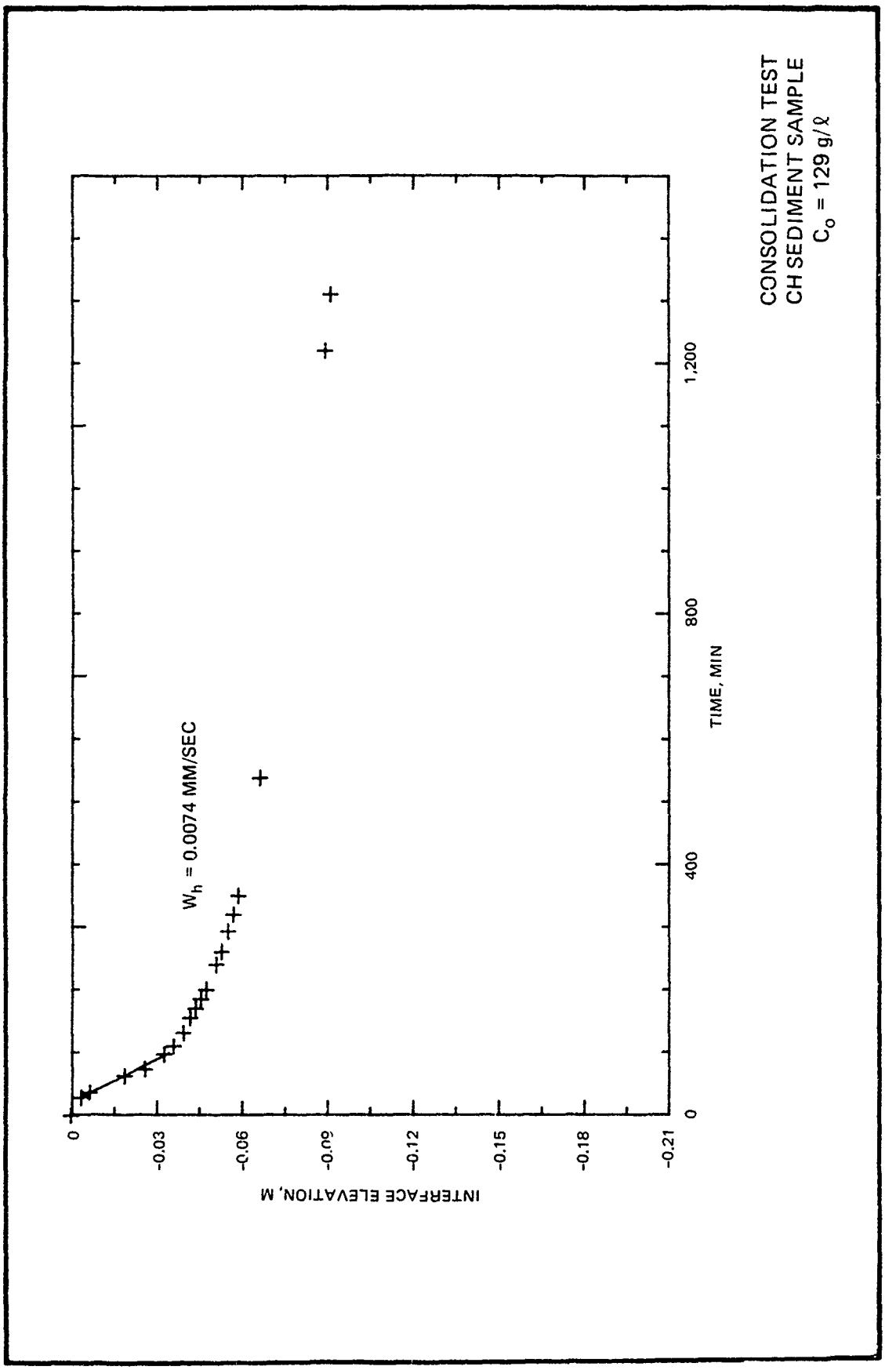
CONSOLIDATION TEST
CH SEDIMENT SAMPLE
C_o = 129 g/ℓ
W_h = 0.0074 MM/SEC
INTERFACE ELEVATION, M
0
-0.03
-0.06
-0.09
-0.12
-0.15
-0.18
-0.21
0
400
800
1,200
TIME, MIN

PLATE A11

PLATE A12

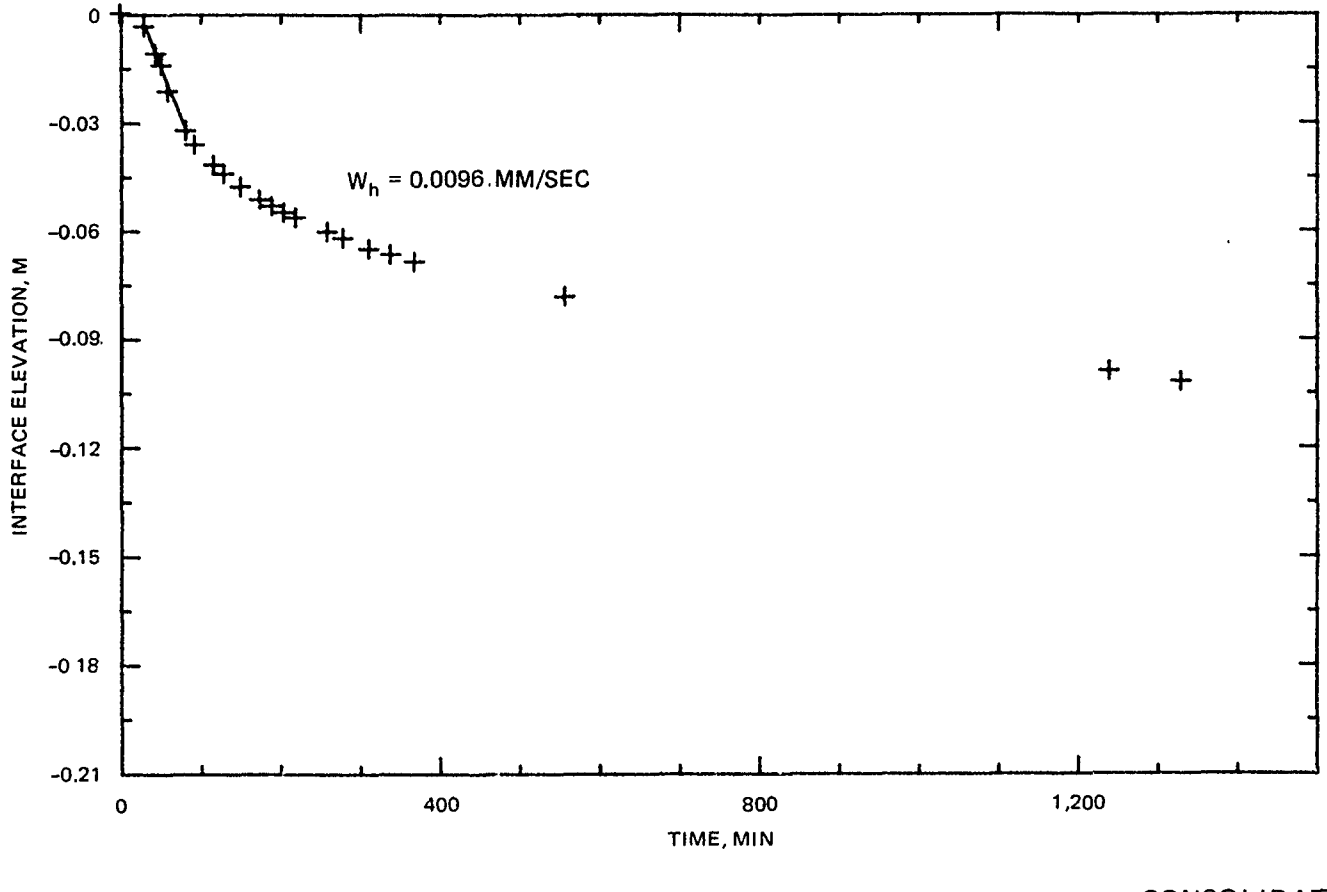

CONSOLIDATION TEST
CH SEDIMENT SAMPLE
C_o = 175 g/ℓ

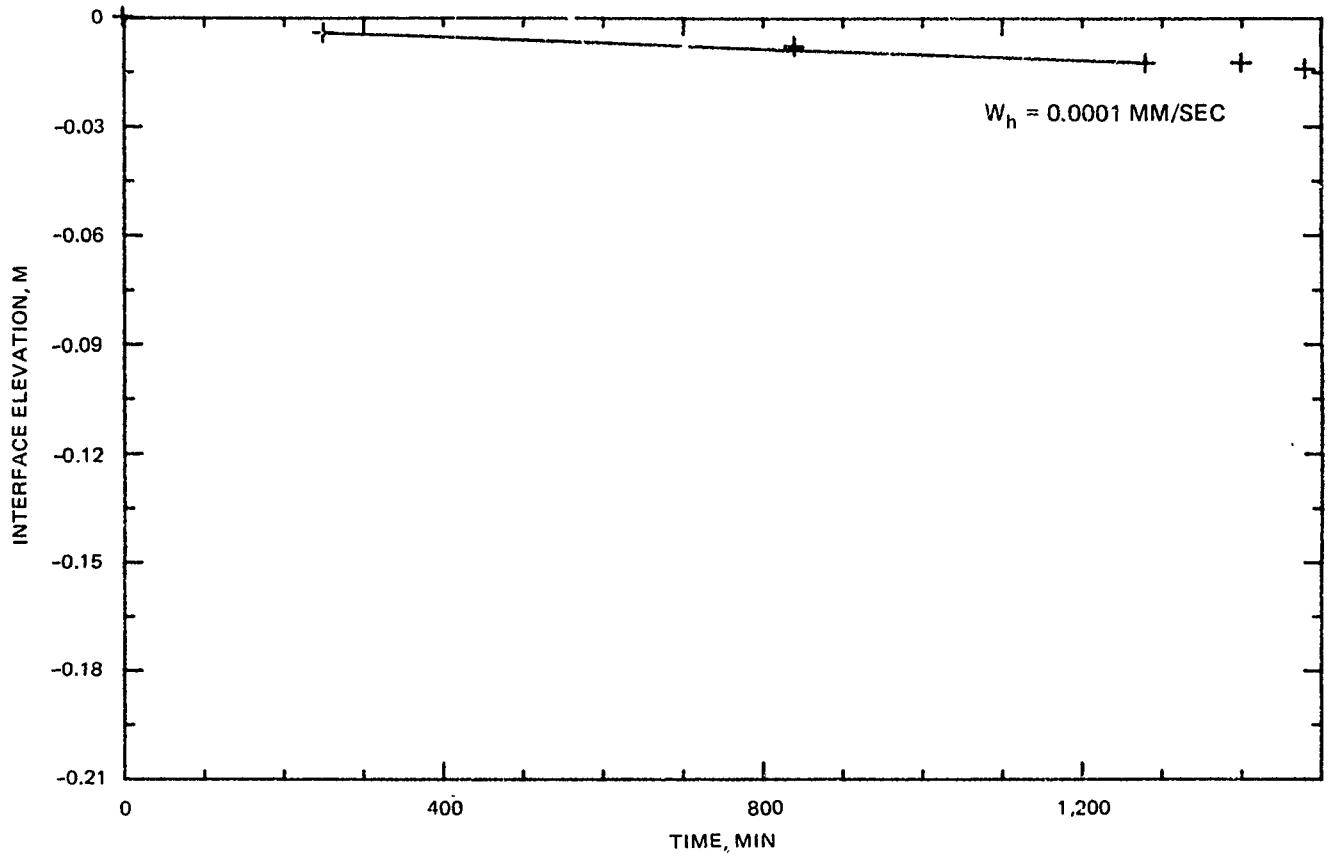

CONSOLIDATION TEST
CH SEDIMENT SAMPLE
C_o = 198 g/ℓ

PLATE A13

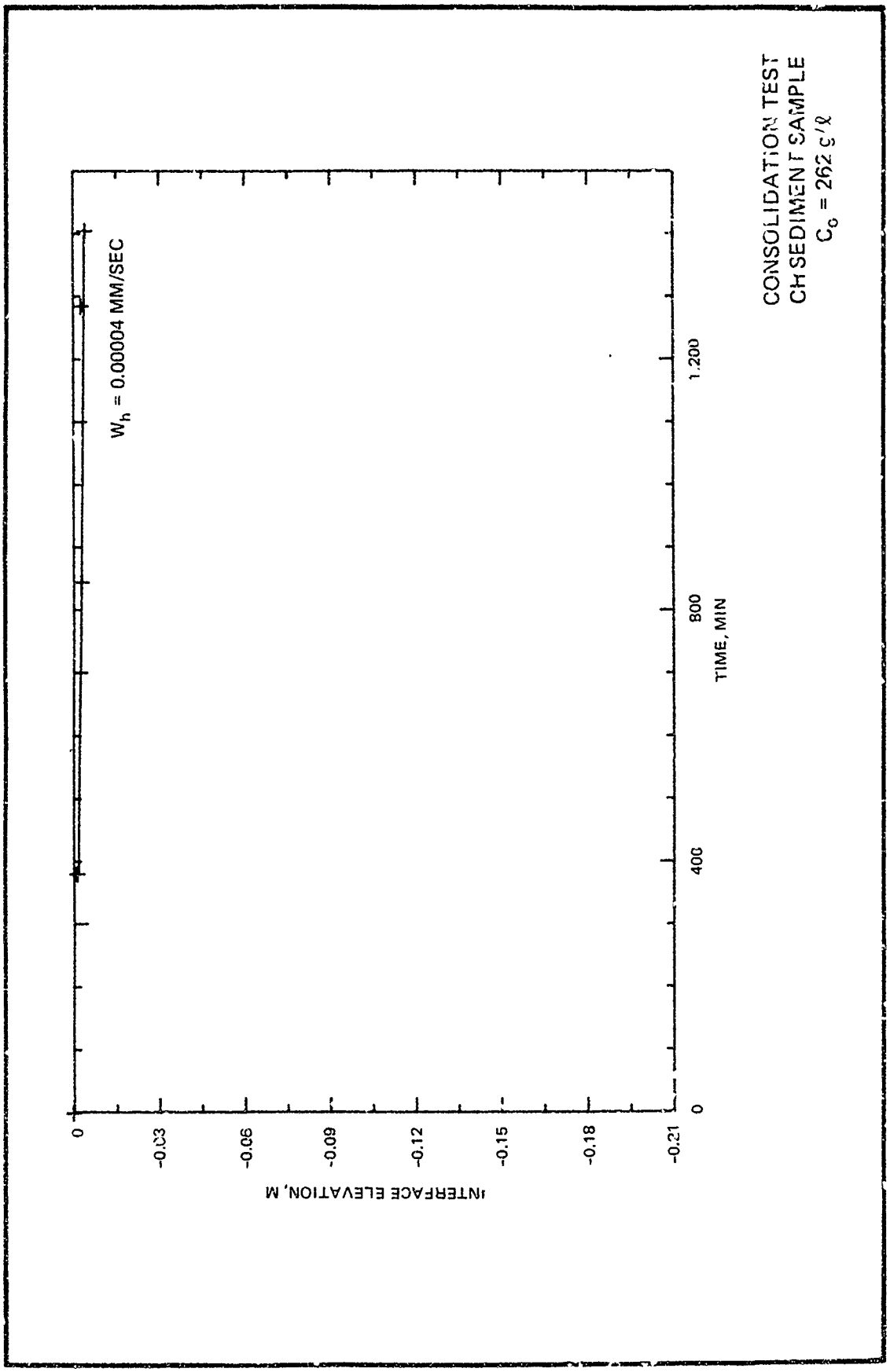
CONSOLIDATION TEST
CH SEDIMENT SAMPLE
C_o = 262 g/ℓ
W_h = 0.00004 MM/SEC
INTERFACE ELEVATION, M
0
-0.03
-0.06
-0.09
-0.12
-0.15
-0.18
-0.21
0
400
800
1,200
TIME, MIN

PLATE A14

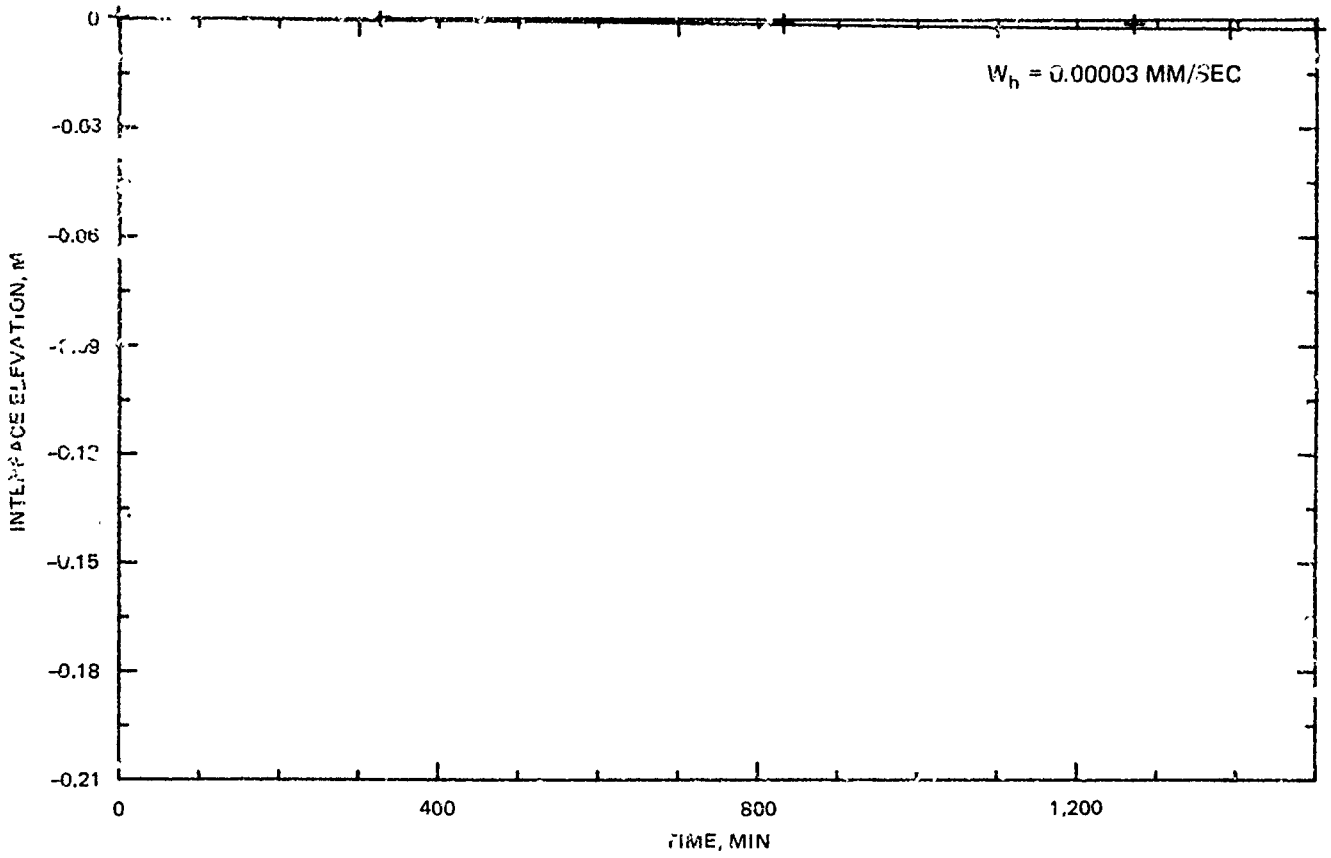

CONSOLIDATION TEST
CH SEDIMENT SAMPLE
C_o = 323 g/ℓ

PLATE A15

APPENDIX B: SEDIMENT EROSION TESTS IN THE UNIVERSITY OF FLORIDA FLUMES

(Previously published as "Experiments on the Erosion of Deposited and Placed Cohesive Sediments in an Annular Flume and a Rocking Flume," by Catherine Villaret and Mary Paulic, Report No. UFL/COEL-86/007, June 1986, Coastal and Oceanographic Engineering Department, University of Florida, Gainesville, Florida.)

PART I. KAOLINITE AND CEDAR KEY MUD

I. INTRODUCTION

The erosion of fine, cohesive sediments in estuaries is important to both the engineer and the scientist. The resuspension and transport of fine sediments can cause shoaling in ship channels resulting in increased time and cost of dredging. From an environmental perspective, resuspension of sediment increases turbidity, thus degrading water quality and possibly harming aquatic organisms.

Under mild to moderate flow conditions in the estuary, erosion of the mud surface typically occurs by the entrainment of aggregates rather than by mass erosion. The erosional behavior of a mud bed depends on four principal factors; physico-chemical properties of the mud, chemical properties of the eroding fluid, flow characteristics, and bed structure (Parchure and Mehta, 1985). Bed structure can be classified as either placed or deposited, in relation to the procedure for bed preparation. For the purposes of this report, a placed bed is defined as one in which the bed has been prepared by placing a thick slurry of mud into the laboratory apparatus. A deposited bed is produced by allowing a dilute mud suspension to settle from the water column and consolidate. The deposited bed represents the top sediment layers of an estuarine sediment which are frequently resuspended by the action of waves and currents. A placed bed is more representative of the lower sediment layers which do not regularly receive perturbations from waves and currents.

The influence of the first three parameters on the erosion rate of cohesive sediments has been extensively studied (Parchure and Mehta, 1985). The majority of laboratory experiments performed have used only one bed structure and flow regime without comparative studies of different bed structures and flow regimes. The main purpose of this study was to show the effect of bed structure on the rate of surface erosion under both steady and oscillatory currents. Two different apparatuses, a rotating annular flume and a rocking flume, were used to generate a steady current and an oscillatory current, respectively. Both bed types, using both kaolinite and estuarine mud, were tested in each apparatus. Table 1 is a list of the experiments performed.

Table 1. Experimental Design

Apparatus	Sediment/Bed	
	Kaolinite	Estuarine Mud
Annular Flume	Deposited bed Placed bed	Deposited bed Placed bed
Rocking Flume	Deposited bed Placed bed	Deposited bed Placed bed

Bed Structure

The primary difference between placed and deposited beds is the distribution of bed shear strength (and density) with depth. A deposited bed shows an increase in shear strength with increasing depth into the bed (Figure 1). This is a Type I profile. Placed beds have a nearly constant shear strength from top to bottom (Figure 2). Such a profile is referred to as Type II (Parchure, 1984; Hunt and Mehta, 1985).

A profile of density with depth is critical to determining erosion rates. Bed density increases in a deposited bed from top to bottom. On the other hand, a placed bed has nearly uniform density from top to bottom. Deposited beds undergo both primary and secondary consolidation as compared to mainly secondary consolidation for placed beds (Parchure, 1984). Due to their mode of preparation, deposited beds are generally weaker (lower density and shear strength) than placed beds for a comparable period of consolidation.

Concentration-Time Profiles

For a deposited bed the rate of erosion, ε (the time-rate of change of suspended sediment mass per unit bed surface area), which is proportional to the time-rate of change of suspension concentration, decreases as erosion proceeds and eventually stops. Once this steady state condition has been reached, the concentration of suspended mass remains constant, as in Figure 3a. Erosion is no longer occurring. At this stage, the bed shear strength at the mud-fluid interface is equal to the applied shear stress, τ_b.

Placed beds behave differently. The suspended sediment concentration increases linearly with time for a given shear stress in excess of the shear strength, as in Figure 3b. Thus, the rate of erosion of these beds is constant for a given shear stress.

Erosion Rate Expressions

Erosion of a deposited bed can be empirically modeled as a logarithmic relationship correlating the erosion rate to the excess shear stress above the bed shear strength. This relationship is:

$$\log \frac{\varepsilon}{\varepsilon_f} = \alpha[\tau_b - \tau_s(z)]^{1/2} \qquad (1)$$

where ε is the erosion rate, τ_b is the time-mean bed shear stress, $\tau_s(z)$ is the bed shear strength as a function of depth, z, below the bed surface, α is an empirical rate constant and ε_f is defined as the floc erosion rate (Parchure, 1984; Parchure and Mehta, 1985).

The erosion rate of a placed bed can be related to the bed shear stress by:

$$\varepsilon = M \frac{(\tau_b - \tau_s)}{\tau_s} \qquad (2)$$

where τ_s is the constant (critical) bed shear strength and M is an empirical coefficient (Parchure and Mehta, 1985).

II. METHODS AND MATERIALS

Apparatus

Two different flumes were used for these experiments; a rotating annular flume and a rocking flume.

Annular Flume. The annular flume had a channel width of 20 cm, depth of 46 cm, and a mean radius of 76 cm. Inside the channel a 20 cm plexiglass annular ring was suspended by means of four vertical supports attached by horizontal supports to the central vertical shaft (Figure 4). The equipment was calibrated to produce a bed shear stress up to 0.9 N/m^2. Complete details of flume calibration are contained in Mehta (1973). The total depth of

sediment and water in the flume could be up to 33 cm. For the described experiments a bed of 7 cm depth and water column height of 23 cm were used.

When the ring was rotated, a shear stress was transmitted to the sediment bed through the water column. To operate properly the ring was required to be in complete surface contact with the water column. During operation the ring and channel were rotated in opposite directions to minimize the effects of secondary currents and to maintain a uniform flow in the channel.

Taps were located on the outside wall of the channel to allow sampling from the water column. Samples were collected over a variable time regime. Total suspended sediment was determined by filtering water samples with a 0.45 micron Millipore filter and filtering apparatus. Samples were then dried at 50°C for at least two hours and then weighed on a Mettler balance (model H80) with an accuracy of 0.1 mg.

Rocking Flume. The rocking flume was constructed of 1.25 cm thick plexiglass. It was 2.4 meters in length and 36 cm high with an inner width of 15 cm. A false bottom was built into the flume at a height of 7 cm. The actual depth of the flume channel was therefore 29 cm. Figures 5a, 5b and 6a illustrate plan, elevation and side views of the flume. The entire assembly was mounted on a table with dimensions of 2.75 meters in length, 91 cm in width, and 91 cm in height. The flume was mounted on a pivot 16 cm above the table allowing it freedom of rocking motion. Directly above the pivot the channel had been deepened an additional 5 cm for a length of 54 cm to allow for the placement of a sediment bed. The flume was operated by a hydraulic transmisison attached to a 3/4 hp motor. A metal shaft (rocking arm) at one end of the flume was attached by a circular hub to the flume and to the hydraulic transmission by a hub attached to a rotating plate (Figures 5a,b and 6a). When the flume was in operation, the transmission turned a shaft which turned the rotating plate. This caused the shaft to move up and down resulting in the flume rocking back and forth. Different periods of rocking could be obtained by increasing the speed of the motor and the attached shaft. Amplitude of rocking motion could be varied by changing the eccentricity of the rocking arm/rotating plate connection.

When the flume was operated a standing wave was produced which had its node at the center of the flume, in the middle of the sediment bed. The waves produced were of shallow water type so that the oscillatory velocities were

nearly uniform over depth. Maximum horizontal displacement occurred at the node where the velocity was predominantly in the horizontal direction, along the bed surface. Wave period could be determined by timing the rotation of the plate. Wave amplitude could be determined by measuring the vertical displacement of water from still water level at the end of the flume.

A modification was made to the flume to increase the flow velocity at the bed surface. A plexiglass top constriction of height 19 cm and 54 cm length was placed in the water column above the sediment bed (Figure 6b,c). The ends of it were sloped to reduce turbulence at the entrance to the bed. Its height above the bed could be varied. With the top constriction in place, free surface flow in the flume was thus replaced by flow in a "tunnel" in the central portion of the flume. Over time the current generated at the sediment surface had a sinusoidal velocity variation.

Flume Calibration. The flume was calibrated to produce a maximum shear stress up to 0.8 N/m^2. Maximum shear stress was calculated as $0.5\ \rho f_w u_m^2$, where ρ is water density, f_w is the coefficient of friction, and u_m is the maximum horizontal water velocity. A number of different techniques were used to determine velocity. These included direct measurement of the displacement of the water level relative to the mean, mean surface particle displacement at the node, and velocity of the water above the bed. For these experiments a water depth of 10 cm was maintained above the bed and 17.5 cm at the ends. Complete details, calculations, and calibration curves are contained in the Appendix.

Bed Preparation

Placed Bed. A thick slurry of sediment and salt water (salinity 10 ppt) was mixed for one hour in a mixer and then placed into the flume to uniform depth. Water was then carefully added to the flume to the appropriate depth. A separate bed was placed in a bucket for determination of bed density.

Deposited Bed. An appropriate volume of sediment was added to the annular flume and water added to a depth of 30 cm. The flume was then rotated to generate a bed shear stress of 0.9 N/m^2, in order to assure complete mixing. After 24 hours, the flume was stopped and the sediment allowed to settle under quiescent conditions. After mixing, but before significant

settling of the sediment, water containing suspended sediment was withdrawn from the channel and deposited into removable beds (Figure 6d) that could be placed directly into the rocking flume. The ends of these beds were temporarily sealed with plexiglass to allow a water column to be poured over the bed. A second sample was withdrawn from the annular flume and allowed to deposit in a bucket. This was later used for bed density measurement.

Test Procedure

Annular Flume. For each experiment six different shear stresses were selected. They were applied in a step-wise fashion starting at 0.1 N/m^2 and continuing until 0.6 N/m^2 in increments (90 min duration) of 0.1 N/m^2. Suspension samples were removed, in approximately 50 ml aliquots, at 2,5,10, 15,20,25,30,40,50,60,75, and 90 minutes with an initial sample taken at the start of the test. Samples were taken from taps at the top and bottom of the water column to give an average suspension concentration for the entire water column. Salt water was periodically added to the flume to maintain a 23 cm water depth.

Rocking Flume. Shear stresses selected in this flume were 0.1, 0.2, 0.3, and, in some cases, 0.4 N/m^2. Note that these are wave-averaged rather than maximum values. Samples were collected over the same time regime as for the annular flume, excluding the 2 minute sample. Samples were taken from the center of the flume, at one-quarter reach and at one end, including the top and bottom at each location. Salt water was added periodically to the flume to replace the volume of water lost to samples.

The test procedure with regard to the applied shear stress is summarized in Figure 7 for both flumes. Note that with respect to deposition and consolidation, the duration of deposition was typically quite small compared with that of consolidation. In what follows, the combined duration is referred to as consolidation period.

Materials

Estuarine Sediment. The mud was collected from a tidal flat in Cedar Key, Florida. Mineralogically it was composed of 73% montmorillonite, 21% kaolinite and 6% quartz. Prior to being used, the mud was sieved through a 1 mm screen to remove shells and plant materials. The median (dispersed)

particle size was ~ 2 microns, as obtained by hydrometer (ASTM, 1981). The cation exchange capacity was ≈ 100 millequivalents per hundred grams. Total organic matter corresponded to 11% loss on ignition, as obtained by standard procedure (American Public Health Association, 1976).

Kaolinite. The kaolinite was obtained from a commercial source. It was prepared by soaking 90 kg dry kaolinite in thirty gallons of salt water (salinity 10 ppt) for one month. The kaolinite-water mixture was stirred every few days to ensure equilibration of the sediment with the fluid. The median (dispersed) size was ~ 1 μm. The cation exchange capacity was ~ 6 milliequivalents per hundred grams and loss on ignition was 12%.

Fluid. All experiments were performed with salt water at a salinity of 10 ppt. Salt water was prepared by mixing sodium chloride in tap water. Salinity was checked by a refractometer. Fluid temperature during the tests was in the range of 24°-27°C. The pH varied from 8.5 to 9.5.

Density Measurement

The method used for determining bed density followed the procedure of Parchure (1984). The apparatus used consisted of a 2.0 cm diameter coring tube and a 15 cm diameter plexiglass cylinder with a 2.5 cm diameter metal tube in the middle (Figure 8). Cores were taken from the bed and then the cylinder was placed over the coring tube. The inside of the cylinder was filled with ethanol and dry ice to snap freeze the cores *in situ*. Once frozen the cores were sliced into thin sections between 2 mm and 10 mm, dried at 40°C and weighed.

III. RESULTS

Density Measurement

Deposited Bed. The density of deposited bed typically increases with depth. Such a trend was observed for both kaolinite and estuarine mud. Density (dry) profiles are contained in Figure 9 for kaolinite and Figure 10 for mud.

Placed Bed. The density of a placed bed is fairly constant with depth. Density (dry) profiles are contained in Figure 11 for kaolinite and Figure 12 for mud. The measured values indicate deviations from uniformity with depth.

Concentration-Time Profiles

Deposited Bed. Figures 13 through 16 are plots of suspension concentration versus time. Where deemed important, comments on the observed trends have been made within the figures, e.g. Figure 16. Most comments made here and in subsequent figures are either self-explanatory, or are discussed in the text. The total (instantaneous) suspension concentration is represented as a depth-averaged value for each flume. In general, deposited beds in both flumes exhibited a series of steady states (characterized by constant final concentrations). Higher suspension concentrations were obtained with kaolinite than with mud at the same applied shear stress. At high shear stresses, particularly in the annular flume, plots appear to indicate a nearly linear increase of concentration with time (Figure 15). In these cases, either the samples were not collected for a sufficient time period to reach steady state concentrations, or the bed shear stress had exceeded the maximum bed shear strength (Parchure, 1984).

Placed Bed. Figures 17 through 20 are concentration-time profiles of placed beds. Again, the suspension concentration is a depth-averaged quantity. In general, the profiles are linear. The placed mud bed in the annular flume, Figure 19, exhibits an initial pattern of steady states at low shear stresses. This behavior occurred because it was difficult to add water to the flume initially without disturbing the bed; thus the top sediment layers behaved like deposited beds. Also observed in this figure is a sudden drop in the concentration at the beginning of the last three steps. It should be noted that the concentration plotted here is based on measurements at a single elevation approximately half way between the suspension surface and the bed. The concentration drop can be attributed to a change in the vertical concentration profile, rather than deposition, as a consequence of a change in the inter-particle collision frequency at the beginning of each step (Parchure, 1984). In the rocking flume, little erosion of the placed beds occurred before 0.3 N/m^2. In particular, the placed mud bed in the rocking flume Figure 20, did not start to erode until 0.4 N/m^2. Note that erosion occurred suddenly without any increase in applied shear stress. This type of behavior may be attributed to a decrease in the bed shear strength (bed softening) under the oscillatory velocity field in the rocking flume (Maa, 1986).

Bed Shear Strength

Deposited Bed. The final, steady state suspension concentration for each shear stress was first converted to mass per unit bed area and then plotted against the applied bed shear stress. Two linear plots of slopes M_1 and M_2 are obtained (see for example Fig. 21). By extrapolating the M_1 line back to the abscissa the bed surface shear strength τ_{so}, corresponding to initiation of erosion can be determined (Parchure and Mehta, 1985). Likewise the point of intersection of lines M_1 and M_2 gives the characteristic shear strength, τ_{sc}, above which the rate of erosion increases significantly. Bed surface (z=0) shear strength, τ_{so}, and characteristic shear strength, τ_{sc}, values are given in Table 2. Figures 21 and 22 are plots of suspended sediment mass per unit bed surface area versus applied shear stress from which the values given in Table 2 have been obtained. Both the rocking flume and the annular flume data are on the same plot. For the kaolinite beds, Figure 21, the same curves were obtained in both flumes. Values of τ_{so} and τ_{sc} in Table 2 suggest that the mud generally had a somewhat higher resistance to erosion than kaolinite.

Table 2. Bed Surface Shear Strength, τ_{so}, and Characteristic Shear Strength, τ_{sc}, of Deposited Beds in the Annular Flume and the Rocking Flume

	Kaolinite		Mud	
Apparatus	τ_{so} (N/m^2)	τ_{sc} (N/m^2)	τ_{so} (N/m^2)	τ_{sc} (N/m^2)
Annular Flume	0.08	0.25	0.18	0.40
Rocking Flume	0.08	0.25	0.03	0.20

Placed Bed. Table 3 contains values of bed shear strength (uniform over depth) for placed beds in each apparatus. Figures 23 and 24 are plots of suspended sediment mass eroded per unit bed surface area per unit time (i.e. rate of erosion) versus shear stress for placed kaolinite and mud beds, respectively. These plots were used to obtain values given in Table 3. The mud bed may be considered to have a somewhat higher shear strength than the kaolinite bed. However, contrary to the bed softening trend expected in the rocking flume, the shear strength was higher in this flume than in the annular flume. A possible explanation is noted later.

Table 3 Shear Strength of Placed Beds in the Annular Flume and the Rocking Flume

Apparatus	τ_s (N/m^2)	
	Kaolinite	Mud
Annular Flume	0.25	0.22
Rocking Flume	0.28	0.40

Relationship of Shear Strength to Depth

The density profiles coupled with concentration-time profiles presented earlier were used to produce profiles of the bed shear strength with depth. Details of procedure are given by Parchure and Mehta (1985).

Deposited Bed. Figures 25 and 26 are plots of bed shear strength versus depth. The same density profile for a given sediment was used for both flumes. The bed shear strength is observed to increase with depth below the bed surface. For the kaolinite bed, the profiles resulting from the two flumes are nearly coincident. For the mud bed, the profiles from the two flumes differ; the shear strengths from the rocking flume are lower. This difference is believed to be due to bed softening.

At corresponding depths in the bed, the shear strength of the mud is generally higher than that of kaolinite in the annular flume. In the rocking flume, shear strengths of kaolinite and mud at corresponding depths are nearly the same.

Placed Bed. The kaolinite bed yielded a constant depth versus shear strength profile, with a shear strength of 0.25-0.28 N/m^2, see Table 3, with only a small difference between the values obtained in the two apparatuses. Figure 27 is a plot of depth versus shear strength for the placed mud bed in the annular flume. Unlike the kaolinite beds, the profile is not constant, but has a lower shear strength in the top few millimeters, due to the deposited bed-like behavior noted previously. The shear strength of the placed mud bed in the rocking flume was 0.40 N/m^2, as estimated from Figure 24.

Erosion Rate

Deposited Bed. For a deposited bed under a constant shear stress the rate of erosion decreases with time. The relationship given by Eq. 1 describes the rate of erosion. The calculated rate coefficients α and ε_f are contained in Table 4 (Parchure and Mehta, 1985). Figures 28 and 29 are plots of the log of the erosion rate versus the square root of the applied shear stress minus the bed shear strength, i.e., square root of the excess shear stress.

Table 4. Values of α and ε_f for Deposited Beds

Apparatus	Kaolinite		Mud	
	α ($m/N^{1/2}$)	ε_f (mg/cm^2-hr)	α ($m/N^{1/2}$)	ε_f (mg/cm^2-hr)
Annular Flume	5.1	2.1×10^{-3}	7.9	3.2×10^{-3}
Rocking Flume	5.1	2.1×10^{-3}	7.9	2.0×10^{-3}

Placed Bed. For a placed bed the rate of erosion is given by Eq. 2. The values of M and τ_s are given in Table 5. Figures 23 and 24 are plots of erosion rate versus applied shear stress for kaolinite and mud, respectively. The erosion coefficient, M, was the same in both flumes for the kaolinite beds until the applied shear stress equalled 0.4 N/m^2 at which point the erosion rate increased rapidly in the rocking flume. However, there were insufficient data points to evaluate the coefficient M. The same situation occurred with

Table 5. Values of M and τ_s for Placed Beds

Apparatus	Kaolinite		Mud	
	M (mg/cm^2-hr)	τ_s (N/m^2)	M (mg/cm^2-hr)	τ_s (N/m^2)
Annular Flume	18.6	0.25	5.8	0.22
Rocking Flume	18.6	0.28	-	0.40

the mud bed in the rocking flume. It is noteworthy that in the rocking flume, the erosion rate increased suddenly in both cases (kaolinite and mud) in spite of the fact that the shear stress was constant at 0.4 N/m^2 (see Figs. 18 and 20). It is believed that bed softening under oscillatory current was a possible cause of this behavior.

IV. CONCLUDING REMARKS

A comparison of results obtained in both the annular flume and the rocking flume indicates trend similarities as well as quantitative differences in the erosional behavior of the two cohesive sediments.

Comparisons have been made of concentration-time profiles, shear strength variation with depth as a function of bed structure, and erosion rate. The concentration-time profiles for deposited beds were characterized by a series of steady states in both flumes and for both sediments. At high shear stresses (equal to or greater than 0.5 N/m^2), the concentration typically continued to increase linearly for the entire sampling period. The explanation for this behavior is the nature of the vertical distribution of shear strength. With increasing depth the shear strength increased, but at smaller rates until it was nearly constant. A one and a half hour sampling period was apparently insufficient to erode away the material to a depth at which the applied shear stress equalled the shear strength. Alternatively, the same type of behavior can be shown to result if the applied bed shear stress exceeds the maximum bed shear strength (Parchure and Mehta, 1985).

Placed beds exhibited a linear increase in suspension concentration with time. The initial period of testing may exhibit a pattern more like that of a deposited bed, as in Figure 19. The reason for this trend is that upon initial addition of water to the flume some disruption of the surface occurred even though care was taken in the addition of water. In general, the values obtained for suspension concentration from the placed beds were lower than for the deposited beds under the same flow conditions. Placed beds are typically more dense to begin with and are less erodible than deposited beds.

An important observation to note about placed beds in the annular flume is that after the applied shear stress was increased, the concentration of sediment in suspension actually decreased, in some instances. A similar

observation was made by Parchure (1984). There are two possible mechanisms involved in an interpretation of this phenomenon. The first is simply a delay in the response of the bed to an increase in the shear force being exerted on it. Secondly, increasing the rate of turbulent shearing in the water column increases the number of collisions between particles which enhances the rate of aggregation. Larger aggregates would be able to deposit, thereby reducing the suspension concentration.

The deposited mud bed had a lower bed shear strength (with respect to erosion) when subjected to an oscillatory current (in the rocking flume) as compared to a steady current (in the annular flume). The difference between shear strengths obtained with the two types of currents also increases with depth in the bed (see Figure 26). In general, the bed shear strength was lower under oscillatory currents than under steady currents. This feature is probably due to the bed softening under oscillatory currents, implying a degradation of bed shear strength due to a breakdown of the structure of the deposited aggregates. The coefficients α and ϵ_f of the erosion rate expression were comparable, however.

Placed beds in the rocking flume showed a sudden increase in the erosion rate without increasing the applied shear stress. The mud bed began to erode after about one hour at a shear stress of 0.4 N/m^2, while the erosion rate of kaolinite approximately doubled after about 45 minutes at the same shear stress (0.4 N/m^2). These sudden increases in erosion rate imply that at the time of occurrence of these changes, the bed shear strength decreases to a level below the applied shear stress.

The bed shear strength of placed beds was nearly the same for kaolinite in both flumes, but was higher for mud in the rocking flume than in the annular flume. This trend is seemingly in contradiction to the bed softening phenomenon noted. Maa (1986) however noted that under certain conditions depending upon the initial bed structure and flow conditions, a breakdown of aggregate structure within the bed is accompanied by an enhanced rate of consolidation. If the influence of consolidation on bed erodibility exceeds that due to structural breakdown, the bed would become more erosion resistant under oscillatory flows in comparison with steady flows.

The coefficient M of the erosion rate expression for kaolinite was the same under both types of currents. The results for mud could not be compared because there were insufficient data for mud from the rocking flume.

As noted, differences in the results between the two flumes may be the result of softening of the bed when subjected to an oscillatory current. The degree of softening is also dependent on the bed properties. The kaolinite bed was weaker than the mud bed, partly because it was less cohesive than the mud which contained montmorillonite as the predominant constituent. In a sense, kaolinite was already "softer" so it was not as readily affected by softening as mud.

The type of sediment used for an experiment had measurable influence on the results obtained. Kaolinite had a narrower distribution of (primary) particle size making a more homogeneous bed. The mud contained a sand fraction which does not erode by the same mechanism that fine particles do. The sand fraction can move as bedload or as suspended load, rather than as suspended load alone. Also, the mud contained an organic fraction which can sometimes lead to increased flocculation of particles.

In conclusion, higher bed shear strengths were generally obtained for mud than kaolinite, making the mud more resistant to erosion than kaolinite. Likewise, the erosion coefficient M for placed beds was 3 to 4 times larger for kaolinite as compared to mud. The type of current (steady or oscillatory) eroding the sediment appears to be an important factor in determining the erosion rate.

PART 2. SAN FRANCISCO BAY MUD

I. INTRODUCTION

Erosion tests conducted with mud from San Francisco Bay were for the purpose of evaluating the erosion potential of the mud at various bed densities. The test methodology, apparatus and procedure were the same as those of kaolinite and Cedar Key mud. Here therefore emphasis is placed predominantly on data analysis and interpretation.

II. SEDIMENT AND FLUID PROPERTIES

The predominant clay mineral constituent in the bay mud is montmorillonite, followed by illite, kaolinite, halloysite and chlorite. Among the non-clay minerals, quartz is predominant. There is also some iron (both structural, replacing some of the aluminum in illite, and non-structural, i.e., independent of the clay mineral) and organic matter. The cation exchange capacity of the samples used was 61 milliequivalents per hundred grams.

Suspended or recently deposited bay mud typically has a light brown color, while sediment from a depth of a few centimeters below the surface has a color ranging from light grey to black. When a sample of wet dredged sediment is placed in a glass cylinder and thoroughly stirred in water, a color change from dark grey to brown takes place. When allowed to stand, the color slowly changes back to greenish grey, and finally back to dark grey. These color changes occur due to the following reasons: in the dark grey sediment iron is present as ferrous sulfide. When stirred, ferrous sulfide is easily oxidized due to aeration to ferric hydroxide, which imparts a brownish color to the sediment. If allowed to stand, bacterial reduction first changes ferric iron to ferrous iron which is greenish, and then finally back to ferrous sulfide.

Table 6 gives sediment sample numbers and corresponding locations within the bay. In Table 7, sample properties - median size, bulk density, ρ_B, sediment density, ρ_s, and total organic matter are given. Sample 3A contained a sizeable fraction of sand; hence its median size (75 μm) was in the fine

sand range. This sample was therefore discarded from further analysis. The remaining samples were mixed in approximately equal proportions since they all had similar properties. Thus, erosion tests reported here are for the composited sample, a mixture of 1, 2A, 2B and 2C.

Table 6. Bay Mud Sample Locations

Sample No.	Location
1	Larkspur Channel
2A	Richmond Longwharf Manuevering Area
2B	Richmond Longwharf Manuevering Area
2C	Richmond Longwharf Manuevering Area
3A	Southampton Shoal Channel

Table 7. Bay Mud Sample Properties

Sample No.	Median size (μm)	Bulk density, ρ_B (g/cm^3)	Sediment density, ρ_s (g/cm^3)	Total organics (%)
1	3	1.52	2.76	10.0
2A	7	1.56	2.67	7.6
2B	30	1.69	2.76	3.4
2C	12	1.65	2.72	4.7
3A	75	1.90	3.11	2.2

The (eroding) fluid was tap water to which sodium chloride was added to raise the salinity to 33 ppt. The pH was maintained at ~ 9. The mean fluid temperature was 24°C during the experiments.

In tests with deposited beds, the pore fluid composition may be considered to have been the same as the eroding fluid composition given above. In the single test with a placed bed at natural density, the pore fluid composition was as follows: Na^{++} 9,700 ppm, Ca^{++} 940 ppm, Mg^{++} 1,150 ppm, K^{+} 770 ppm, Cl^{-} 16,930 ppm and SO_4^{--} 2,640 ppm. Solution conductivity was 33 mmhos/cm.

III. TEST RESULTS

Test conditions are summarized in Table 8. Test 1 was with a placed (dense) bed in the annular flume at the natural bulk density of 1.63 g/cm^3 (corresponding to a dry density of 0.96 g/cm^3). Tests 2 through 5 were for deposited (soft) beds with consolidation periods of 0.5 day and 3.8 days.

Table 8. Bay Mud Test Conditions

Test No.	Apparatus	Consolidation (days)	ρ_D (g/cm^3)	ρ_B (g/cm^3)
1	Annular flume	dense bed	0.96	1.63
2	Annular flume	0.5	0.22	1.17
3	Rocking flume	0.5	0.22	1.17
4	Annular flume	3.8	0.40	1.28
5	Rocking flume	3.8	0.40	1.28
P1	Straight flume[a]	40 (placed)	0.61[b]	1.36
P2	Straight flume[a]	15 (placed)	0.57[b]	1.34

[a]Tests of Partheniades (1965).

[b]Sediment density was 2.24 g/cm^3

Density profiles for the dense bed (test 1) and soft beds (tests 2,3,4,5) are given in Fig. 30. These are dry densities, ρ_D (not to be confused with sediment density, ρ_s). The dense bed density did not vary with depth. For the soft beds, ρ_D and ρ_B values given in Table 8 are representative depth-mean values corresponding to the top bed layers which eroded during the tests. Thus they are not averages over the entire mud bed thickness shown in Fig. 30.

Tests P1 and P2 corresponding to series I and II of Partheniades (1965) were conducted on remolded, placed beds. Since Partheniades also used sediment from the San Francisco Bay which is spatially well mixed (Krone, 1978), results from these tests are included in the subsequent analysis.

Time-concentration data for tests 1 through 5 are given in Figs. 31 through 35. Data from P1 and P2 appear elsewhere (Partheniades, 1962).

The erosion rate, ε, against bed shear stress, τ_b, relationship from test 1 (annular flume) is compared with P1 (series I) and P2 (series II) in

Fig. 36. The annular flume data agree with series I up to $\tau_b = 0.8$ N/m^2. Disparities for larger τ_b are attributed to likely corresponding differences in the bed structure due to differences in the method of bed preparation, i.e., the manner in which the beds were remolded and placed. In series II, iron oxide from rust in the return pipe of the flume used by Partheniades enhanced bed resistance to erosion due to cementing of aggregates. Characteristically however, incipient erosion is observed to have begun at the same $\tau_b = \tau_{co}$, ~ 0.1 N/m^2, in all three cases.

In Fig. 37, erosion rate, ε, is plotted against τ_b for tests 1 through 5, i.e. for dense as well as soft beds, for the mere purpose of demonstrating similarities and differences. For the dense bed, time-concentration profiles (Fig. 31) were characteristically linear, hence ε was constant for a given τ_b. On the other hand, time-concentration response of the soft beds (Figs. 32, 33, 34, 35) was a series of steady state steps also characteristic of such beds. For all tests, ε was calculated for each τ_b by substracting the initial concentration from final concentration for each particular step and dividing the difference by the step duration (90 minutes). Thus, the ε value is a representative mean for the entire step. The most significant feature of Fig. 37 is the considerably higher resistance to erosion offered by the dense bed compared to the soft beds. In tests with soft beds, the bed softening role of oscillatory flow in the rocking flume is also evident, particularly in the 0.5 day consolidation test, when compared with the corresponding results from the annular flume.

The following analysis is directed towards determining the erosion rate constants, M and τ_c (= τ_s) of Eq. 2, from all the tests. τ_c is then correlated empirically to the bulk density and, finally, M is likewise correlated to τ_c. Equation 2 is an acceptable approximation for the erosion behavior of dense beds. For soft beds, Eq. 1 is applicable (Parchure and Mehta, 1985). However, Eq. 2 is a reasonable approximation of the erosion behavior of soft beds, provided the erosion rate is calculated as a representative mean of each steady state step as noted (Fig. 37).

In Figs. 38 and 39, ε-τ_b relationships for soft beds have been replotted for clarity. With reference to Fig. 39 as an example, τ_{co} is the value of τ_b corresponding to incipient erosion, while τ_c is the "operational" or "design" value of the critical shear stress for erosion applicable to Eq. 2. M is

evaluated from the slope of the second line. In Fig. 38, erosion rates at $\tau_b = 0.1$ N/m^2 appear to be excessively high in comparison with the trends implied by other data from both flumes. These values, corresponding to points A and B, suggest mass erosion as opposed to surface erosion behavior (Parchure and Mehta, 1985). Therefore, points A and B were disregarded.

For the dense bed as well as tests of Partheniades, linear approximations (dashed lines) shown in Fig. 36 were used to evaluate τ_c and M. For the soft beds, Parchure (1984) used an alternative procedure for estimating τ_c. This involves plotting the final suspension concentration in a steady state step against the corresponding τ_b. This is done in Figs. 40 and 41 where C_{90} is the (final) concentration at 90 minutes, the step duration.

Results are summarized in Table 9. Characteristically, τ_{co} values are close to each other with a mean of 0.12 N/m^2. For the same sediment, incipient erosion occurs at the same shear stress because the surface shear strength (equal to applied shear stress) is unaffected by overburden. Hence bed preparation procedure or density do not significantly influence τ_{co}. τ_c has been calculated by two methods - A corresponding to Figs. 38, 39 and B corresponding to Figs. 40 and 41; the latter method being applied to deposited (soft) beds only, since for dense beds the two methods yield identical results. Values obtained by B are generally slightly lower (except in test 4) than A, but are of comparable magnitudes. M values are obtained from linear slopes in Figs. 36, 38 and 39.

In Fig. 42, τ_c (both methods) is plotted against ρ_B. The following may be considered as a representative relationship encompassing all data:

$$\tau_c = 1.04\ (\rho_B - 1) \tag{3}$$

In Fig. 43, M is plotted against τ_c yielding the following relationship (without consideration for the influences of bed structure or flow):

$$M = 1.06 \times 10^{-3} e^{-2.33\ \tau_c} \tag{4}$$

With respect to Eq. 3, the trend of increasing τ_c with bed density is in agreement with previous observations (Mehta et al., 1982). Likewise, others have previously reported the trend of decreasing M with increasing τ_c evident in Fig. 43 and Eq. 4 (Ariathurai and Arulanandan, 1978; Hunt, 1981).

Table 9. Bay Mud Erosion Rate Constants

Test No.	τ_{co} (N/m^2)	τ_c		M (g/cm^2-min)
		A (N/m^2)	B (N/m^2)	
1	0.12	0.65	-[b]	2.8×10^{-4}
2	0.16	0.35	0.23	3.2×10^{-4}
3	-[a]	0.12	0.05	5.0×10^{-4}
4	0.10	0.26	0.30	7.4×10^{-4}
5	0.10	0.28	0.20	7.4×10^{-4}
P1	0.12	0.38	-[b]	2.1×10^{-5}
P2	0.12	1.20	-[b]	7.8×10^{-5}

[a]Insufficient data

[b]Method A not applied

IV. CONCLUDING REMARKS

The relationships considered to be representative of the rate of erosion of bay mud are as follows:

$$\varepsilon = M \left(\frac{\tau_b}{\tau_c} - 1\right) \tag{2}$$

$$\tau_c = 1.04 \ (\rho_B - 1) \tag{3}$$

$$M = 0.00106 \exp(- 2.33 \ \tau_c) \tag{4}$$

$$\tau_b = \frac{\rho g n^2}{h^{1/3}} u^2 \tag{5}$$

noting that in Eq. 2, τ_c and τ_B, used previously, have the same meaning.

In Eq. 5, n is Manning's bottom resistance coefficient, h is depth of flow and u is current speed. An example is considered in Fig. 44 where the rate of erosion, ε, is plotted against current speed, u, (0-1.5 m/sec), for different values of the bed bulk density, ρ_B (1.2, 1.4 and 1.6 g/cm^3). h = 10 m and n = 0.020 were selected arbitrarily as typical representative estuarine values. The influence of ρ_B (which also reflects bed "aging") on ε

in this "design chart" is observed to be quite significant. Soft beds (1.2 g/cm^3) generally have an order of magnitude (~ 10^{-2} g/cm^2 min) greater rate of erosion than do dense (1.6 g/cm^3) beds (~ 10^{-3} g/cm^2-min) at the same speed (~ 1.3 m/sec).

APPENDIX

VELOCITY AND SHEAR STRESS CALCULATIONS

The original plan for the rocking flume designated a height of 22 cm. Early experiments determined that this height would not allow for sufficient water depth to generate a large enough shear stress on the bed surface. The height of the flume was therefore increased to 36 cm. A second modification was made with the addition of a plexiglass top constriction over the center of the flume (Fig. 6b,c). This constriction increased the flow velocity over the sediment bed. The top could be set at any selected depth over the bed.

Flume Calibration. To calculate the shear stress in the flume it was necessary to know the velocity of water above the bed. Three different techniques were used to measure velocity. In all cases maximum velocity was measured. Following is a brief description of the methods employed and a comparison of the results obtained. Calculations are made of the shear stress with and without the top in place. Calibration marks were added to the speed controller of the flume, so that wave period and velocity could be determined at specific settings.

For a shallow water wave the velocity profile over the water depth is fairly constant, at least within the detection limits employed. The simplest method of measuring velocity is to determine the horizontal displacement of a particle floating on the surface at the node. From the distance traveled the maximum velocity can be calculated from the relationship $u_m = \pi d/T$ where d is displacement and T is wave period. This measurement could only be made without the top constriction in the flume. Once the top was in place new estimates of velocity were made by assuming that the only effect of the top was to increase water velocity at the center of the flume. From the equation of continuity, the same volume of water, 17.5 cm deep, had to pass the center, but there were only 10 cm of depth for it below the top. New velocities were calculated from a ratio of water depths at the ends and the middle of the flume. A ratio of 1.75 (velocity with top divided by velocity without top) was determined. Table A.1 contains velocities obtained by the method of horizontal displacement.

Table A.1. Maximum Velocities Obtained by Measurement of Horizontal Displacement, without and with Top Constriction

Wave period, T (sec)	Horizontal displacement, d (cm)	Maximum velocity, u_m without top (cm/sec)	Maximum velocity, u_m with top (cm/sec)
13.0	25	6.0	10.6
8.0	27	10.6	18.6
6.6	28	13.3	23.3
6.1	30	15.5	27.0
5.7	33	18.2	31.8
5.4	36	20.8	36.4
5.2	38	23.0	40.2
5.1	40	24.6	43.1
5.0	50	31.7	55.5

The most direct method of measuring velocity was with a current meter. The current meter was an electro-magnetic unit made by Marsh McBirney (model 523), with an accuracy of 3 cm/s. Measurements were taken at a height of 2 cm above the bed at the center of the flume. Data were recorded on a Hewlett-Packard strip chart recorder so that the mean maximum velocity could be determined. Table A.2 contains velocity (and wave period) data obtained using the meter.

The third method involved measuring the displacement of water above and below still water level, at the ends of the flume. Velocity was calculated by determining the total volume of water that moved through the flume without and with the top in place over one-half a wave period (see Fig. A.1). The maximum velocity, u_m, without the top is

$$u_m = \frac{\pi A_d}{T h} \qquad (A.1)$$

where A_d is the longitudinal (vertical) area of water displaced during one-half period, and h is the still water depth. A_d is obtained from (for small displacements):

Table A.2. Periods of Oscillation and Velocities Obtained from Current Meter in the Rocking Flume

Period, T (sec)	Max.velocity, u_m (cm/sec)
33.6	3.1
35.0	3.7
21.5	4.6
13.0	10.5
11.0	13.7
9.1	16.3
7.8	19.1
7.4	20.1
7.2	20.8
6.6	23.4
6.1	27.0
5.7	32.3
5.5	36.4
5.2	43.0
5.1	47.0

Table A.3. Maximum Velocities Obtained by Considering Flow Continuity

Wave period, T (sec)	Maximum velocity, u_m without top (cm/sec)	Maximum velocity, u_m with top (cm/sec)
13.0	4.8	8.1
8.0	9.2	15.4
6.6	12.0	20.7
6.1	14.3	26.0
5.7	15.9	32.1
5.5	19.5	36.2
5.2	20.7	45.0
5.1	23.8	52.0

$$A_d = L\left(\frac{A}{\pi} + \frac{B}{4}\right) \qquad (A.2)$$

where A/2 = vertical displacement amplitude at flume ends relative to still water level, B/2 = vertical displacement amplitude of flume bottom and L = flume length. In Eq. A.2, the water surface profile is assumed to vary sinusoidally. With the top in place, A_d was appropriately modified. Results are presented in Table A.3.

The maximum applied shear stress was calculated from the following relationships established by Jonsson (1966); $\tau_{max}=0.5\rho f_w u_m^2$, where ρ is water density, f_w is the coefficient of friction, and u_m is maximum velocity. The coefficient of friction can be calculated as $f_w=0.09\ Re^{-0.2}$, where Re is the wave Reynolds number. The Reynolds number can be calculated as $u_m^2/\sigma\nu$, where u_m is maximum velocity, σ is wave angular frequency ($2\pi/T$), and ν is kinematic viscosity of water. For these experiments the kinematic viscosity was taken to be 1×10^{-2} cm^2/sec and ρ as 1 g/cm^3. These calculations are based on fresh water.

Calculation of shear stress using Jonsson's formula yields the maximum applied shear stress. This formula is valid for progressive waves generating (smooth) turbulent flows. In dealing with a standing wave, the applied shear stress is not constant, but oscillates as a square sine function. To adjust for this difference the maximum velocity was used to calculate a maximum shear stress, τ_m. By integrating shear stress over one-half a wave period the mean shear stress was determined. The result is that mean shear stress is one-half the maximum shear stress. Justification for this manipulation was based on the correlation of results of critical shear stresses obtained in the rocking flume compared to those obtained in the annular flume.

A calibration curve between maximum velocity, u_m, and wave period, T, is presented in Fig. A.2, based on data in Tables A.1, A.2 and A.3. The corresponding relationship between the average bed shear stress, τ_b, and wave period, T, is given in Fig. A.3.

LITERATURE CITED

American Public Health Association, Standard Methods for the Examination of Water and Wastewater, 14th ed., American Public Health Association, New York, 1975.

Ariathurai, R., and Arulanandan, K., "Erosion of Cohesive Soils," Journal of the Hydraulics Division, ASCE, Vol. 104, No. HY2, February, 1978, pp. 279-283.

ASTM, 1981 Annual Book of ASTM Standards, American Society for Testing and Materials, Philadelphia, Pennsylvania, 1981.

Hunt, S.D. and Mehta, A.J., "An Evaluation of Laboratory Data on Erosion of Fine Sediment Beds," Paper Presented at the Annual Meeting of the Fine Particle Society, Miami, Florida, April, 1985.

Jonsson, I.G., "Wave Boundary Layers and Friction Factors," Proceedings of the 10th Coastal Engineering Conference, ASCE, Vol. 1, Tokyo, Japan, 1966, pp. 127-148.

Krone, R.B., "Sedimentation in San Francisco Bay System," In: San Francisco Bay: The Urbanized Estuary, California Academy of Sciences, San Fancisco, California, 1979, pp. 177-190.

Maa, P.Y., "Erosion of Soft Muds by Waves," Ph.D. Dissertation, University of Florida, Gainesville, Florida, 1986.

Mehta, A.J., "Depositional Behavior of Cohesive Sediments," Ph.D. Dissertation, University of Florida, Gainesville Florida, 1973.

Mehta, A.J., Parchure, T.M., Dixit, J.G., and Ariathurai, R., "Resuspension of Deposited Cohesive Sediment Beds," In: Estuarine Comparisons, V.S. Kennedy Editor, Academic Press, New York, 1982, pp. 591-609.

Parchure, T.M., "Erosional Behavior of Deposited Cohesive Sediments," Ph.D. Dissertation, University of Florida, Gainesville, Florida, 1984.

Parchure, T.M. and Mehta, A.J., "Erosion of Soft Cohesive Sediment Deposits," Journal of Hydraulic Engineering, ASCE, Vol. 3, No. 10, October 1985, pp. 1308-1326.

Partheniades, E., "A Study of Erosion and Deposition of Cohesive Soils in Salt Water," Ph.D. Dissertation, University of California, Berkeley, California, 1962.

Partheniades, E., "Erosion and Deposition of Cohesive Soils, Journal of the Hydraulics Division, ASCE, Vol. 91 No HY1, January, 1965, pp. 105-139.

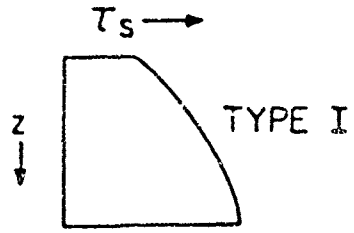

Fig. 1. Variation of Bed Shear Strength with Depth for a Deposited Bed, Type I Profile (after Parchure, 1984).

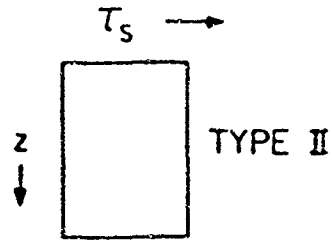

Fig. 2. Variation of Bed Shear Strength with Depth for a Placed Bed, Type II Profile (after Parchure, 1984).

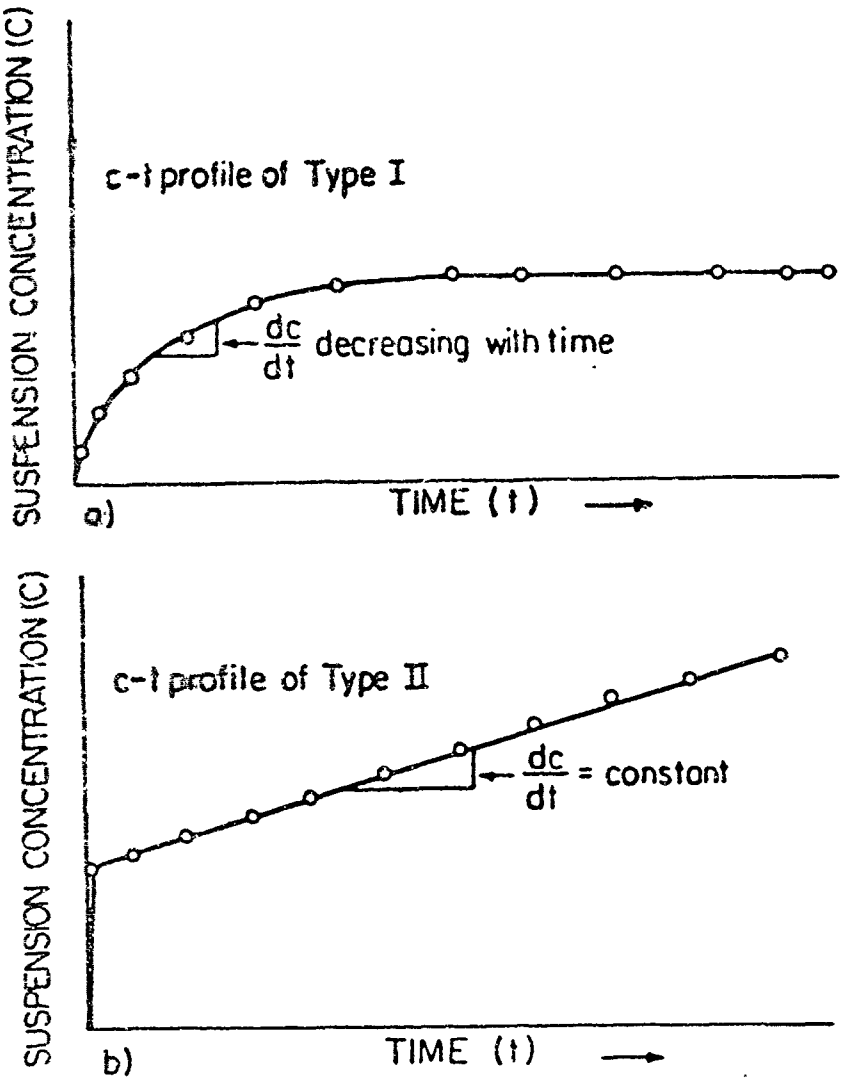

Fig. 3a. Concentration-Time Profile for a Deposited Bed (Type I) (after Parchure, 1984).

Fig. 3b. Concentration-Time Profile for a Placed Bed (Type II) (after Parchure, 1984).

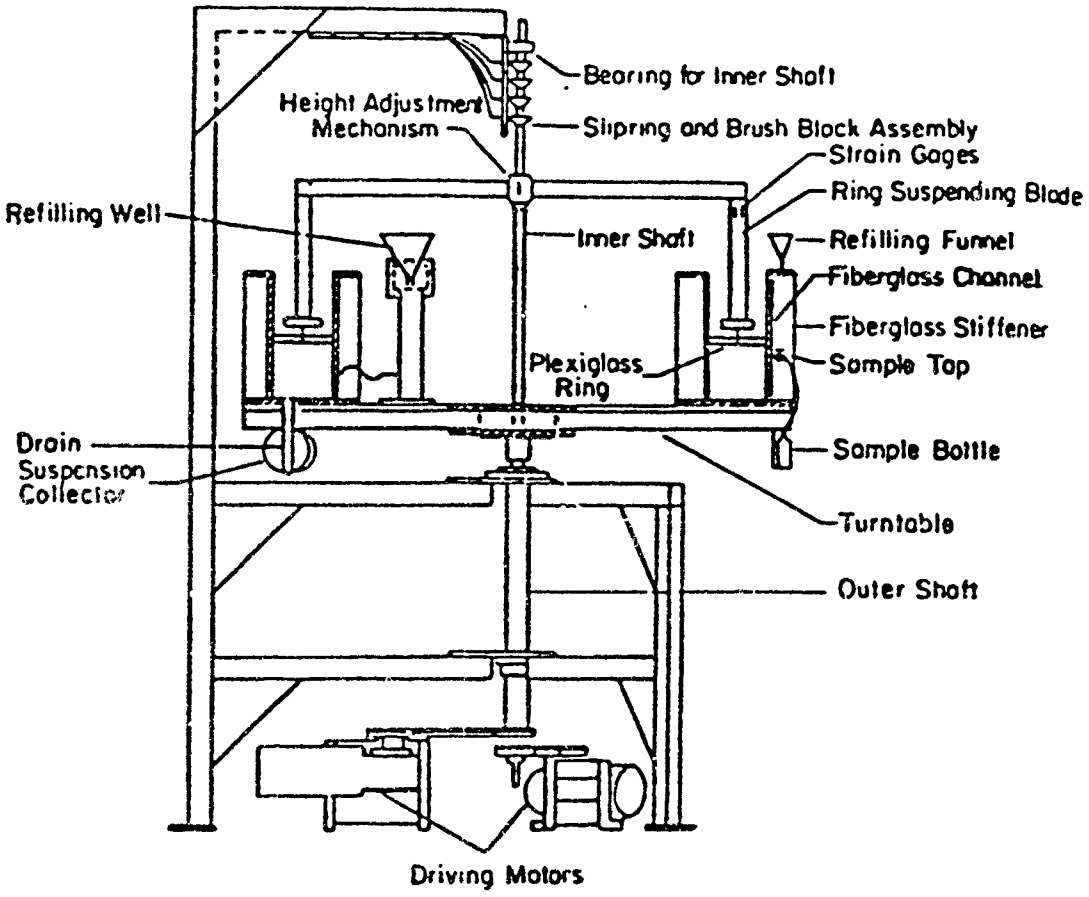

Fig. 4. Schematic View of Annular Flume (after Mehta, 1973).

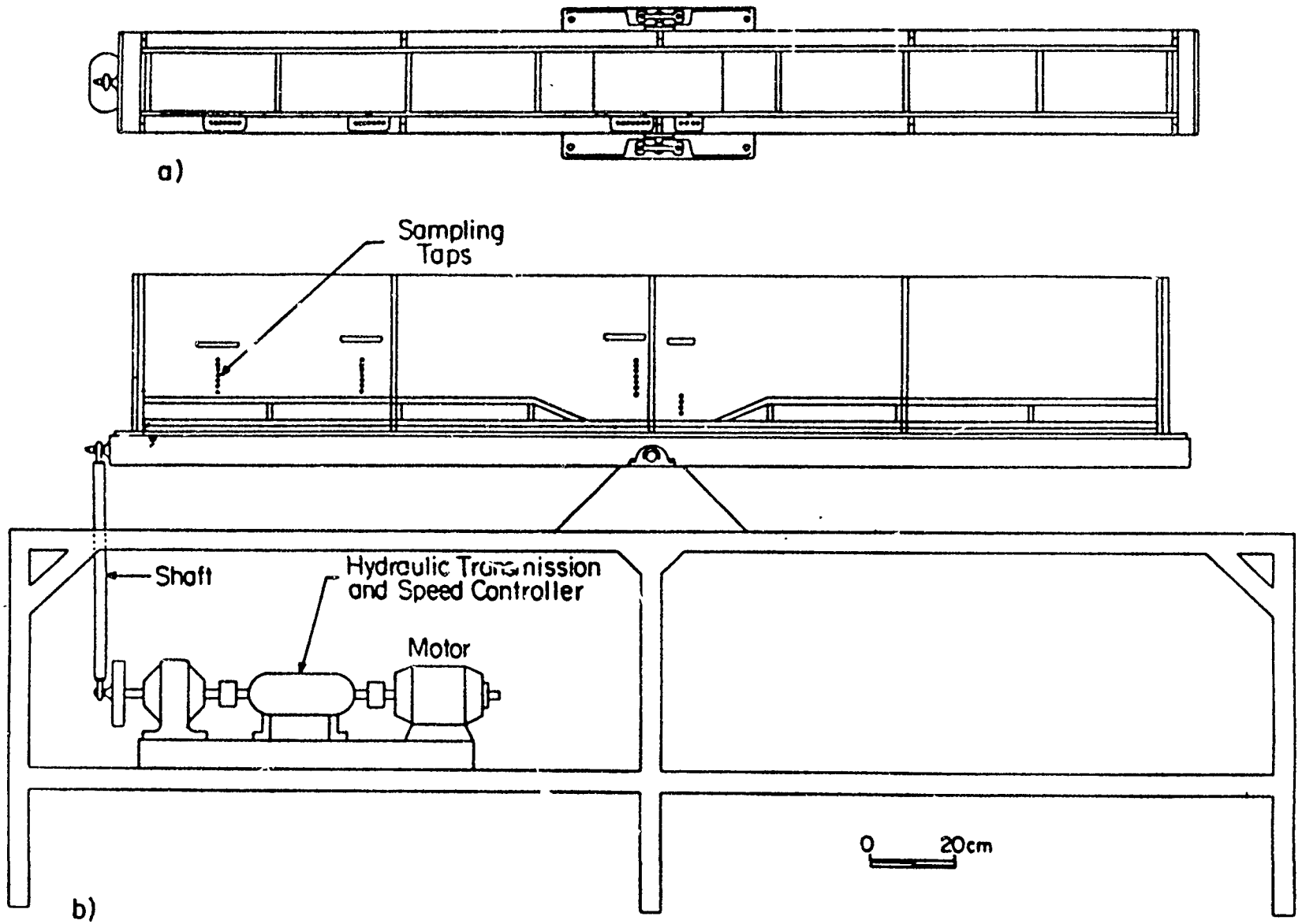

Fig. 5a. Plan View of Rocking Flume.
Fig. 5b. Elevation View of Rocking Flume.

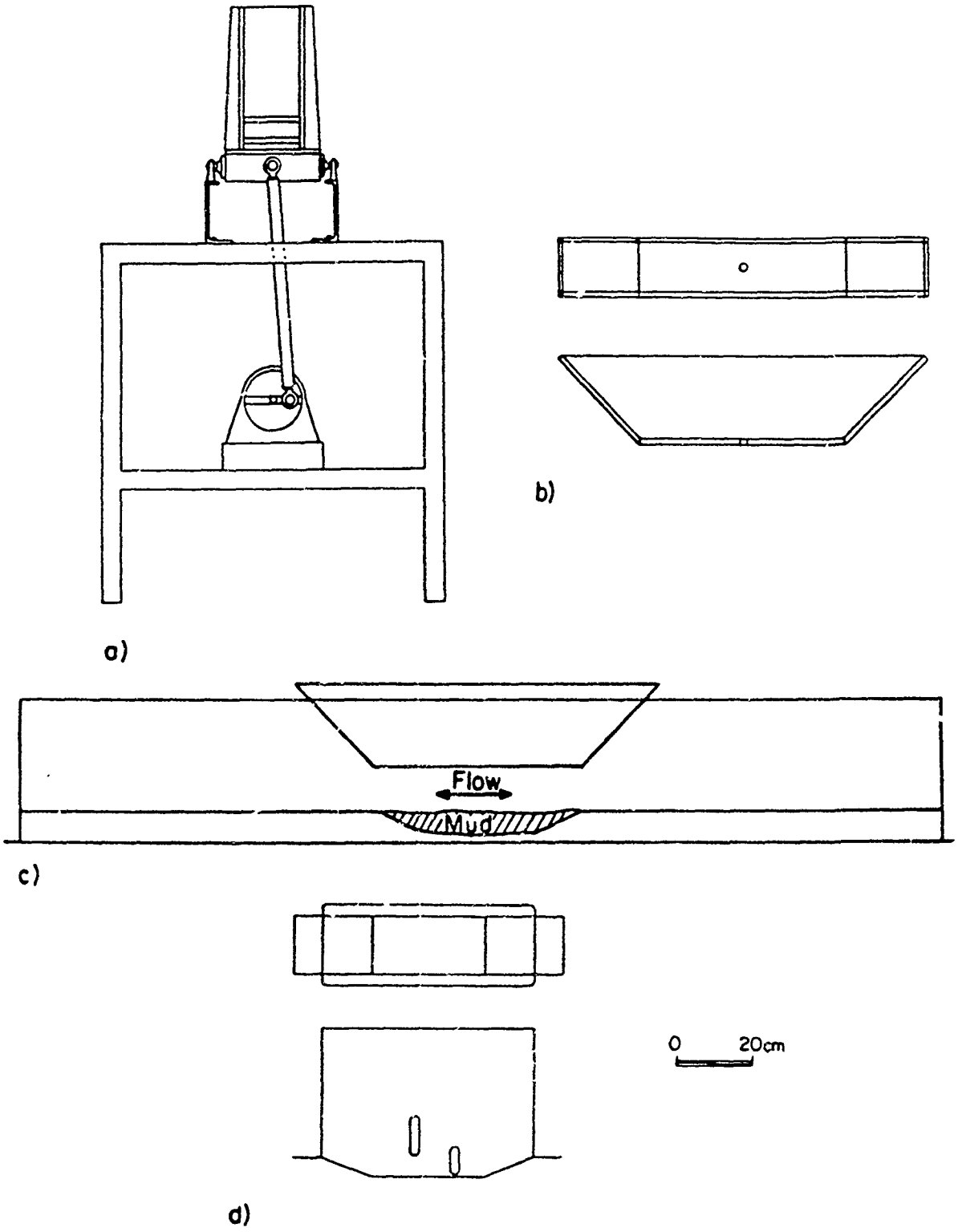

Fig. 6a. Side View of Rocking Flume.
Fig. 6b. Top Constriction for Rocking Flume.
Fig. 6c. Top Constriction Placed in the Rocking Flume.
Fig. 6d. Removable Sheet Metal Bed for Rocking Flume.

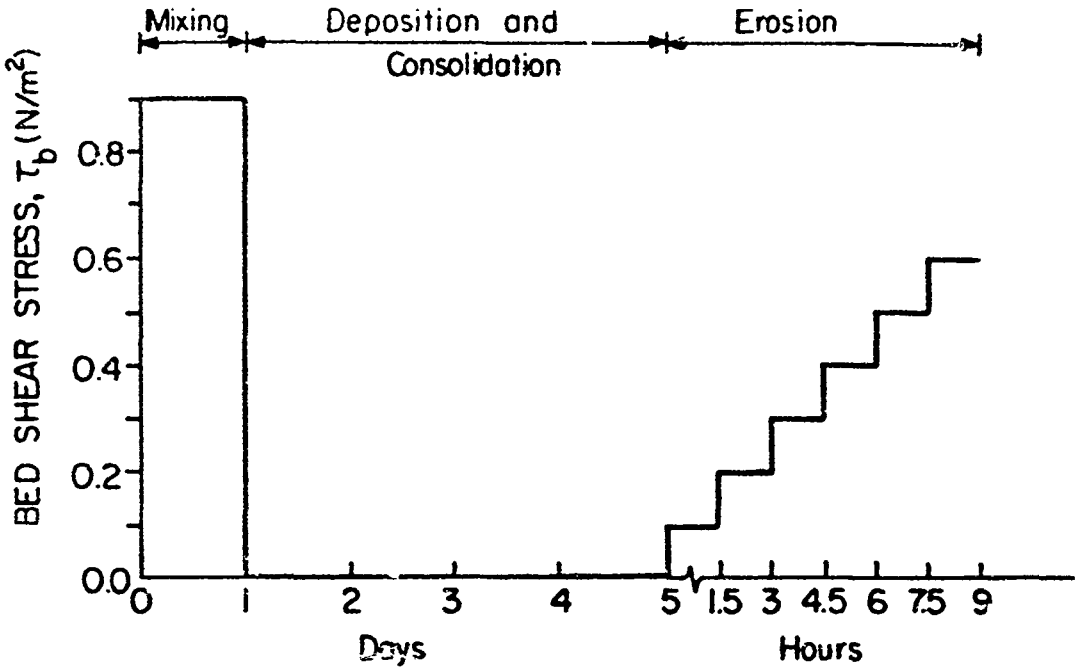

Fig. 7. Experimental Test Procedure (Shear Stress Variation).

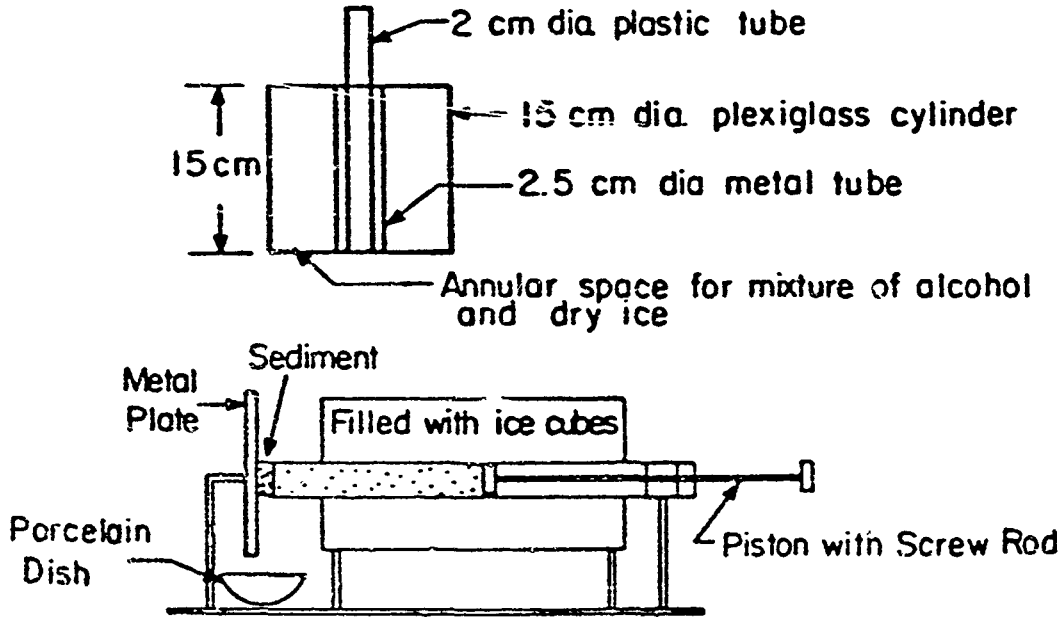

Fig. 8. Apparatus for Measurement of Density as a Function of Depth (after Parchure, 1984).

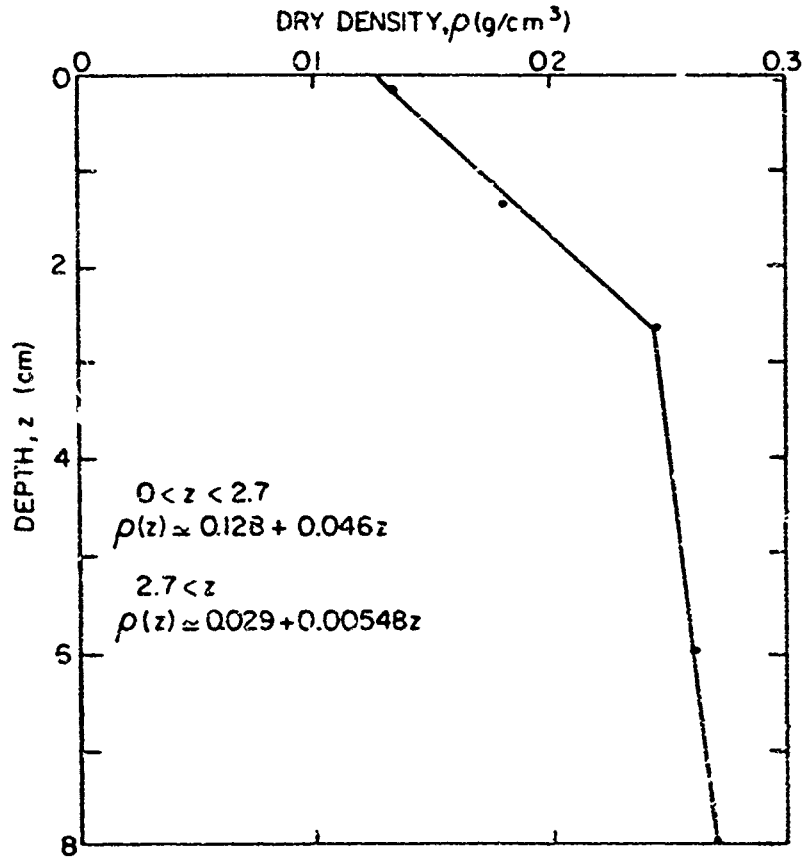

Fig. 9. Density (Dry) Profile as a Function of Depth for Deposited Kaolinite.

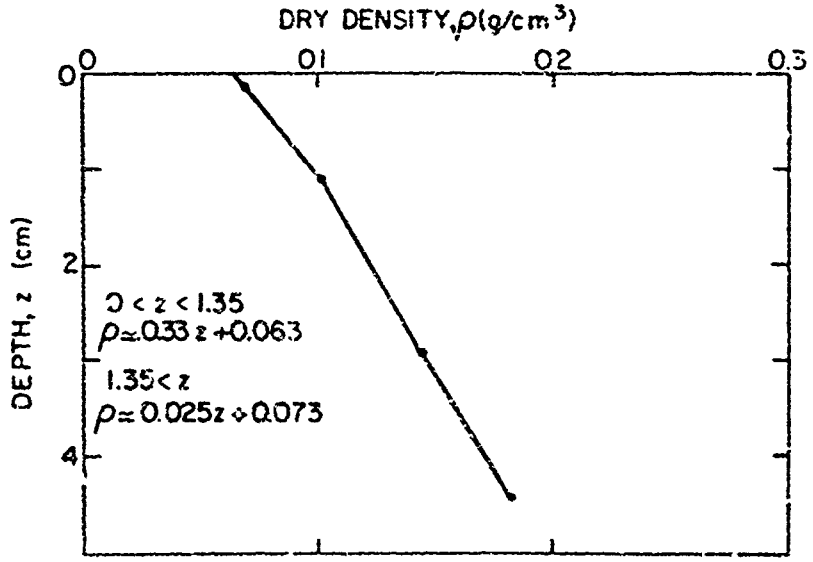

Fig. 10. Density (Dry) Profile as a Function of Depth for Deposited Cedar Key Mud.

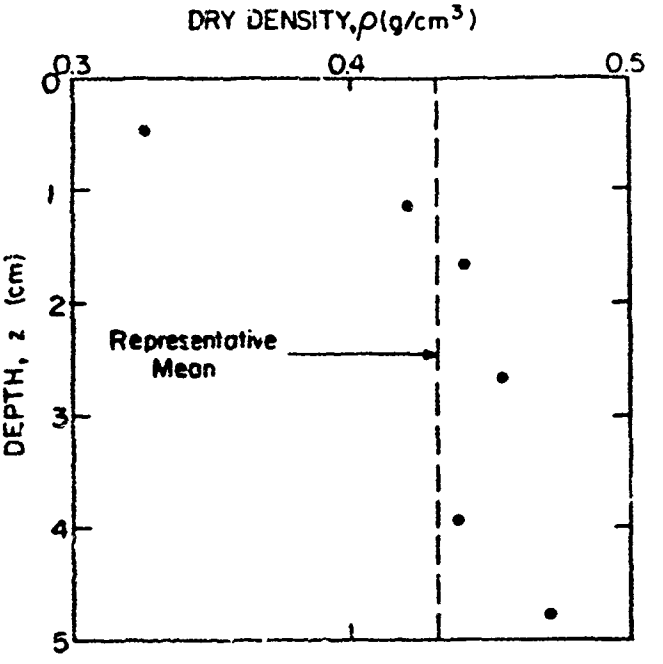

Fig. 11. Density (Dry) Profile as a Function of Depth for Placed Kaolinite.

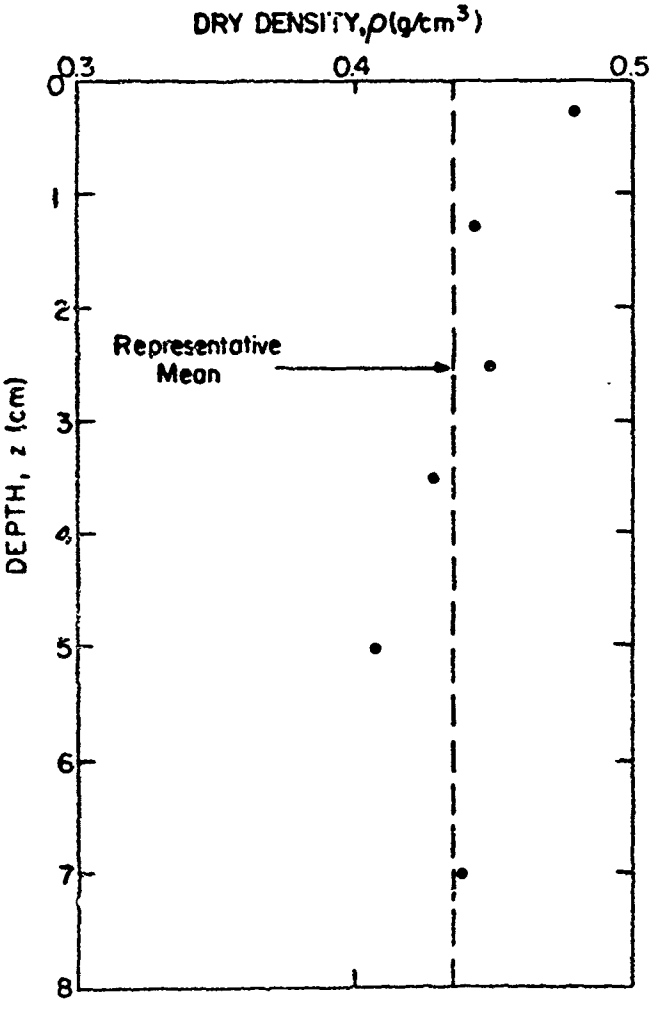

Fig. 12. Density (Dry) Profile as a Function of Depth for Placed Cedar Key Mud.

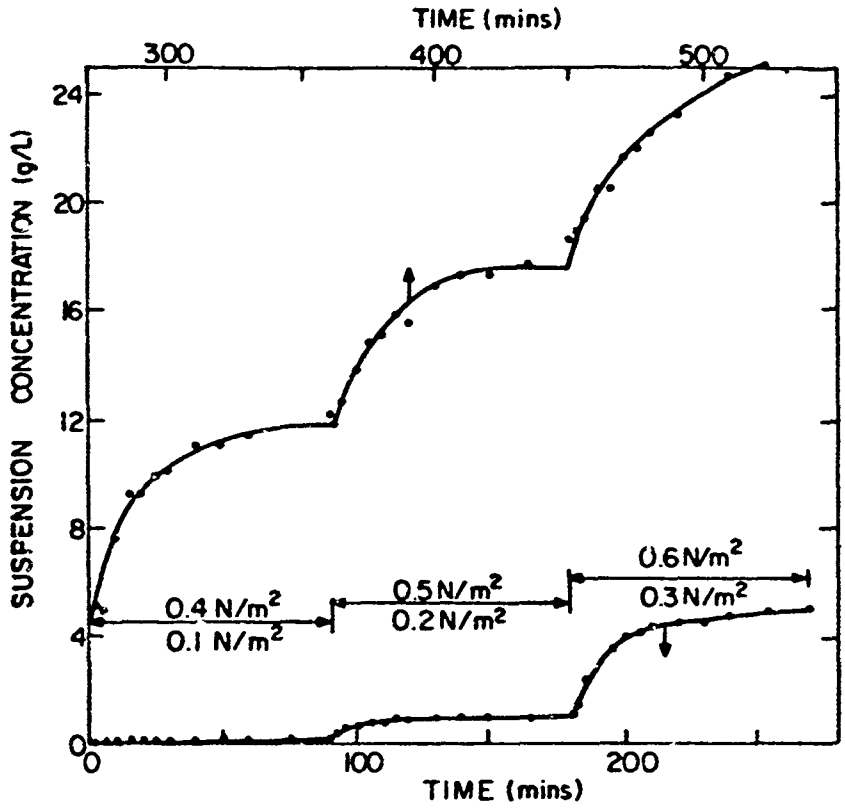

Fig. 13. Suspended Sediment Concentration versus Time for Deposited Kaolinite, Annular Flume.

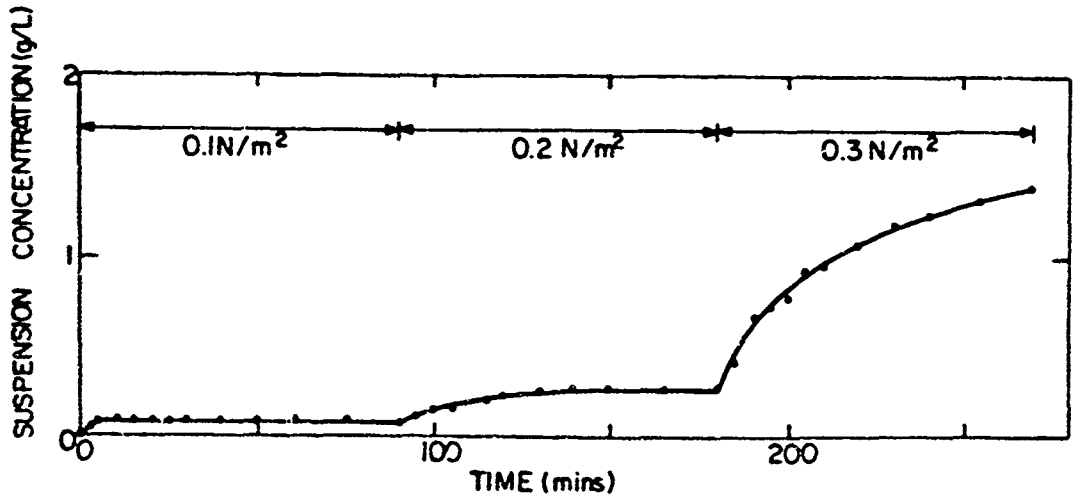

Fig. 14. Suspended Sediment Concentration versus Time, Deposited Kaolinite, Rocking Flume.

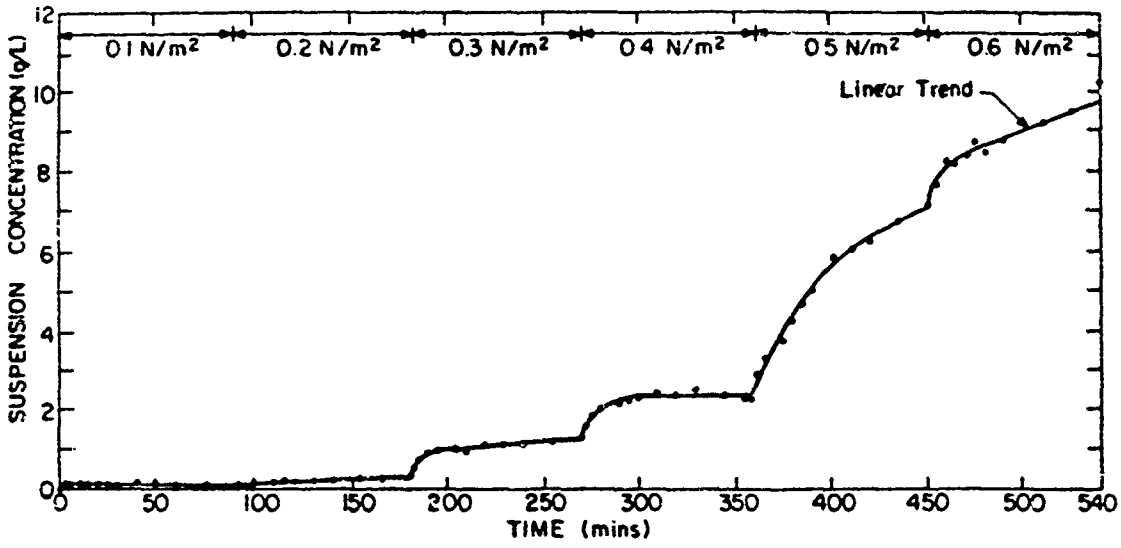

Fig. 15. Suspended Sediment Concentration versus Time for Deposited Cedar Key Mud, Annular Flume.

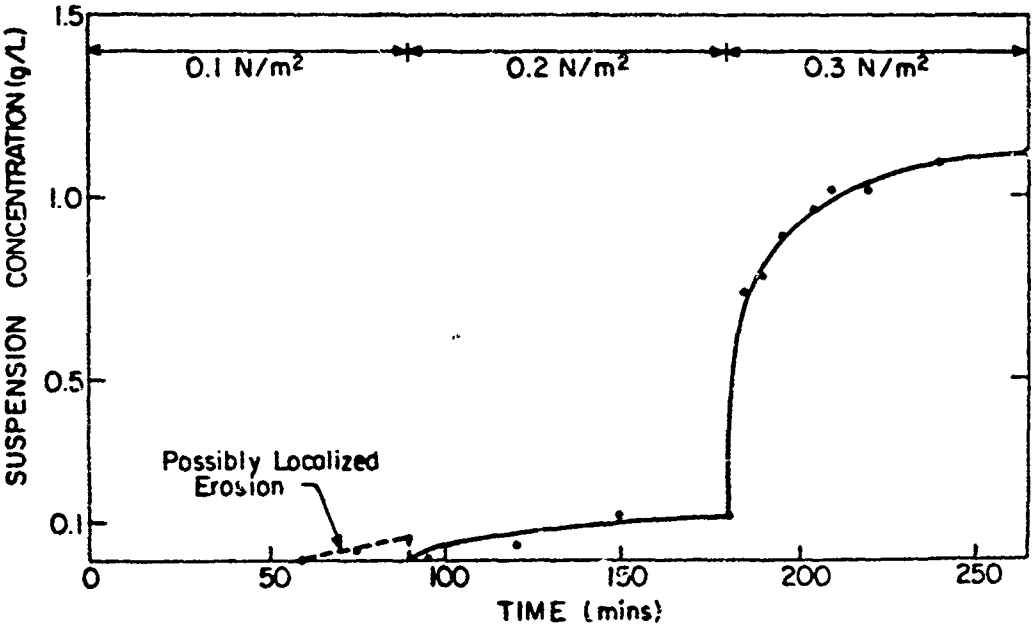

Fig. 16. Suspended Sediment Concentration versus Time, Deposited Cedar Key Mud, Rocking Flume.

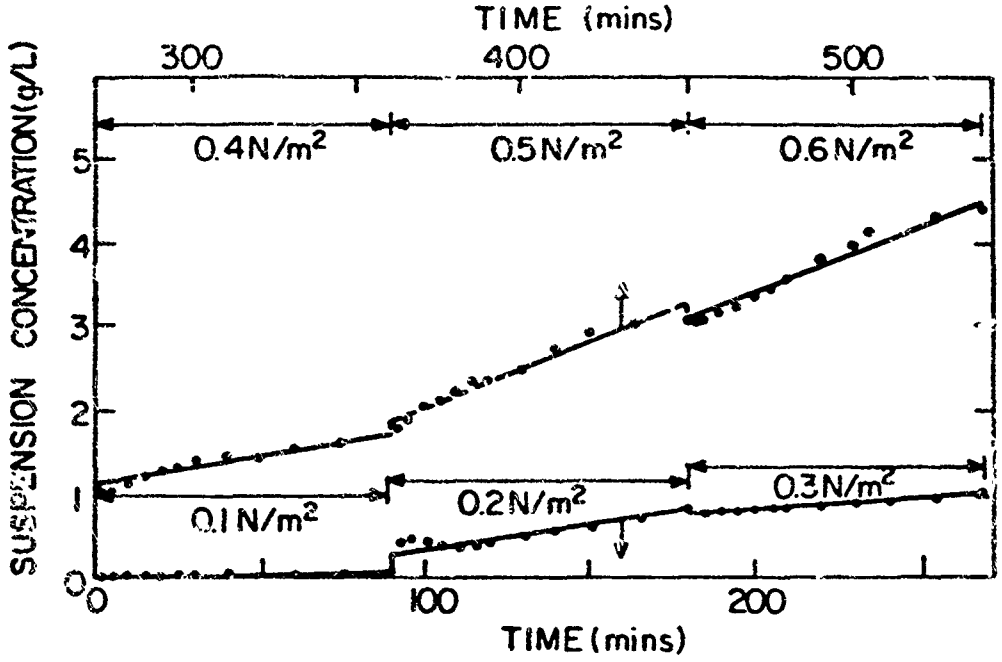

Fig. 17. Suspended Sediment Concentration versus Time, Placed Kaolinite, Annular Flume.

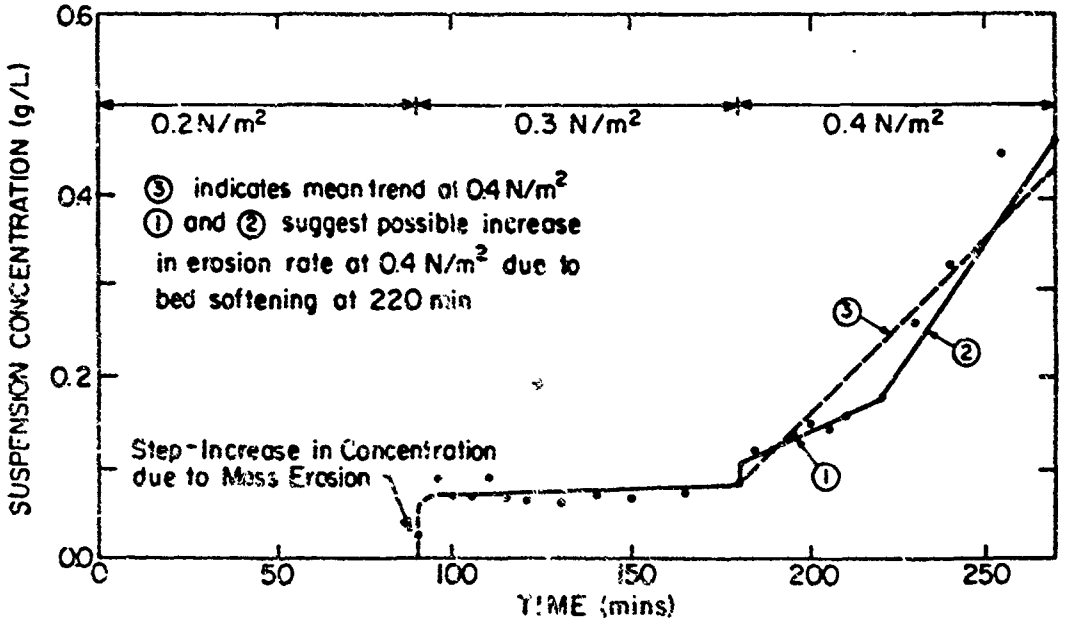

Fig. 18. Suspended Sediment Concentration versus Time, Placed Kaolinite, Rocking Flume.

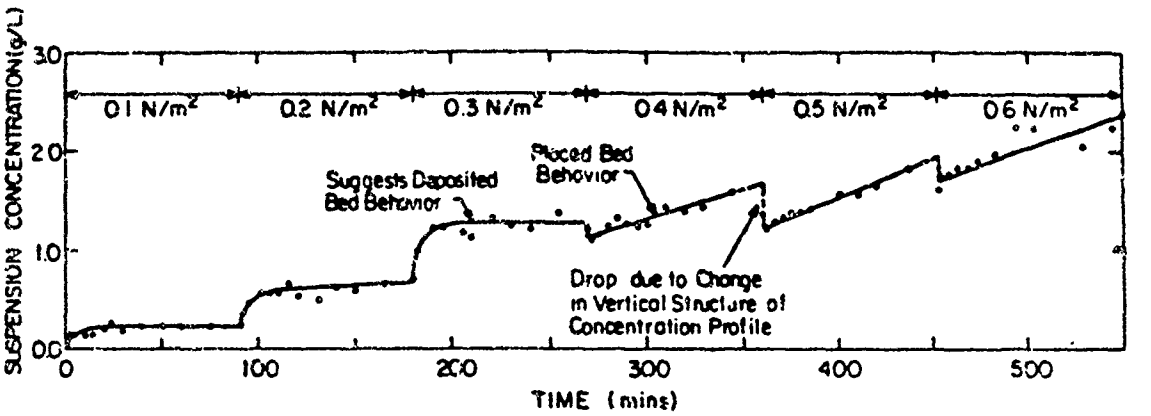

Fig. 19. Suspended Sediment Concentration versus Time, Deposited Cedar Key Mud, Annular Flume.

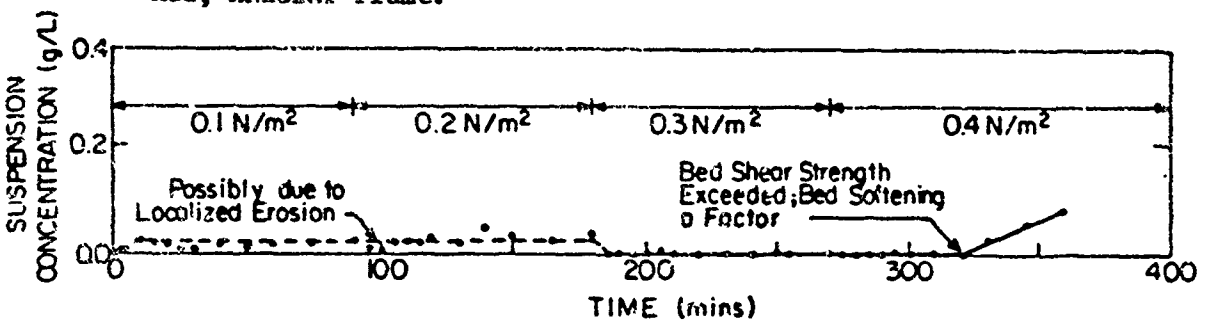

Fig. 20. Suspended Sediment Concentration versus Time, Placed Cedar Key Mud, Rocking Flume.

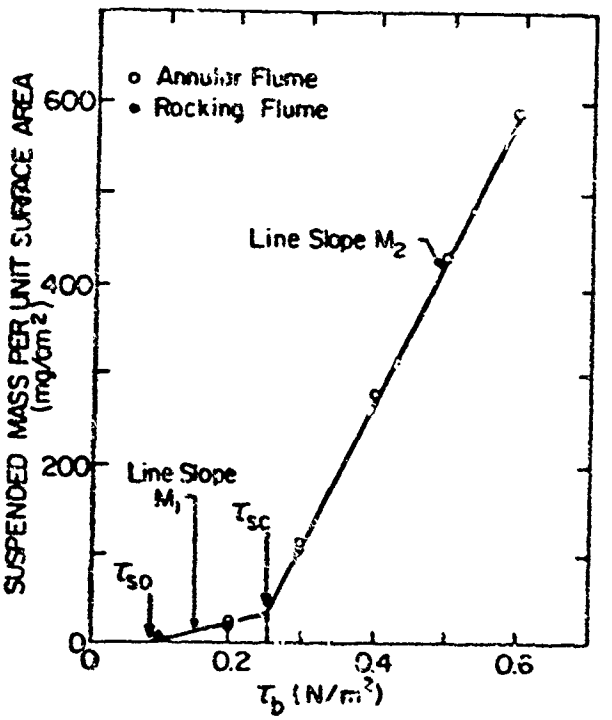

Fig. 21. Mass Per Unit Surface Area versus Shear Stress, Deposited Kaolinite, Both Flumes.

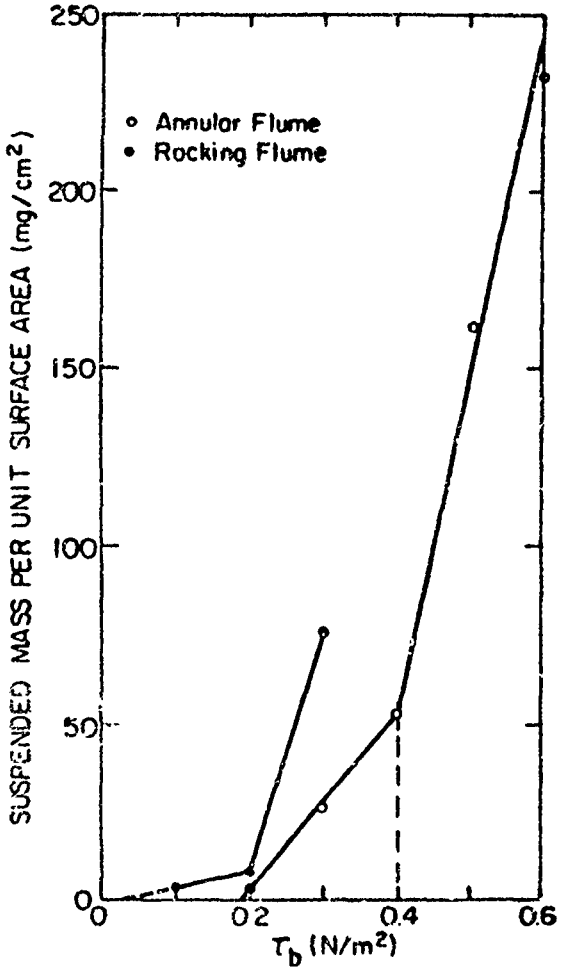

Fig. 22. Mass Per Unit Surface Area versus Shear Stress, Deposited Cedar Key Mud, Both Flumes.

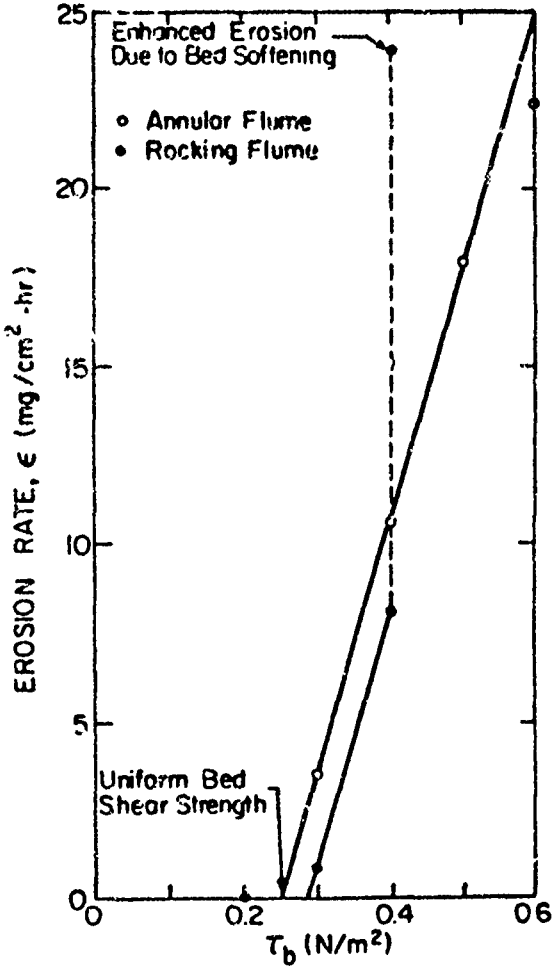

Fig. 23. Erosion Rate versus Shear Stress, Placed Kaolinite, Both Flumes.

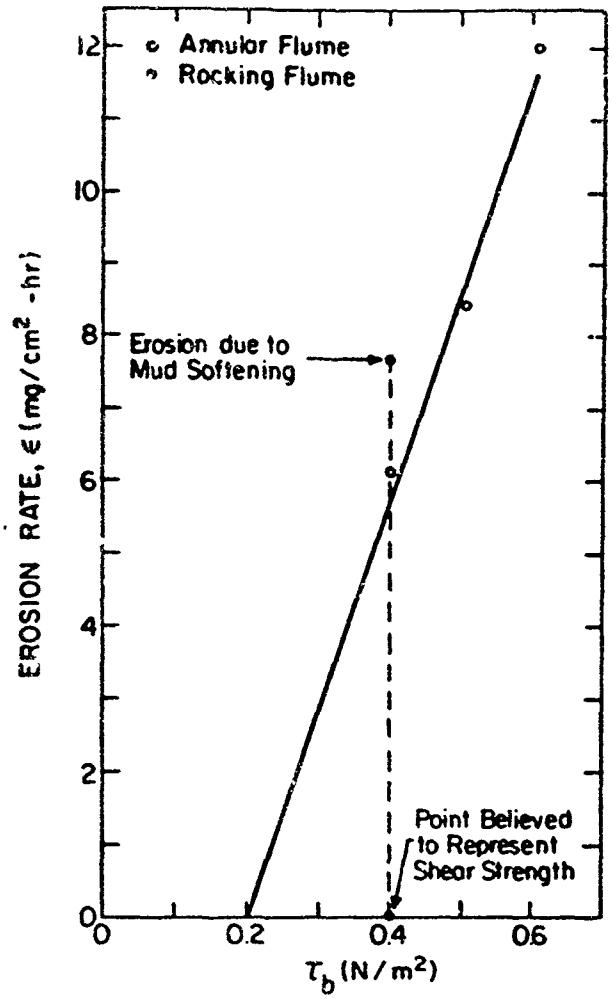

Fig. 24. Erosion Rate versus Shear Stress, Placed Cedar Key Mud, Both Flumes.

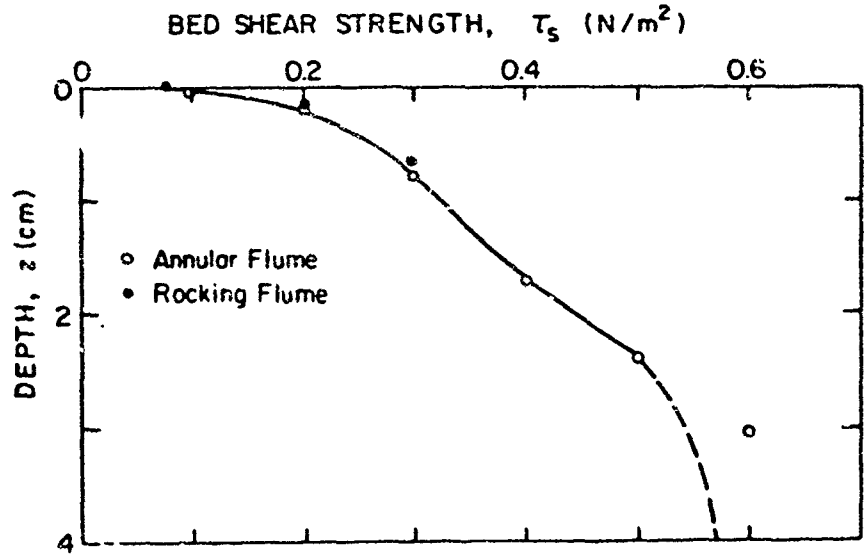

Fig. 25. Variation of Bed Shear Strength with Depth for Deposited Kaolinite, Both Flumes.

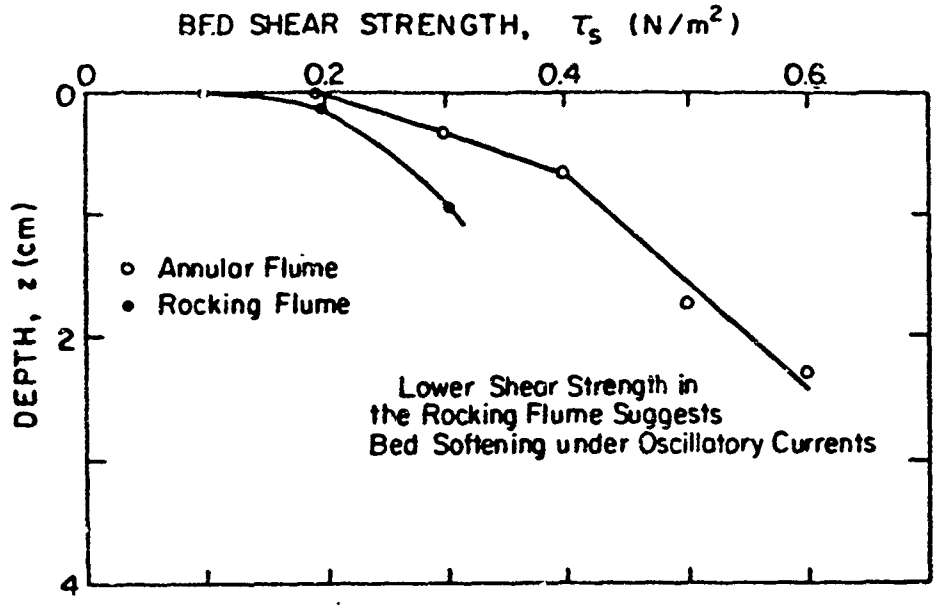

Fig. 26. Variation of Bed Shear Strength with Depth for Deposited Cedar Key Mud, Both Flumes.

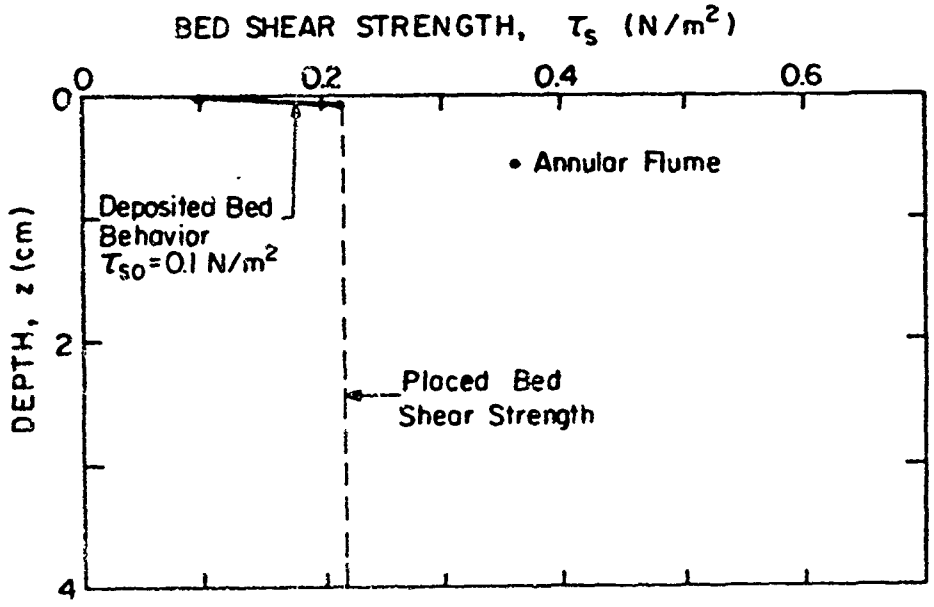

Fig. 27. Variation of Bed Shear Strength with Depth for Placed Cedar Key Mud, Annular Flume.

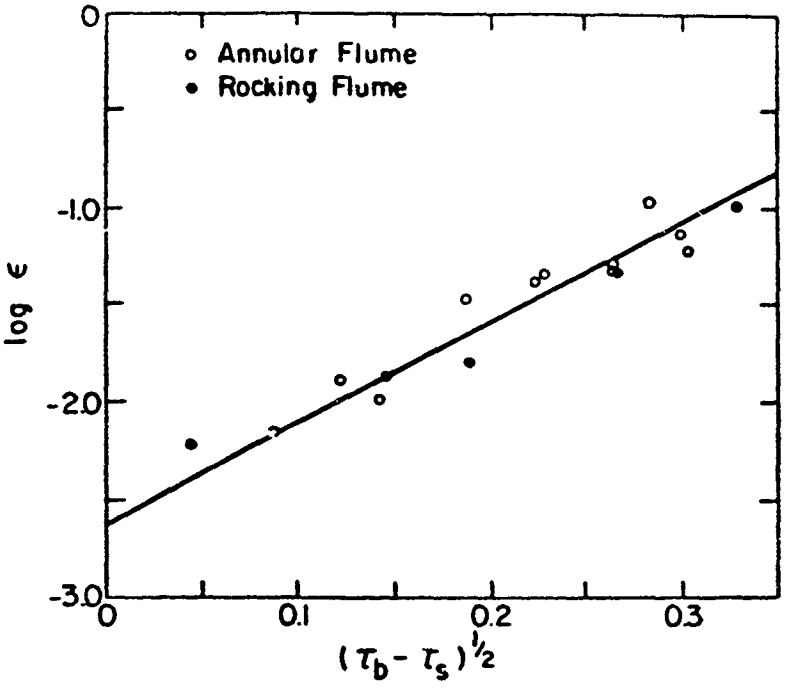

Fig. 28. Log ε versus $(\tau_b - \tau_s)^{0.5}$ for Deposited Kaolinite, Both Flumes.

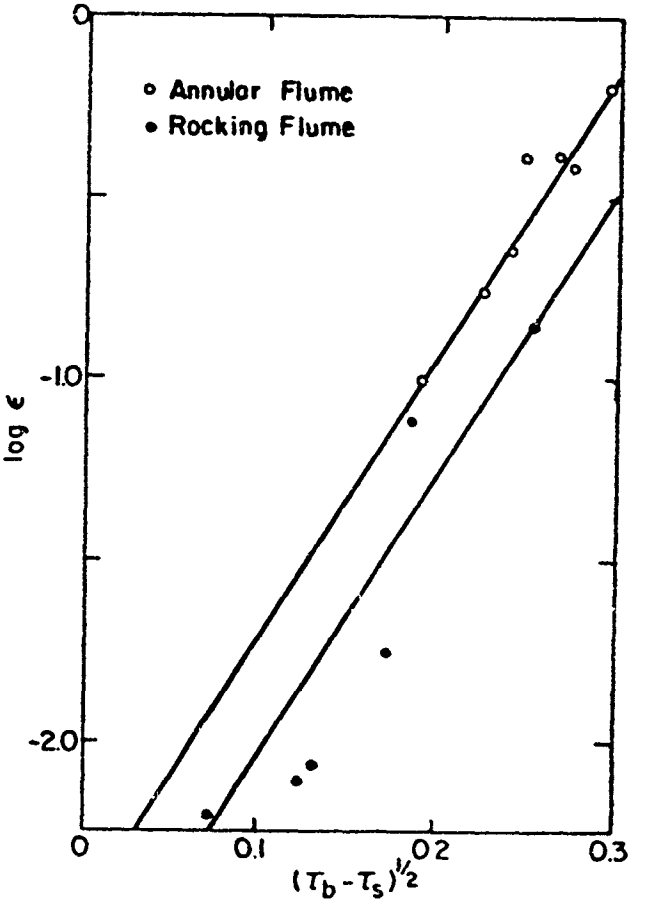

Fig. 29. Log ε versus $(\tau_b - \tau_s)^{0.5}$ for Deposited Cedar Key Mud, Both Flumes.

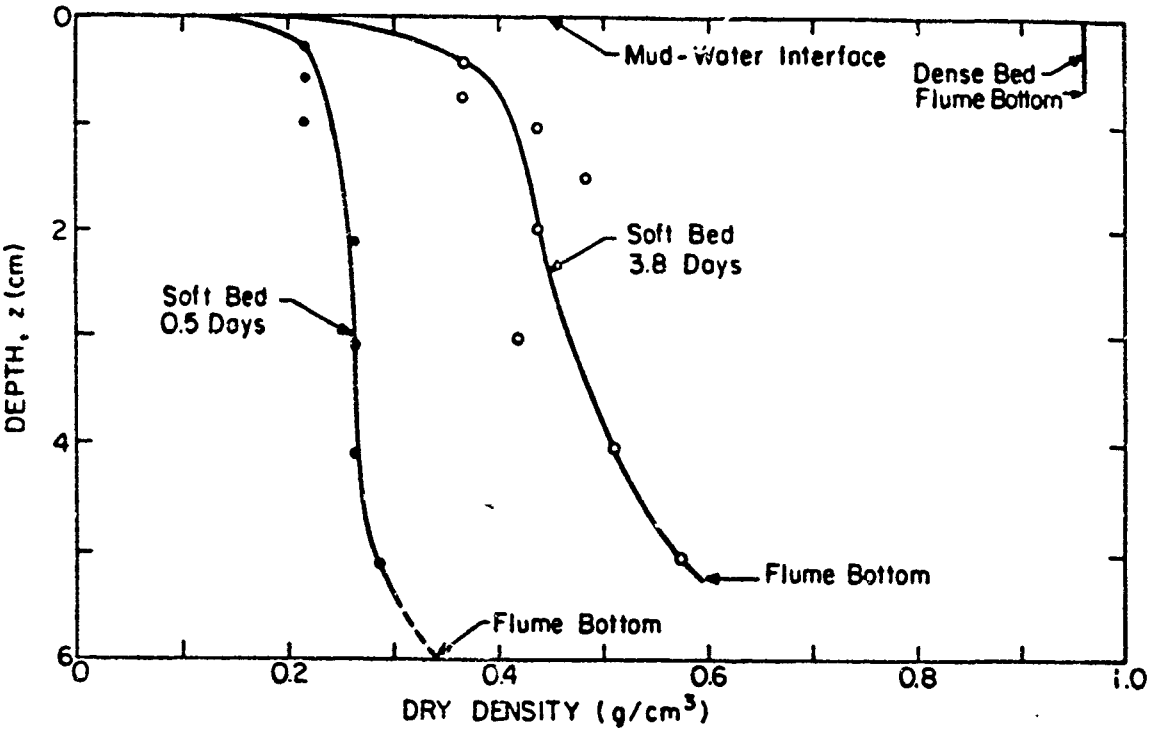

Fig. 30. Bed Dry Density Profiles, Bay Mud.

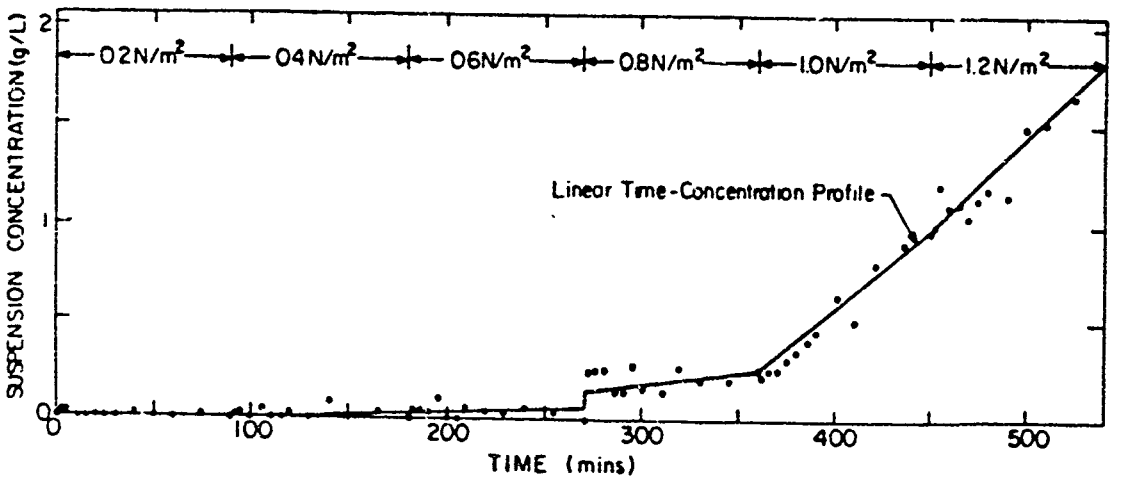

Fig. 31. Time-Concentration Relationship, Bay Mud, Dense Bed, Annular Flume (Test 1).

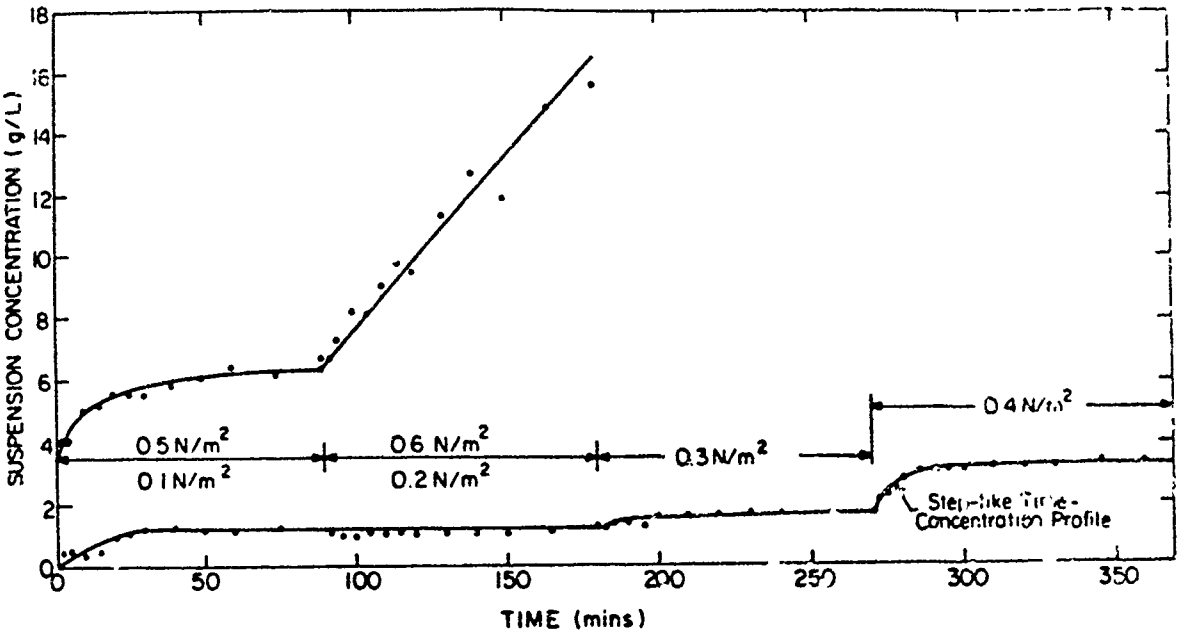

Fig. 32. Time-Concentration Relationship, Bay Mud, Deposited Bed, 0.5 Day Consolidation, Annular Flume (Test 2).

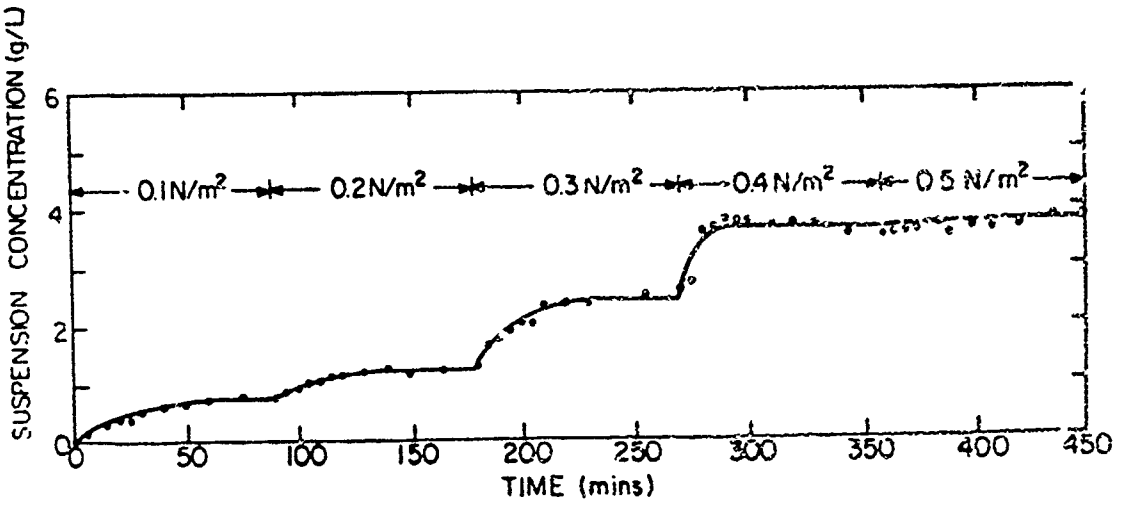

Fig. 33. Time-Concentration Relationship, Bay Mud, Deposited Bed, 0.5 Day Consolidation, Rocking Flume (Test 3).

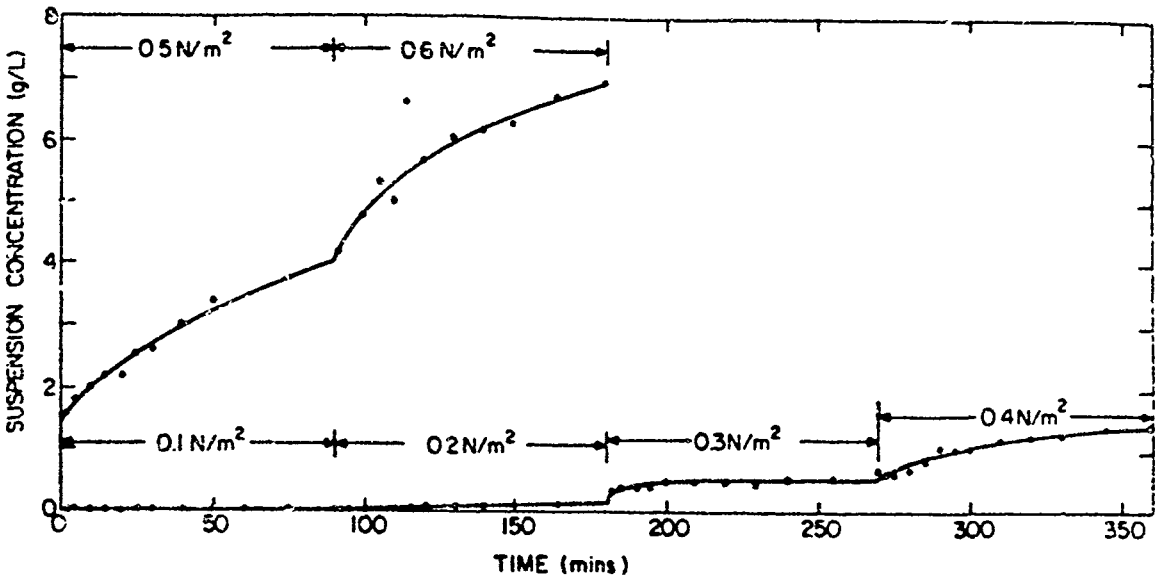

Fig. 34. Time-Concentration Relationship, Bay Mud, Deposited Bed, 3.8 Day Consolidation, Annular Flume (Test 4).

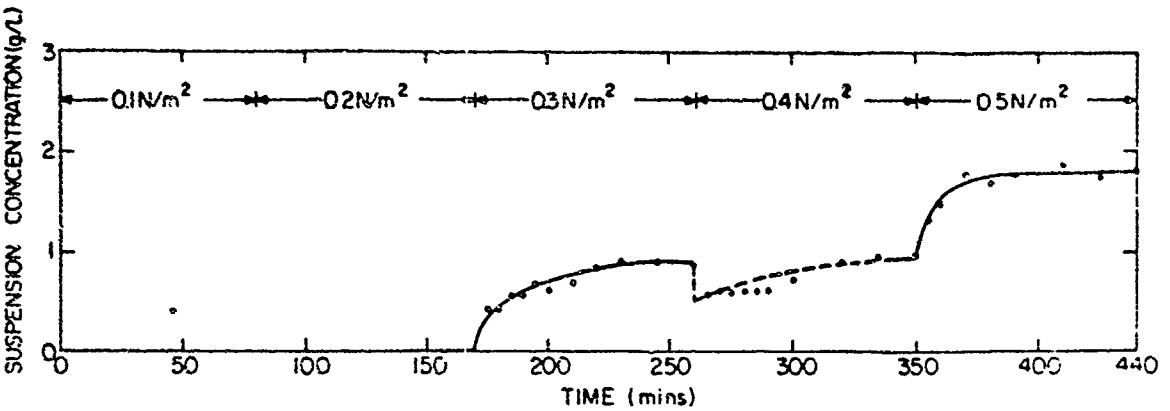

Fig. 35. Time-Concentration Relationship, Bay Mud, Deposited Bed, 3.8 Day Consolidation, Rocking Flume (Test 5).

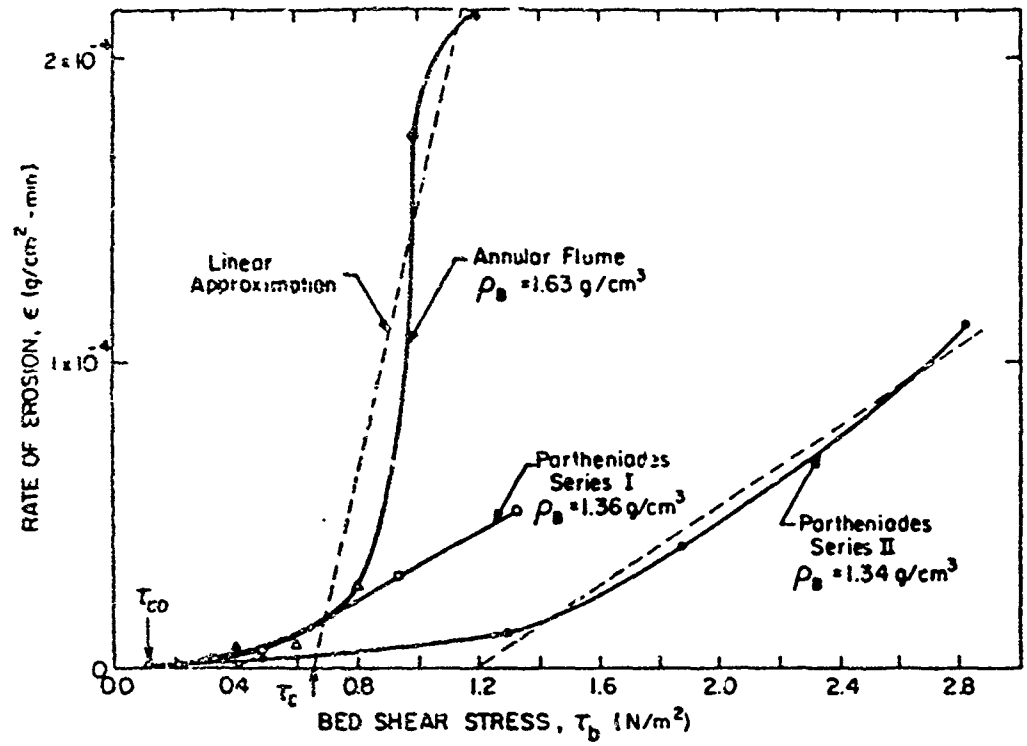

Fig. 36. Rate of Erosion versus Bed Shear Stress, Bay Mud, Dense Bed and Results of Partheniades.

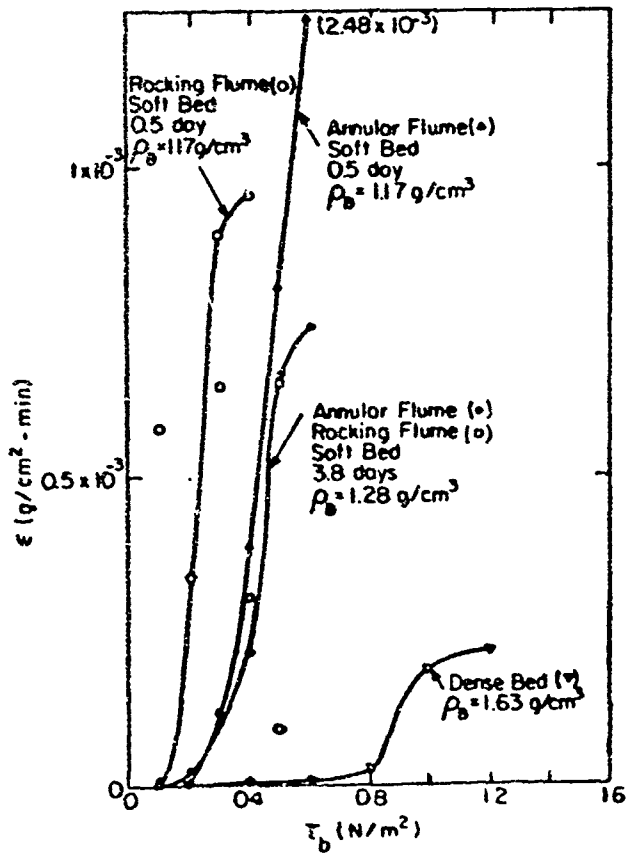

Fig. 37. Rate of Erosion versus Bed Shear Stress, Bay Mud, Dense Bed and Soft Beds.

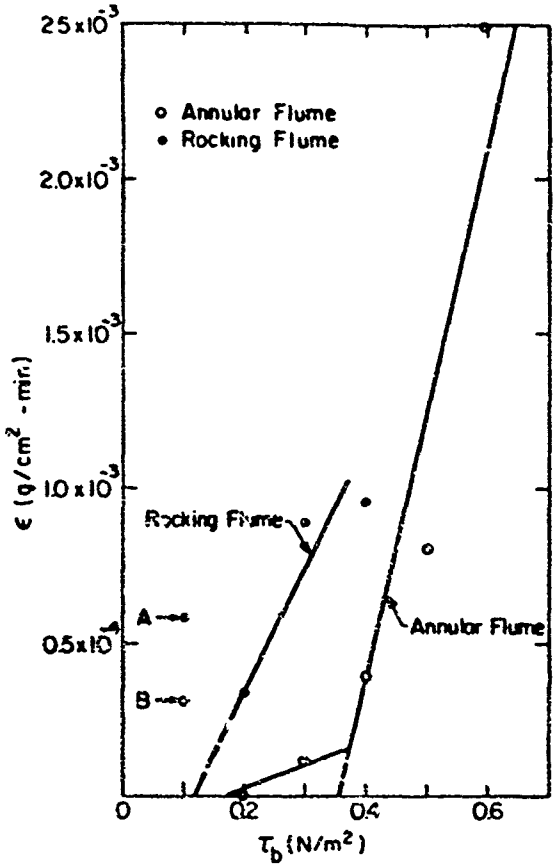

Fig. 38. Rate of Erosion versus Bed Shear Stress, Bay Mud, Soft Beds, 0.5 Day Consolidation.

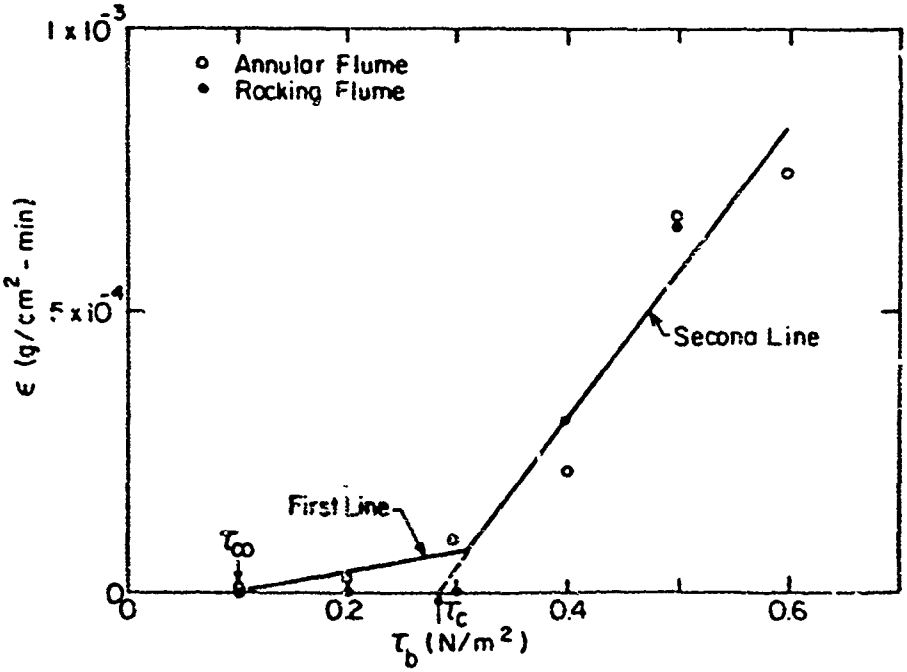

Fig. 39. Rate of Erosion versus Bed Shear Stress, Bay Mud, Soft Beds, 3.8 Day Consolidation.

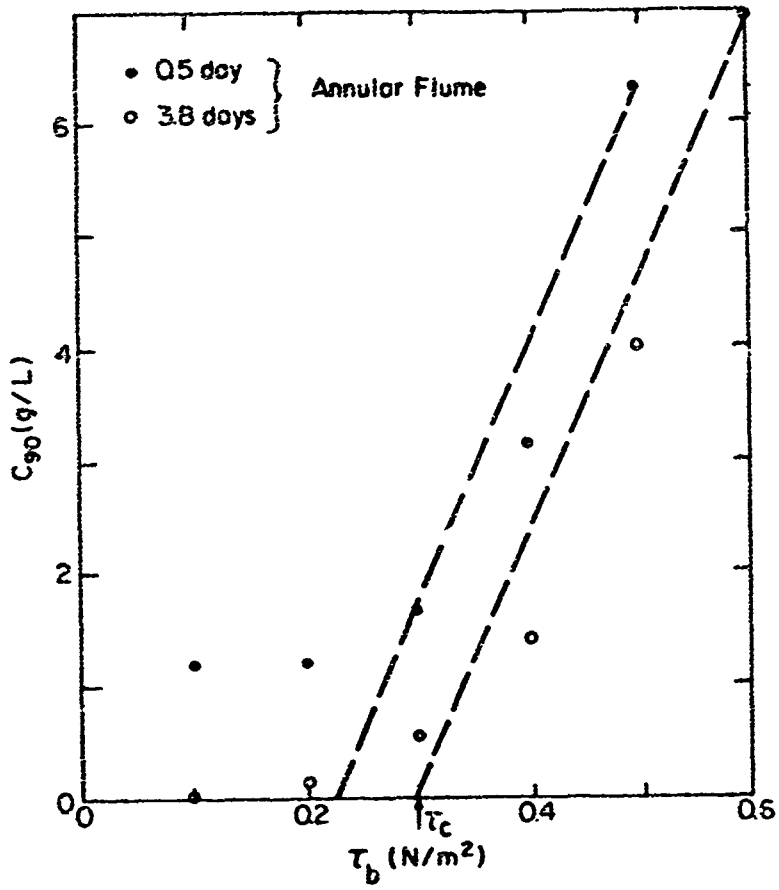

Fig. 40. Final Concentration, C_{90}, versus Bed Shear Stress, τ_b, Bay Mud, Soft Beds, Annular Flume.

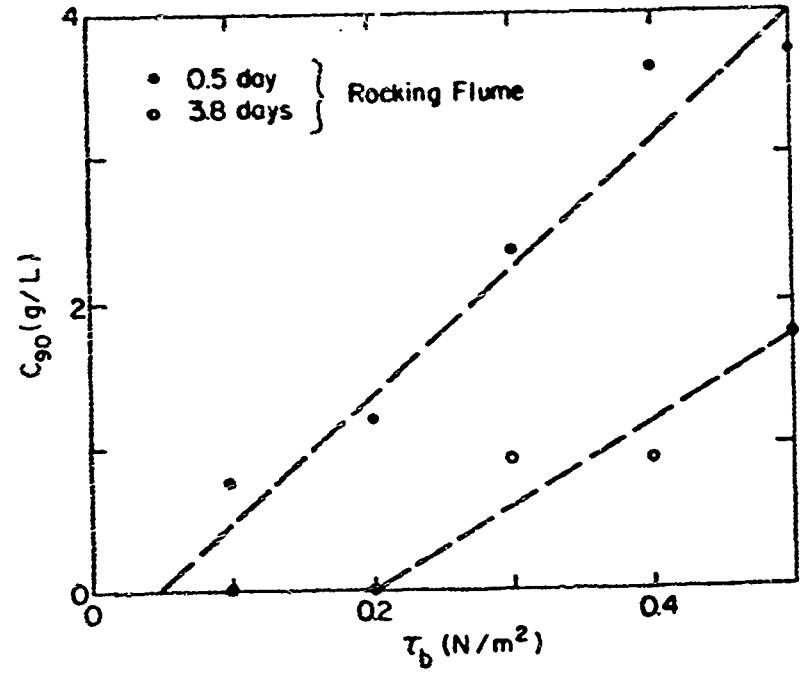

Fig. 41. Final Concentration, C_{90}, versus Bed Shear Stress, τ_b, Bay Mud, Soft Beds, Rocking Flume.

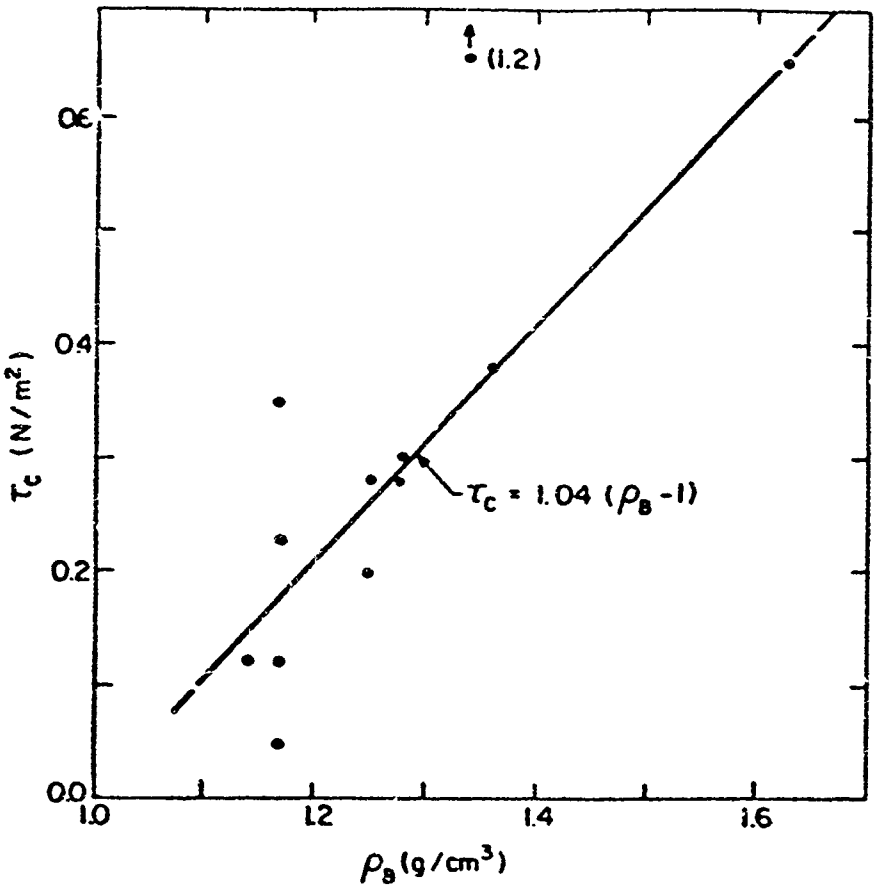

Fig. 42. Critical Shear Stress, τ_c, as a Function of Bed Bulk Density, ρ_B, Bay Mud.

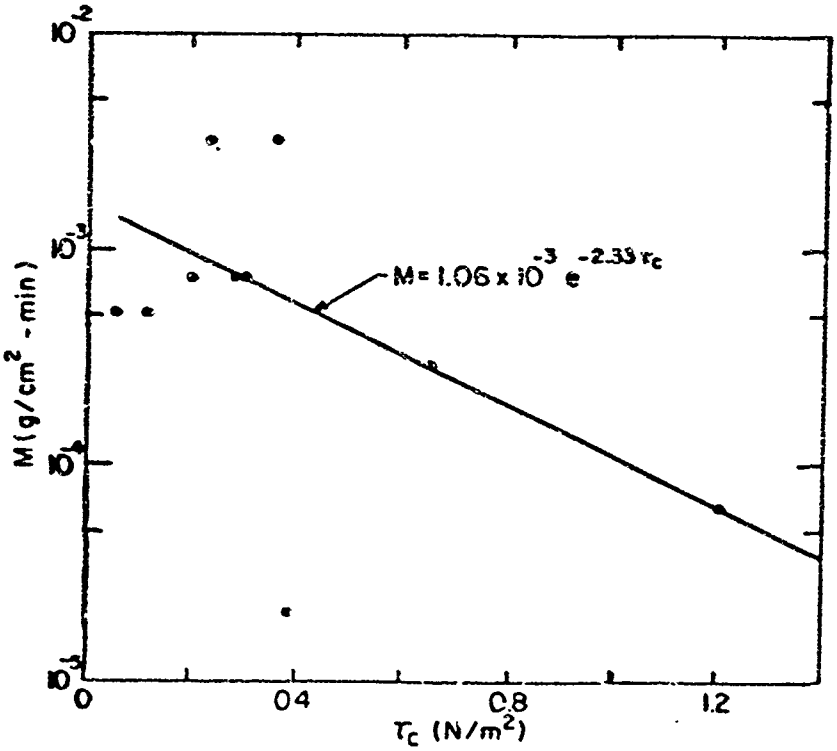

Fig. 43. Erosion Rate Constant, M, as a Function of Critical Shear Stress, τ_c, Bay Mud.

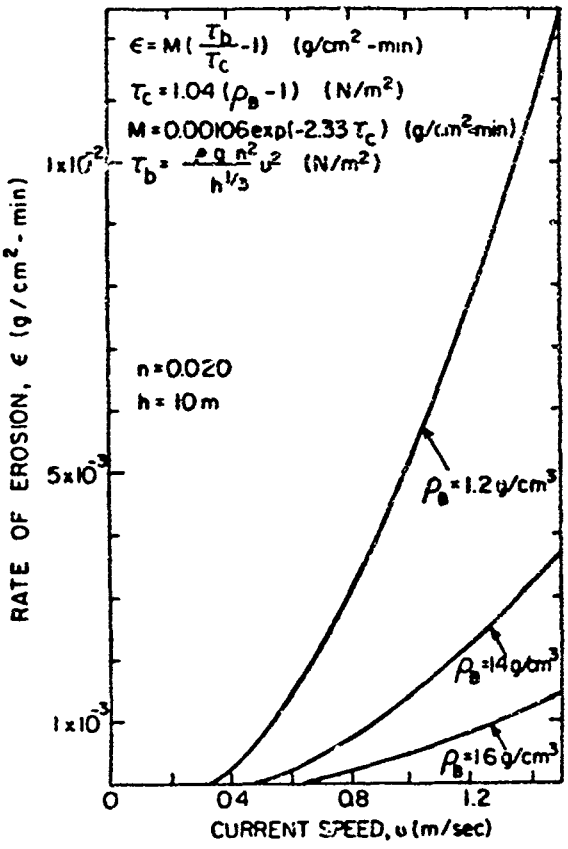

Fig. 44. Erosion Rate Dependence on Bed Bulk Density and Current Speed, Bay Mud.

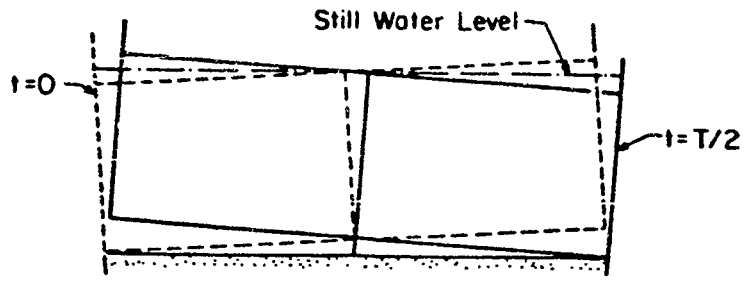

Fig. A.1. Oscillatory Motion of the Rocking Flume.

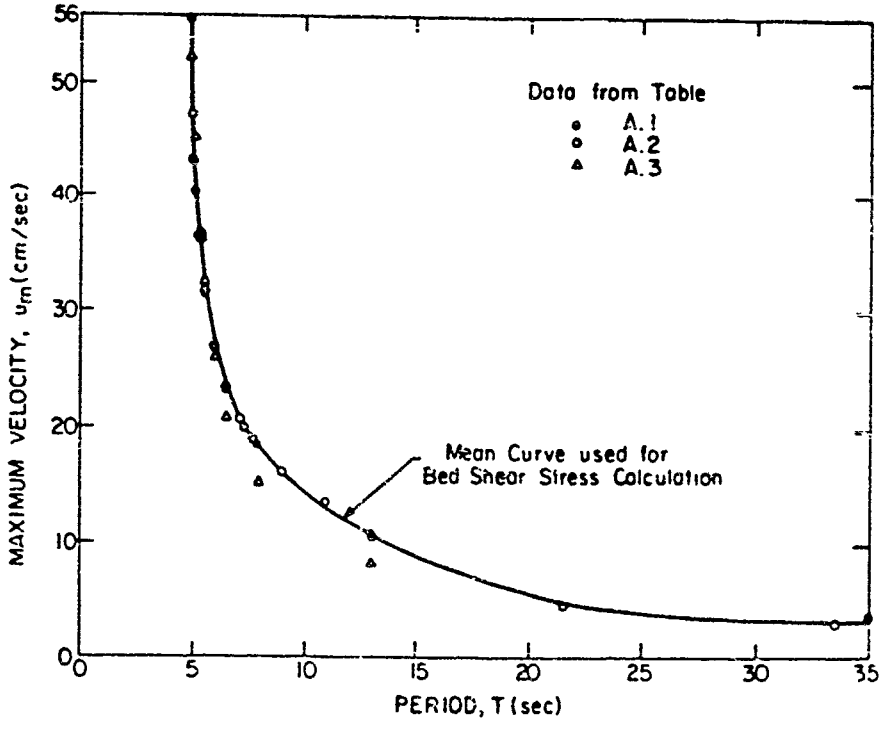

Fig. A.2. Calibration Curve between Maximum Velocity, u_m, and Wave Period, T, in the Rocking Flume.

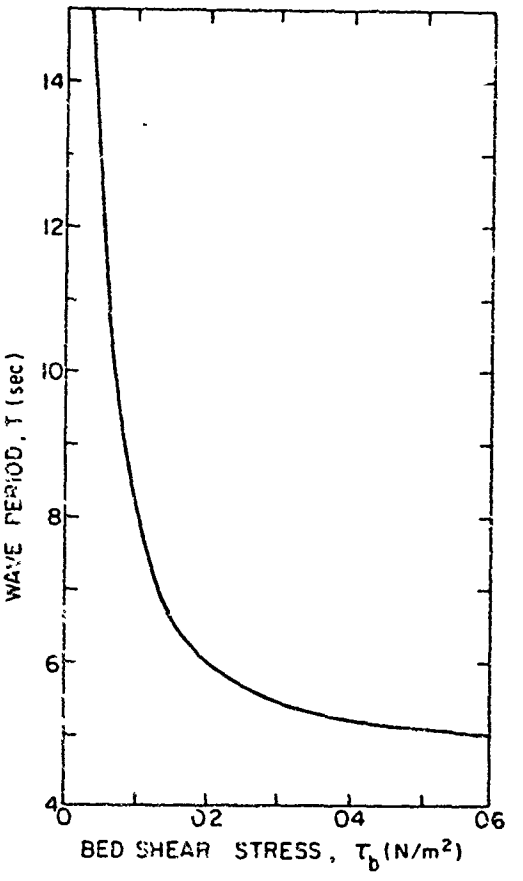

Fig. A.3. Calibration Curve between Bed Shear Stress, τ_b, and Wave Period, T, in the Rocking Flume.

APPENDIX C: NOTATION

BWD	Bulk wet density
C	Concentration
C_o	Initial vertically uniform concentration
CEC	Cation exchange capacity
E	Erosion rate
g	Gravity (9.81 m/sec^2)
H	Flow depth
M	Erosion rate constant
n	Friction coefficient (0.020)
P	Probability of sediment depositing once reaching the bed
SAR	Sodium adsorption ratio
U	Depth-averaged current speed, m/sec
W_h	Hindered settling velocity
W_s	Settling velocity
X	Radius of the site
γ_f	Specific weight of the fines in the material, g/cu cm
ρ	Flow density (1,025 kg/cu m)
ρ_b	UF term for BWD
τ_b	Bed shear stress, N/sq m
τ_c	Critical shear stress for erosion, N/sq m
$\tau_i - \tau_{i-1}$	Maximum excess shear stress where τ_i is the bed shear stress at the termination step i and $i-1^i$ refers to the previous step